

UNCLASSIFIED



AD NUMBER

AD-357 955

CLASSIFICATION CHANGES

TO **UNCLASSIFIED**

FROM **CONFIDENTIAL**

AUTHORITY

DNA Ltr; Dec 6, 1985

19990805006

THIS PAGE IS UNCLASSIFIED

UNCLASSIFIED



AD NUMBER

AD-357 955

NEW LIMITATION CHANGE

TO

DISTRIBUTION STATEMENT: A

Approved for public release; Distribution Unlimited.

LIMITATION CODE: 1

FROM

No Prior DoD Distr Scty Cntrl St'mt Assgn'd

AUTHORITY

DNA Ltr; Dec 6, 1985

THIS PAGE IS UNCLASSIFIED

UNCLASSIFIED

AD 357 955

CLASSIFICATION CHANGED

TO: UNCLASSIFIED -
FROM: CONFIDENTIAL

AUTHORITY:

DAP 142, 6 Dec 85



UNCLASSIFIED

UNCLASSIFIED

WT-1620

This document consists of 130 pages

No. 163 of 225 copies, Series A

857955

357955

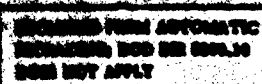
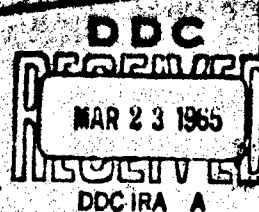
HARDTACK

Project 2.2

SHIPBOARD CONTAMINANT INGRESS FROM UNDERWATER BURSTS (U)



issuance Date December 14, 1964



This material contains neither recommendations nor conclusions of the Defense Department. It has been reviewed and approved for public release by the Defense Department.

UNCLASSIFIED

Reproduced From
Best Available Copy

UNCLASSIFIED

Inquiries relative to this report may be made to

Chief, Defense Atomic Support Agency
Washington 25, D. C.

When no longer required, this document may be
destroyed in accordance with applicable security
regulations.

DO NOT RETURN THIS DOCUMENT

UNCLASSIFIED

UNCLASSIFIED

FOREIGN ANNOUNCEMENT AND DISSEMINATION OF THIS REPORT BY EDG
IS NOT AUTHORIZED.

13 DEC

19

WT-1620

R.G.T. OPERATION HARDTACK--PROJECT 2.2 217

SHIPBOARD CONTAMINANT INGRESS FROM
UNDERWATER BURSTS (U)

M. M. Bigger, ~~Executive Officer~~
J. K. Cong,
F. K. Kihahara,
R. K. Fuller,
W. L. Milne,
S-H. Cohn

(U) 2 Dec 61
U.S. Naval Radiological
Defense Laboratory
San Francisco 28, California

U. S. GOVERNMENT AGENCIES MAY OBTAIN COPIES OF THIS REPORT DIRECTLY
FROM CDC. OTHER QUALIFIED CDC USERS SHALL REQUEST THROUGH

This material contains information affecting
the national defense of the United States
within the meaning of the espionage laws
Title 18, U. S. C., Secs. 793 and 794, the
transmission or revelation of which in any
manner to an unauthorized person is pro-
hibited by law.

Director
Defense Atomic Support Agency
Washington, D. C. 20301

UNCLASSIFIED

ABSTRACT

The objectives were to obtain data in selected interior compartments of one destroyer located within the dynamic radiological environment following two underwater nuclear detonations (Wahoo and Umbrella) from which it might be possible (1) to determine whether an inhalation hazard existed in these compartments because of the ingress of contaminants via ventilation or combustion air systems, (2) to estimate the external gamma radiation dose or dose rate in these compartments due to the ingress of contaminants, and (3) through the measurement of particle-size distribution in several size ranges and activity associated with these size ranges, to attempt correlation between biological dosimetry (primary measurements for Rem 1) and physical measurements, and to provide information on these parameters for use in Rem 2.

Three ventilated compartments were instrumented on the moored and washed destroyer (DD-593). The test conditions were designed to simulate the operational situation with ventilation blowers turned off but with no closures in the ventilation systems. Exhaust blowers were installed to induce 20 percent of the rated airflow through each ventilation system. This airflow represents a maximum that has been measured in shipboard tests under the most favorable conditions for induced airflow with ventilation blowers turned off. The after fireroom was also instrumented to provide data for estimating the dose due to boiler air casting leakage. In this fireroom, full-power airflow was maintained through an unfired boiler, and the compartment was sealed to prevent the ingress of contaminants via the ventilation system. These test compartments were instrumented with air samplers, surface samplers, small animals (mice and guinea pigs), film badges, and recording gamma radiation detectors.

The DD-593 was moored with its starboard side to surface zero, 4,600 feet downwind during Shot Wahoo and 3,000 feet downwind during Shot Umbrella. Two other target ships were also moored downwind with their sterns to surface zero: the DD-474 at 2,900 feet and the DD-593 at 8,900 feet for Shot Wahoo; and the DD-474 at 1,900 feet and the DD-593 at 7,900 feet for Shot Umbrella. The forward firerooms of all three destroyers had one boiler fired for operational reasons with an airflow about half of the full-power airflow. These firerooms were instrumented with film badges and recording radiation detectors by another project.

Because of operational difficulties, the only results obtained as a function of time on the DD-593 for Shot Umbrella were the gamma radiation data. Only animal data and film badge data were obtained on the DD-593 for Shot Wahoo, with ventilation systems open but fans inoperative.

The necessity to estimate the external gamma radiation dose due to the ingress of contaminants into the DD-593 from Shot Umbrella resulted in a wide range of values (and quite a bit of uncertainty). The lower dose estimates were: 0.6 to 2 r for ventilated compartments and 3 to 4 r for the firerooms. These lower dose estimates represent less than 1 percent of the total dose in the ventilated compartments and between about 3 and 18 percent of the total dose in the firerooms. The higher dose estimates were 16 r for a fireroom (only one of two boilers in operation) and 31 r for the ventilated engine room. The higher dose estimates represent approximately 50 percent of the total dose in these compartments. The higher dose estimates for the two ventilated machinery compartments, though quite unreliable, are less than 30 percent of the total dose in three lightly shielded compartments. Estimates of maximum internal dose to man were 0.6 to 1.6 rad/s to the skeleton (critical organ) for the first 7 days after shot.

It was found that 90 to 98 percent of air sample activities collected in the test compartments were due to particles in the less-than-1-micron size range and hence were readily airborne and were capable of being respired.

UNCLASSIFIED

were shown equal to those for ~~the~~ ^{the} ~~Umbrella~~ ^{Umbrella} film badge data. It was also estimated that deposited radioactivity contributed a higher fraction of these doses, because ~~the~~ ^{the} ~~Umbrella~~ ^{Umbrella} Survey dose rates in test compartments were 3 to 4 times the comparable Umbrella dose rates. Estimates of maximum internal dose were 1.8 to 3.4 rads to the skeleton for the first 7 days after shot. In the ventilated engine room, there was one higher estimate of 7 rads to the gastrointestinal tract (also a critical organ). The low estimate in this case was 0.7 rad.

It was concluded that the dose due to ingress of contaminants was of relatively lesser importance than the dose from sources external to the compartment. The dose due to deposited radioactivity in the body was always insignificant compared to the total exposure dose.

In all cases, it is estimated that the doses due to the ingress of contaminants are secondary to the doses due to exterior transient radiation sources, but that, if shielding were provided to reduce the doses due to radiation sources external to the ship, the doses due to the ingress of contaminants would require consideration under any concept of dosage control for repeated exposures.

UNCLASSIFIED

FOREWORD

This report presents the final results of one of the projects participating in the military-effect programs of Operation Hardrock. Overall information about this and the other military-effect projects can be obtained from ITR-1060, the "Summary Report of the Commander, Task Unit 3." This technical summary includes: (1) tables listing each detonation with its yield, type, environment, meteorological conditions, etc.; (2) maps showing shot locations; (3) discussions of results by programs; (4) summaries of objectives, procedures, results, etc., for all projects; and (5) a listing of project reports for the military-effect programs.

PREFACE

The gamma-intensity-time data utilized in this report was obtained by Project 2.1 personnel as an extension of their own experiment design, instrumentation, and data reduction. In addition, they had cognizance of common instrumentation support functions such as gamma-intensity-time recorders and animal-cooling system and the instrument-starting system for both projects. The cooperation and assistance of personnel of Project 2.1, particularly H. R. Rinwert, H. A. Zagories, and R. G. Page, is gratefully acknowledged.

Recovery operations required manpower beyond that available from within the project. Task Element 7.3.1.5, the decontamination unit of Task Group 7.3, furnished four men—R. L. Kopp, DC2; A. P. Brown, FN; J. W. Cox, SN; and W. P. Morones, SN—to assist in this work. In addition they were assigned many miscellaneous tasks, such as sample processing, air sampler preparation for test, and decontamination of air samplers. The highly cooperative and able manner in which they carried out this work was of material assistance.

Project 2.2 also gratefully acknowledges its indebtedness to the officers and crews of the Task Group 7.3 Special Projects Unit, who manned the three target destroyers, for their frequent and cheerful assistance in maintaining support equipment, accomplishing repair and alteration work, and furnishing work parties when required.

UNCLASSIFIED

CONTENTS

ABSTRACT	5
FOREWORD	7
PREFACE	7
CHAPTER 1 INTRODUCTION	15
1.1 Objectives	15
1.2 Background	15
1.2.1 Countermeasure Studies	15
1.2.2 Inhalation Hazard	17
1.2.3 Experimental Considerations and Scope of Tests	17
1.3 Theory	20
1.3.1 Estimates of Dose Rates Due to Radiation Sources Inside a Compartment	20
1.3.2 Inhalation Hazard	23
CHAPTER 2 PROCEDURE	28
2.1 Instrumentation	28
2.1.1 Gamma-Intensity-Time Recorders (GITR's)	28
2.1.2 Total Air Sampler	28
2.1.3 Incremental Air Samplers	28
2.1.4 Animals	29
2.1.5 Surface Samplers	29
2.1.6 Temperature-Humidity Recorder and Counting Apparatus	29
2.1.7 Test and Instrument Installations	30
2.1.8 Test Compartment Airflow Characteristics	30
2.1.9 Air Sampler Efficiency	31
2.2 Operations	31
2.2.1 Shot Wahoo	31
2.2.2 Shot Umbrella	31
2.2.3 Postrecovery Operations	32
2.3 Description of Required Data	32
2.3.1 Data Obtained and Data Available from Other Projects	32
2.3.2 Reduction of Gamma-Intensity-Time Data	32
2.3.3 Reduction of Air and Surface Sample Data	33
2.3.4 Film Badge Data	33
2.3.5 Animal Tissue Dose	33
2.3.6 Correlation of Data	34
CHAPTER 3 RESULTS AND DISCUSSION	52
3.1 Radiation Environment, Shot Umbrella	52
3.1.1 Total Gamma Radiation as a Function of Time	52
3.1.2 Estimates of Some Characteristics of the Enveloping Base Surge	53
3.1.3 Air Sample Data	54
3.1.4 Surface Sample Data	55

UNCLASSIFIED

3.2.1 Estimates of External Radiation Doses Due to the Ingress of Contaminants, Based on GITR Data	56
3.2.2 Estimates of External Gamma Radiation Dose Due to Airborne Activity and Airborne Activity Concentrations Within Test Compartments, Based on Air Sample Data	57
3.2.3 Estimates of External Radiation Dose Due to Deposited Activity Within Test Compartments	58
3.2.4 Summary of External Gamma Dose Estimates Due to the Ingress of Contaminants	58
3.2.5 Comparison of Estimates of External Gamma Dose Due to the Ingress of Contaminants, Shot Wilson and Umbrella	59
3.3 Animal Tissue Dose	59
3.3.1 Internal Dose to Animals—General Trends	60
3.3.2 Estimates of Internal Dose to Man	60
3.3.3 Assessment of the Internal Hazard to Man	61
3.4 Correlation of Air Sample and Animal Data	61
3.5 Summary	62
3.5.1 External and Internal Doses	62
3.5.2 General Considerations	62
CHAPTER 4 CONCLUSIONS AND RECOMMENDATIONS	121
4.1 Conclusions	121
4.2 Recommendations	121
APPENDIX A EQUATIONS FOR ESTIMATION OF GAMMA DOSE RATES FROM RADIOACTIVITY MEASUREMENTS OF AIR AND SURFACE SAMPLE COLLECTIONS AS A FUNCTION OF TIME IN A SHIPBOARD COMPARTMENT	122
A.1 Gamma Dose Rate Due to Airborne Activity	122
A.2 Gamma Dose Rates Due to Airborne Activity and Estimation of Airborne Activity Concentrations from Total Air Sample Data	123
A.3 Gamma Dose Rate Due to Deposited Activity	125
APPENDIX B DECAY FACTORS TO CORRECT r/hr TO EQUIVALENT r/hr AT H+30 SECONDS	126
REFERENCES	127
TABLES	
2.1 Test Compartment Volumes and Surface Areas	35
2.2 Test Compartment Air Volumes and Airflow Data, Shot Umbrella	35
2.3 Sacrifice Schedule	36
3.1 Data from Incremental Air Samplers, Shot Umbrella	63
3.2 Data from Total Air Samplers, Shot Umbrella	63
3.3 Summary of Surface Sample Data, Shot Umbrella	64
3.4 Normalization Factors Used in Simulation of Decay-Corrected Nominous Dose Rate Data	64
3.5 Estimates of External Gamma Dose, Based on GITR Data, Due to Ingress of Contaminants, DD-592, Shot Umbrella	65
3.6 Estimated Airborne Radioactive Concentrations and Resulting External Dose Rates Within Galley of DD-592 After Shot Umbrella	66

3.10 Estimated External Gamma Radiation Dose Due to Airborne Radioactivity Within Test Compartments of DD-592, After Shot Umbrella	66
3.8 Estimated Airborne Radioactive Concentrations and Resulting External Dose Rates Within After Fireroom of DD-592 After Shot Umbrella	67
3.9 Estimated Airborne Radioactive Concentrations and Resulting External Dose Rates Within the After Crews Quarters of DD-592 After Shot Umbrella	67
3.10 Estimated External Gamma Radiation Dose Due to Airborne Radioactivity Within Test Compartments of DD-592, After Shot Umbrella	68
3.11 Estimated Maximum Dose Rates Due to Contaminated Surfaces in Test Compartments Calculated from Surface Samples, DD 592, Shot Umbrella	68
3.12 Estimated Dose Rates and Dose in Curies from H-1 to H-10 Minutes Due to Deposited Contaminants, DD-592, Shot Umbrella	69
3.13 Total Dose and Summary of Estimates of External Gamma Dose Due to the Ingress of Contaminants, DD-592, Shot Umbrella	69
3.14 Gamma Survey Readings Taken Aboard DD-592 After Shots Wahoo and Umbrella	70
3.15 Average 24-Hour Gamma Doses Aboard DD-592, Based on Film Badge Data, and Ratio of Shot Wahoo Doses to Shot Umbrella Doses	70
3.16 Total Dose and Estimates of External Gamma Doses Due to Ingress of Contaminants, DD-592, Shots Wahoo and Umbrella	71
3.17 Estimated External Dose in Forward Fireroom Due to Contaminated Boiler Combustion Air; DD-474, DD-592, and DD-593; Shots Wahoo and Umbrella	71
3.18 Whole-Body Internal Dose to Animals on DD-592	72
3.19 Internal Dose to Organs of Animals on Director Platform of DD-592	72
3.20 Internal Dose to Organs of Animals in Galley of DD-592	73
3.21 Internal Dose to Organs of Animals in After Engine Room of DD-592	73
3.22 Internal Dose to Organs of Animals in After Fireroom of DD-592	74
3.23 Internal Dose to Organs of Animals in Crews Quarters of DD-592	74
3.24 Internal Dose to Man, Estimated from Mouse and Guinea Pig Data, Shot Wahoo	75
3.25 Internal Dose to Man, Estimated from Mouse and Guinea Pig Data, Shot Umbrella	75
3.26 Comparison of Air Sample and Animal Data, Shot Umbrella	76
3.27 Estimated External and Internal Doses Due to the Ingress of Contaminants, DD-592	76

FIGURES

1.1 Hypothetical curve for the ingress of radioactive material, showing a relation between airborne and deposited material	25
1.2 Hypothetical curves for the ingress of radioactive material, assuming all material to be airborne	26
1.3 Hypothetical curve for the ingress of radioactive material, assuming all material to be deposited	26
1.4 Steps in normalizing noningress compartment dose rates to ingress compartment dose rates to obtain dose rates due to ingress by difference	27
2.1 Typical GITR station	37

2.1	Anderson sampling head	39
2.5	Anderson sampler calibration curves	39
2.6	A. C. Schmidt 2-APR constant-flow suction unit	40
2.7	Typical incremental air sampler station, DD-592	41
2.8	Typical animal station, DD-592	41
2.9	Cooling system on DD-592	42
2.10	Instrument locations on DD-592	43
2.11	Location and designation of GITR stations on target destroyers	44
2.12	General arrangement of gallery, DD-592	45
2.13	General arrangement of crews quarters, DD-592	45
2.14	General arrangement of after engine room	46
2.15	Boiler combustion air system, Boiler No. 3, DD-592	47
2.16	General arrangement of after fire room	48
2.17	General arrangement of gun space, DD-592	49
2.18	General arrangement, 5-inch-ammo handling room, schematic, DD-592	49
2.19	Uptake space, DD-592	50
2.20	Surface sample locations. Sample numbers shown are for Shot Wahoo. Add 190 to each sample number for Shot Umbrella	51
3.1	Average gamma dose rates on weather decks of DD-592 after Shot Umbrella	77
3.2	Gamma dose rates in wheelhouse of DD-592 after Shot Umbrella. Compartment sealed, no ventilation	78
3.3	Gamma dose rates in crews mess of DD-592 after Shot Umbrella. Compartment sealed, no ventilation	79
3.4	Gamma dose rates in magazine of DD-592 after Shot Umbrella. Compartment sealed, no ventilation	80
3.5	Gamma dose rates in galley of DD-592 after Shot Umbrella. Controlled ventilation, 100 seconds for one air change	81
3.6	Gamma dose rates in forward fireroom of DD-592 after Shot Umbrella. Compartment sealed, no ventilation, one boiler operating with half of full-power airflow	82
3.7	Gamma dose rates in forward engine room of DD-592 after Shot Umbrella. Compartment sealed, no ventilation	83
3.8	Gamma dose rates in after fireroom of DD-592 after Shot Umbrella. Compartment sealed, no ventilation, full-power airflow through one unfired boiler	84
3.9	Gamma dose rates in after engine room of DD-592 after Shot Umbrella. Controlled ventilation, 255 seconds for one air change	85
3.10	Gamma dose rates in after crews quarters of DD-592 after Shot Umbrella. Controlled ventilation, 800 seconds for one air change	86
3.11	Average gamma dose on weather decks of DD-592 after Shot Umbrella	87
3.12	Gamma doses in wheelhouse and galley of DD-592 after Shot Umbrella. Wheelhouse sealed, no ventilation. Controlled ventilation in galley, 100 seconds for one air change	88
3.13	Gamma doses in crews mess (portside, GITR Station 6) and magazine of DD-592 after Shot Umbrella. Both compartments sealed, no ventilation	89
3.14	Gamma doses in crews mess (starboard side, GITR Station 7) and after crews quarters of DD-592 after Shot Umbrella. Crews mess sealed, no ventilation. Controlled ventilation in after crews quarters, 800 seconds for one air change	90

CONFIDENTIAL

3.15	Gamma doses in lower levels of forward fireroom and after fireroom of DD-592 after Shot Umbrella. Both compartments sealed, no ventilation. One boiler operating in forward fireroom with half of full-power airflow-----	91
3.16	Gamma doses in lower levels of forward fireroom and after engine room of DD-592 after Shot Umbrella. Forward fireroom sealed, no ventilation, but one boiler operating with half of full-power airflow. Controlled ventilation in after engine room, 255 seconds for one air change-----	92
3.17	Gamma doses in lower levels of forward engine room and after fireroom of DD-592 after Shot Umbrella. Both compartments sealed, no ventilation, but full-power airflow through one boiler in after fireroom-----	93
3.18	Gamma doses in upper levels of after engine room and after fireroom of DD-592 after Shot Umbrella. Controlled ventilation in after engine room, 255 seconds for one air change. After fireroom sealed, no ventilation, but full-power airflow through one unlit boiler-----	94
3.19	Decay-corrected dose rates for the weather deck GITR Stations 2 and 3, and for the average of Stations 2 and 3; DD-592, Shot Umbrella-----	95
3.20	Decay-corrected dose rates for the crew mess GITR Stations 6 and 7, and for the average of Stations 6 and 7; DD-592, Shot Umbrella-----	96
3.21	Decay-corrected dose rates for all noningress compartment GITR stations normalized to the average of Stations 2 and 3 at 360 seconds; DD-592, Shot Umbrella-----	97
3.22	Decay-corrected dose rates for the galley GITR Station 9, and for the normalized average of Stations 2 and 3; DD-592, Shot Umbrella-----	99
3.23	Decay-corrected dose rates for the lower level of the forward fireroom GITR Station 11, and for the normalized average of Stations 2 and 3; DD-592, Shot Umbrella-----	100
3.24	Decay-corrected dose rates for the lower level of the after fireroom GITR Station 18, and for the normalized average of Stations 2 and 3; DD-592, Shot Umbrella-----	101
3.25	Decay-corrected dose rates for the lower level of the after engine room GITR Station 20, and for the normalized average of Stations 2 and 3; DD-592, Shot Umbrella-----	102
3.26	Decay-corrected dose rates for the upper level of the forward fireroom GITR Station 10, and for the normalized average of Stations 6 and 7; DD-592, Shot Umbrella-----	103
3.27	Decay-corrected dose rates for the upper level of the after fireroom GITR Station 17, and for the normalized average of Stations 6 and 7; DD-592, Shot Umbrella-----	104
3.28	Decay-corrected dose rates for the upper level of the after engine room GITR Station 19, and for the normalized average of Stations 6 and 7; DD-592, Shot Umbrella-----	105
3.29	Decay-corrected dose rates for the after crews quarters GITR Station 21, and for the normalized average of Stations 6 and 7; DD-592, Shot Umbrella-----	106
3.30	Estimated dose rates in the galley due to the ingress of contaminants into the DD-592 for Shot Umbrella-----	107
3.31	Estimated dose rates in the upper level of the forward fireroom, due to the ingress of contaminants into the DD-592 for Shot Umbrella-----	108

3.33	Estimated dose rates in the upper level of the after fireroom, due to the ingress of contaminants into the DD-592 for Shot Umbrella	110
3.34	Estimated dose rates in the lower level of the after fireroom, due to the ingress of contaminants into the DD-592 for Shot Umbrella	111
3.35	Estimated dose rates in the upper level of the after engine room, due to the ingress of contaminants into the DD-592 for Shot Umbrella	112
3.36	Estimated dose rates in the lower level of the after engine room, due to the ingress of contaminants into the DD-592 for Shot Umbrella	113
3.37	Estimated dose rates in the crews quarters, due to the ingress of contaminants into the DD-592 for Shot Umbrella	114
3.28	Radiological and biological decay curve for mice, director platform, Shot Wahoo	115
3.39	Radiological and biological decay curve for guinea pigs, director platform, Shot Wahoo	115
3.40	Radiological and biological decay curve for mice, director platform, Shot Umbrella	116
3.41	Radiological and biological decay curve for guinea pigs, director platform, Shot Umbrella	116
3.42	Radiological and biological decay curves for individual organs of mice, director platform, Shot Wahoo	117
3.43	Radiological and biological decay curves for individual organs of guinea pigs, director platform, Shot Wahoo	118
3.44	Radiological and biological decay curves for individual organs of mice, director platform, Shot Umbrella	119
3.45	Radiological and biological decay curves for individual organs of guinea pigs, director platform, Shot Umbrella	120

CONFIDENTIAL

Chapter 1

INTRODUCTION

Two underwater nuclear detonations were scheduled to obtain data from which safe standoff distances for a weapon of delivery ship (destroyer) could be determined. (Safe half distance is defined as the distance between point of detonation and delivery ship at time of detonation.) Among the effects to be considered was the potential radiological hazard resulting from the ingress of contamination via both ventilation and combustion air systems. Although this project was too limited in scope to provide full information relative to the problem, the data provides a basis for planning and indicates a need for more extensive studies.

1.1 OBJECTIVES

The objectives were to obtain data in selected interior compartments of one destroyer located within the dynamic radiological environment following two underwater nuclear detonations from which it might be possible (1) to determine whether an inhalation hazard existed in these compartments because of the ingress of contaminants via ventilation or combustion air systems, (2) to estimate the external gamma radiation dose or dose rate in these compartments due to the ingress of contaminants, and (3) through the measurement of particle-size distribution in several size ranges and activity associated with these size ranges, to attempt correlation between biological dosimetry (primary measurements for Item 1) and physical measurements, and to provide information on these parameters for use in Item 2.

1.2 BACKGROUND

Following underwater detonation of a nuclear weapon, the delivery ship, if close to surface zero, might be enveloped by base surge or fallout. The ship would thus be exposed to radiation from external sources and to contamination by ingress via the ventilation and combustion air systems. Ingress of small fallout particles would result in a contaminating aerosol as well as deposition of radioactive material within the ship. Both the aerosol and the deposited material would increase the radiation intensities within the ship. The magnitude of these intensities would be a function of (1) the geometry of the ventilation and combustion air systems and associated compartments, (2) the physical, chemical, and radiological properties of the particles, and (3) the mechanism of transport and of deposition of the airborne material. Quantitative measurements upon which estimates of the magnitude of these potential hazards could be made have been lacking in many areas.

1.2.1 Countermeasure Studies. For a number of years, a requirement has existed in the Bureau of Ships to determine whether a need exists for countermeasures against the ingress of radioactive contamination into ships' interiors and to develop radiological countermeasures, if required.

CONFIDENTIAL

on board the ship decks would be expected to lead to significant radioactive aerosol if the ventilation systems had been operating.

Further tests were conducted aboard the LSS Worcester (CL-144). Nonradioactive cobalt chloride was used as a tracer in an aerosol assumed to simulate that which would be generated by a deep underwater explosion. The simulation was studied to determine the deposition characteristics of the aerosol throughout a boiler combustion air system and a fireroom ventilation system. In addition, laboratory tests were conducted at the U.S. Naval Radiological Defense Laboratory (NRDL) using models of typical ventilation-air and combustion-air systems. These studies (unpublished) revealed that large amounts of the tracer were deposited along the walls of the ducts and at obstructions within the system. No attempt was made to estimate the potential radiation hazard had the tracer been radioactive.

Theoretical studies have been made of the radiological situation that would exist on mobile ships exposed to contamination at various resulting from an underwater nuclear detonation. Reference 3 gives the results of hazard analysis for operation for two cases.

Case 1 assumes no deposition of the boiler systems and an outside aerosol activity of 1 curie/ft³ at 1 minute after detonation. It was estimated that the inhalation hazard (due to leakage of contaminated air from the boiler systems into the boiler room) would be less than the permissible amount listed in Reference 3. Estimates of the external hazard in the boiler room and nearby spaces due to radiation from contaminated air in boiler systems, and in the boiler room through leakage from the boiler systems, were maximum based on a ship entry time of 1 minute after shot and a stay time of 10 minutes. The maximum calculated doses were 22 and 20 r respectively for the upper and lower boiler room levels.

For Case 2, estimates of doses to personnel in the upper level of a boiler room were made assuming that all of the contamination from the combustion air was deposited along the duct system. Assuming an outside activity concentration of 1 curie/ft³ at 1 minute and a ship entry time of 10 minutes after shot, the estimated doses were: 600 r in 1 hour, 1,000 r in 10 hours, and 1,600 r in 100 hours. Thus, even at a low deposition efficiency of 10 percent, personnel exposed for 10 hours or more would receive a dose greater than the military permissible dose (Reference 4).

The results obtained in this theoretical study indicated the need for experimental work on deposition of radioactivity in ducts within shipboard spaces supplied by forced-air systems, ventilation or combustion, as well as measurements of external radiation intensity upon which calculations of radiation dose might be based.

Further theoretical studies (Reference 5) were made relative to the radiation hazard from contaminated aerosols entering via the ventilation system. The degree of hazard from airborne radioactivity might be expected to depend on the type and extent of duct contamination and the sequence of "blowers on" or "blowers off" during and after introduction of contaminated air into the system. It was concluded that, had condition "blowers off" existed at all times, the estimated gamma dose would be reduced to approximately 25 percent of that which would be expected with blowers on. Based on activity of 2 to 3 curies/ft³ at 1 minute, it was concluded that the "blowers off" condition would result in no reduction of combat efficiency from external gamma dose.

Tests were conducted on the ventilation and boiler air systems of ships (YAG's 39 and 40) subjected to the fallout from medium-range surface explosions during Operation Castle. From these tests, it was determined that, for the conditions peculiar to Operation Castle, an average airborne-activity concentration in unprotected ventilation test compartments was on the order of 0.02 percent of that average concentration found weather-side (Reference 6). Data from paper-filter and electrostatic-precipitator protective devices in the ventilation systems gave even lower values.

The contaminating events during Castle were basically different from those during Shot Baker. Correlation of results obtained from Operations Castle, Hardtack, and Crossroads will be diffi-

1.2.2 Inhalation Hazard. Acute biological injury resulting from exposure to airborne radioactive fission products in aerosol form, if any, would be caused predominantly by the external whole-body irradiation (Reference 7). Reports from several field studies attempted to delineate the internal radiation hazards due to inhalation of fallout (References 8 through 10). In these studies and by theoretical calculations (Reference 11), it was determined that the inhalation hazard was small compared with the concomitant external radiation hazard.

In the field studies referenced above, though little or no physical characterization of the fallout material was accomplished, the fallout was dry and insoluble. No field data existed on the possible inhalation hazard associated with an underwater nuclear detonation. After such an event, the inhalation hazard might be considerably greater, because of the possible high aerosol concentration and the soluble nature of the contaminated sea water aerosol. Laboratory experiments indicated that the particles are deposited in the respiratory tract to a greater extent than the same material when dry (Reference 12).

Accurate measurements of particle size, air concentrations, photon spectra, and other physical characteristics of fallout material in the field situations of various kinds are not available. Therefore, it is difficult to simulate field conditions in the laboratory. Expressing the internal radiation hazard in terms of airborne concentrations and exposure time does not accurately indicate the radiation dose to the lungs or other tissues. Also it is difficult to characterize an inhalation hazard in terms of the chemical-physical properties of the aerosol.

Biological samples in the form of small animals have been used in laboratory inhalation studies and provide an empirical method for assessing the potential inhalation hazard to man. Mice were used in the laboratory experiments and were selected as one of the animals to be used in the tests. Guinea pigs were also selected for use, because it has been found (Reference 13) that particulate matter of approximately 1 micron in diameter is deposited most easily in both man and guinea pigs, approximately 50 percent in each.

1.2.3 Experimental Considerations and Scope of Tests. The following is presented, in lieu of experimental background, as experimental work on the ingress of radioactive materials suspended after Operation Castle.

The radiation sources contributing to the radiation field in a shipboard compartment may be classed as: (1) airborne and deposited sources enveloping or deposited on the ship's weather surfaces, (2) waterborne sources, (3) airborne and deposited sources within adjacent compartments if there is ingress, and (4) airborne and deposited sources within the compartment if there is ingress. In any compartment in which there is ingress, it may be necessary to consider separately airborne and deposited sources in ducts or structures within the compartment. This consideration applies to any ventilated compartment containing supply ducts and blowers and is particularly applicable to firerooms with their boilers and associated high-capacity air systems.

The dose rate in a compartment is the sum of the dose rates due to irradiation by each source, each dose rate component varying independently as a function of time because of changing amounts of radioactive material, distance, intervening shielding, and various decay rates if fractionation varies among the several sources. The above-mentioned considerations make it obvious that the external dose rate in an ingress compartment due only to the ingress of contaminants is made up of several components and that the sum of these components may be only a fraction of the total dose rate.

Considering only airborne and deposited radioactive material in a ventilated compartment, Figure 1.1 represents a hypothetical relation between the amounts of total airborne and deposited material as a function of time. The first time period, t_1 to t_2 , represents the buildup of material prior to any exhaust and is dependent on the concentration available in particle sizes that can be carried through the air supply system, the quantity of air supplied, and air distribu-

This period, t_1 to t_2 , is of particular significance in that it is the time during which material is thrown out of the air currents before reaching exhaust terminals. During the second time period, t_2 to t_3 , there is both intake and exhaust of material, t_3 being the time when intake ceases. Either during this period or soon afterward, there will be some time, perhaps only momentary, when the rate of intake is equal to the rate of exhaust plus the rate of deposition, and the total material curve may be flat. During the final period, t_3 to t_m , exhaust is the only mechanism changing the amount of material in the compartment.

The equation given in Figure 1.1 for this period is based on the assumption that the rates of change of airborne material due to exhaust and due to deposition are each proportional to the amount of airborne material present. The equation demonstrates that the rate at which material is exhausted from the compartment is dependent on both deposition and exhaust rates. Thus, the higher the rate of deposition the more rapidly will the total material curve approach the final deposit value, because there is less material out of a given total to be exhausted for a given rate of air exhaust.

Figure 1.2 represents the case where all material is of such small particle size that it remains airborne and deposition of material, if any, can be neglected. The time periods are the same as given above. The principal differences are that during the second period the curve may be flat indicating a constant amount of material in the compartment due to equal intake and exhaust of material, and exhaust air movement alone governs the rate of depletion of material in the compartment after intake has ceased. For the final period after intake has ceased and if it is assumed that the material is uniformly distributed—uniform concentrations throughout the compartment—the dilution equation given in Figure 1.2 may apply. Because in this case the rate of material removed is equal to the rate of change of air in the compartment, the constant k is equal to the ventilation flow rate divided by the compartment volume.

Figure 1.3 represents the case where all material is deposited immediately upon introduction and may more nearly approximate the action in a boulder and its air system than a ventilated compartment. The assumption in this case implies that rapidly acting forces such as impaction from a high-velocity airstream are the principal mechanisms governing particle behavior.

Gamma dose rates due to radioactive materials in a compartment are dependent not only on the amount of material in the compartment but also on a number of variables such as radioactive decay, distribution of material, and photon energy. Any of these factors, particularly decay, which is quite rapid at the early times after shot that are of interest in these tests, when used to convert a material curve to a dose rate curve (or vice versa) may change the slopes and times of peaks.

A direct measurement of dose rate as a function of time, due only to the ingress of radioactive material, can only be made in a compartment that is shielded from other radiation sources, a situation not found on a destroyer. If two similar compartments could be found one of which was ventilated and the other sealed and the dose rate differences due to unequal shielding determined, then any remaining dose rate difference would be due to the ingress of radioactive materials. Determination of such a shielding or normalizing factor between two dose rate measurements at different shipboard locations may be quite difficult or at best be accompanied by large uncertainties. Where the ingress dose rate is a small difference between large numbers, and may be equal to the uncertainty in the large numbers, then any determination by differences is almost impossible.

Uncertainties in this estimating technique are maximum for conditions of rapidly changing, nonuniform radiation sources where the exterior dose rate component is the principal dose rate component. Minimum uncertainties result when radiation sources change slowly, are uniform, and the dose rate due to ingress is the predominant dose rate component. If dose rates due to ingress can be determined and corrected for decay, the values so determined are proportional to the amount of radioactive material in the compartment as a function of time and, with some assumptions and approximations, values proportional to airborne and deposited material may be derived. Reconversion of these estimates to dose rates and integrating would give the mag-

Further assumptions and approximations must be used to convert decay-corrected dose rates to estimates of airborne concentrations and deposition of material per unit surface area as a function of time. The uncertainties in the dose rate data, assumptions, and approximations may lead to estimates of such uncertainty that equally qualitative information might be obtained with less effort from an inspection of dose rates and their relative magnitudes at various locations of measurement aboard ship.

An alternative approach is the reverse of the above, the collection and measurement of radioactive material as a function of time, using air and surface samplers. Using the same approximations and assumptions as above, the dose rates due to airborne and deposited radioactive material may be estimated and added to determine the dose rates due to ingress. The samples obtained may also be utilized to determine particle sizes. Sampling at an exterior location would provide data on airborne concentrations and particle sizes available for intake into ventilation systems for comparison with similar data from ventilated compartment air intakes, to provide some insight into the losses or exclusion due to air supply system characteristics.

Location of samplers in a compartment may be very important. Many shipboard ventilation systems are not designed to uniformly change the air in a compartment. Examples are: machinery spaces which employ spot cooling and spaces where air-cooling (ventilation) is provided to remove heat generated by equipment. In these cases, distances between supply and exhaust ventilation terminals may vary considerably, and there may be relatively dead air-spaces due to short circuiting, where supply and exhaust terminals are located to primarily change air in a particular part of the compartment. Therefore a sufficient number of samplers must be located on the basis of airflow patterns in the compartment. Additional samplers at ventilation intakes or supply terminals and exhaust terminals may be used to determine when intake and exhaust of material start and stop if samples are obtained as a function of time.

To obtain samples as a function of time that may be useful for all of the purposes indicated above requires a knowledge of the time history of the enveloping event, which could be only qualitatively predicted, in addition to ventilation airflow rates and patterns.

The considerations given above were weighed against limitations of time, money, personnel, logistic requirements, and operating conditions to determine the scope of tests and the types of instrumentation. The choice in scope was between the measurement of all parameters in a compartment, of simple ventilation geometry and shielded as much as possible from exterior radiation sources, or making limited measurements in as many compartments as possible. The latter choice was made based on the possibility of obtaining gross information from gamma recorded data and postshot surveys for a wide range of ventilation conditions in the event of instrumentation failures or loss of sample data if early recovery and counting could not be accomplished because of high radiation fields.

Accordingly the scope was determined as follows:

1. Tests would be conducted on one ship only.
2. The center destroyer of a 3-ship array was selected as the test ship to be located downwind from surface zero in the predicted base surge or fallout region.
3. Three compartments were selected for ventilation testing to cover a wide range of ventilation flow rates and incidentally a wide range of rates of change of air and a variety of air distribution patterns.
4. Test compartment ventilation systems would operate with an induced airflow of 20 percent of normal to simulate the countermeasure of "blowers off." Prior shipboard tests had shown that, with ventilation blowers off, airflow varied from 0 to 17 percent of normal. Twenty percent of normal was selected to provide a known maximum airflow to simulate countermeasure conditions.
5. In one fireroom, which was not used for any other purpose, full-power airflow would be maintained through an unfired boiler. The ventilation openings for this compartment would be closed so that any radioactive materials in the compartment would be due to leakage from the

CONFIDENTIAL

deposition of radioactive material. While this procedure is not applicable to combustion studies concerned with boiler air leakage alone, the lack of combustion effects would not be expected to produce deposition of radioactive material in the boiler and its air system in the same amount that would occur under full-power operating conditions. This effect would be expected to influence any dose rate measurement.

Each of the four test spaces would be instrumented as follows with:

1. Gamma-intensity-time recorders (GITR's).
2. Air samplers to sample as a function of time, using an available sampler designed to separate particles into several ranges of particle sizes.
3. Surface samplers as total collectors of deposited material. It was not feasible to attempt to obtain these samples as a function of time. The samplers were to use an available film surface that could be used to determine particle sizes by microscopic examination.
4. Guinea pigs and mice would be used for inhalation studies.

Because of circumstances that will be described later, no air sample data was obtained as a function of time, and the combined effects of ingestion and salt on the surface samples made it impossible to distinguish individual particles.

1.3 THEORY

The techniques, assumptions, and approximations used to estimate the dose rates and dose due to the ingress of contaminants are described below.

1.3.1 Estimates of Dose Rates Due to Radiation Sources Inside a Compartment. Two general methods of estimating dose rates due to the ingress of contaminants were discussed in Section 1.2.3 based on gamma dose rate measurements as a function of time or based on radioactive material collections as a function of time.

The steps in the first method are shown graphically in Figure 1.4. As before:

t_0 = time at which intake of radioactive material starts

t_1 = time at which exhaust of radioactive material starts

t_2 = time at which intake of radioactive material stops

R_I = dose rate at any time t in ingress compartment

R_N = dose rate at any time t in noningress compartment or on deck normalized to dose rate in ingress compartment

I = dose rate component at any time t in ingress compartment due to ingress

R_E = dose rate component at any time t in ingress compartment due to exterior radiation sources

N_F = normalizing factor

t_N = time of normalization

t_{N_2} = time after envelopment and close to estimated time t_2 when I can reasonably be distinguished.

The hypothetical curves shown owe their shape to two envelopments by radiation sources as is the case for which data was obtained. Determination of t_0 may not be possible from this data alone, t_1 cannot be determined and is therefore neglected, however t_2 and t_N for estimating purposes may be determined approximately from decay-corrected dose rate data and any other evidence available.

In the first step, Figure 1.4a, the time t_N is selected during a period when nearly all or a major part of the dose rate in an ingress compartment is due to large exterior radiation sources

$$\frac{R_I}{R_N} = N_F \quad I = 0, \quad t = t_N$$

Assuming that N_F is constant, then

$$R_I = (N_F \times R_N) = I \quad t = t_N$$

It seems reasonable that I at t_N should be at least equal to or greater than I at t_∞ , because of some combination of airborne and deposited material in the ingress compartment. Assuming equality, a new normalizing factor is derived. Then

$$\frac{R_I - I_{\infty}}{R_I} = N_F \quad I_{N_2} = I_{N_1} \cdot t \cdot N$$

and a new I is determined at time t_{N_2} using the new normalizing factor. The process is repeated until there is no significant change in I_{N_2} or N_F and it is then assumed that $R_N = R_E$ at any time (Figure 1.4b).

I at any time t between t_0 and t_∞ may be determined where

$$I = R_I - R_E$$

and $R_E = (R_N \times N_F)$

or $I = R_I - (R_N \times N_F) \quad t_0 \leq t \leq t_\infty \quad (1.1)$

In addition to the uncertainties given in Section 1.2.3 for this method must be added the uncertainties as to the correctness of the normalizing factor and the assumption that the normalizing factor is a constant. It is implicit in this latter assumption that the dose rate measurement at each location is equally influenced by all exterior source geometries.

The second general method of estimating ingress dose rates discussed in Section 1.2.3 was the conversion of material collection measurements to dose rates. The basic measurement required to estimate the dose rate due to airborne radioactive material is the determination of the concentration of airborne material as a function of time. The air samples obtained were collected as total samples for a 2-hour period. Therefore, rates of collection had to be approximated, which together with known air sampler flow rates could be used to approximate airborne material concentrations as a function of time. The time of start of intake t_0 was estimated from gamma data and the time when sampling stopped was known. It was assumed that the influx of material was instantaneous and complete at time t_0 , and that thereafter the airborne concentrations were reduced only by exhaust and dilution with clean air.

The equation for conversion of airborne concentrations to dose rates is given in Appendix A based on the determination of the dose rates at the center of a sphere whose volume is equal to the compartment volume and the assumption that concentrations of material are uniform throughout this volume. This equation was modified to include the approximation given above for apportioning the sample collection as a function of time and is also derived in Appendix A. Total air sample measurements were in terms of fissions, and the equation is:

$$R = 10^{-4} \frac{f_1}{V_1} MKr \quad (1.2)$$

CONFIDENTIAL

t_1 = concentration of fissions, t_1 , in compartment of volume V_1 at any time t_1 , fis/cm^3
 V_1 = volume of compartment, cm^3
 M = gamma energy emission rate at any time t_1 , $\text{Mev} (10^6 \text{ fis-sec})$
 K = conversion factor for gamma flux to dose rate, $r, \text{hr per Mev/cm}^2 \cdot \text{sec}$
 r_0 = maximum radius of the sphere, centimeters

To convert the units of the estimated airborne concentrations in the test compartment from fis/cm^3 to equivalent $\mu\text{c}/\text{cm}^3$ at any time t_1 , the following was used

$$A = 10^{-6} \frac{t_1}{V_1} \frac{Y}{K} \quad (1.3)$$

Where: A = airborne concentration, $\mu\text{c}/\text{cm}^3$
 t_1 = concentration as above, fis/cm^3
 V_1 = value of the disintegration rate of gross fission product mixture at various times after slow neutron fission of 10^6 atoms of $U-235$, $\text{dis}/(10^6 \text{ fis-sec})$ (Reference 14)
 $K = 3.7 \times 10^4 \text{ dis}/(\mu\text{c-sec})$

For the assumption of constant concentration

$$\frac{t_1}{V_1} = \frac{F}{w} \quad (1.4)$$

Where: F = total number of fissions collected on sample
 w = volume of air sampled, cm^3

Estimation of the dose rate at the center of a compartment due to radioactive material deposited on the compartment decks or bulkheads is based on material deposited per unit area as a function of time. Samples were not collected as a function of time, and only the most simple approximations will be made. They will be described later as applied.

For a measurement of deposited material per unit surface area, it will be assumed that the total area (deck or bulkhead) is uniformly contaminated and the shape of the area is a;proximated by a disk of equal area. The dose rate is then estimated for a point above the center of the uniformly contaminated disk. For the case of a uniformly contaminated disk the following equation, derived in Appendix A, is used:

$$R = \frac{k_1 K S E \delta}{4 \pi A} \ln [1 + (r_0/h)^2] \quad (1.5)$$

Where: R = dose rate at h feet above the center of a uniformly contaminated disk at time t , r, hr
 r_0 = maximum radius of disk, feet
 S = sample count rate, counts/min
 δ = decay factor to convert dose rate at time of sample count to dose rate at time t , dimensionless
 A = sample area, in^2
 K = gamma flux to dose rate conversion factor, $r, \text{hr per Mev/cm}^2 \cdot \text{sec}$
 E = gamma energy, Mev/Photon
 g = detection efficiency of counter, counts/Photon
 h = perpendicular distance of point from disk, feet
 k_1 = conversion factor for units, $2.6 \times 10^{-3} \text{ in}^2 \cdot \text{min/cm}^2 \cdot \text{sec}$

rates are too crude to hope to derive an accurate dose-rate history. However, they should be adequate for dose-estimating purposes and, for the data obtained, should provide an overestimate rather than an under-estimate of doses. In the air-sample-estimating technique, all of the material is considered to have been collected at the beginning of intake of material. The effect of decay in this case will compensate to a large degree, or overcompensate for the fact that some material came in at later times or was in the compartment for a longer time period.

1.3.2 Inhalation Hazard. The occurrence of an inhalation hazard from radioactive aerosols may be determined by measuring the uptake and retention of airborne radioactivity by the respiratory system of small animals. Precise evaluation of the internal radiation dose from inhaled radioactive contaminants is difficult. However, approximations, based on experimental data obtained from animal studies, are feasible (References 15 through 17). In these studies, the gamma-emitting fission products are used as the basis for estimating beta concentration in tissue. For the most part, the range of beta particles is confined to the organ or tissue containing the contaminant. Calculation of the dose rate is essentially an estimate of the beta energy made available by the decay of a quantity of the isotope per gram of tissue.

The calculation of the dose is based on several assumptions: (1) the gamma activity of the contaminant per gram of tissue is assumed to be proportional to the beta activity, when corrected for the ratio of beta particles to gamma photons in the fission-product mixture at the time of study; (2) the radioactive contaminant is evenly distributed in the organ; and (3) the beta energy emitted in an organ is completely absorbed within that organ.

An approximation of the dose rate to individual tissues can be obtained by the use of the following equation (Reference 17):

$$R_t = K \frac{Q}{W} E_B$$

Where: R_t = dose rate at time t , rad/hr
 K = factor for conversion of units, 1.15×10^{-6} min./hr, ergs/Mev, rads per erg/gram and includes a factor of 1.2 to convert Q to beta disintegrations per minute
 Q = gamma activity of each sample at the time of sample count, dis/min
 W = weight of tissue, grams
 E_B = average energy of beta particles at time t , Mev/disintegration, 0.65

Dose rate or activity as a function of time changes due to both radiological decay and biological processes. These composite curves as a function of time will be referred to as turnover curves.

The total dose received during any time interval may be obtained by integration of R_t over the time interval in question.

$$D = K \frac{E_B}{W} \int_a^b Q dt \quad (1.6)$$

D = dose in rads between Time a and Time b .

The organs of guinea pigs and mice investigated in this project were the alveolar tissue, large intestine, small intestine, stomach and esophagus, liver, heart, kidney, trachea, nasal passage, spleen, and a tibia. After Shot Umbrella, counts of the thyroid were also made. The activity obtained by counting the remaining carcass, when added to the total count of the organs, resulted in a whole-body count.

the dose of alpha particles may not be stopped in any particular organ. However, the range in man is sufficiently large, as compared to the range of beta particles, to make valid the assumption of the equivalence of energy emission and absorption. By extrapolating the dose values as observed in the guinea pigs and mice, an estimate of the dose from inhaled material in man may be made.

CONFIDENTIAL

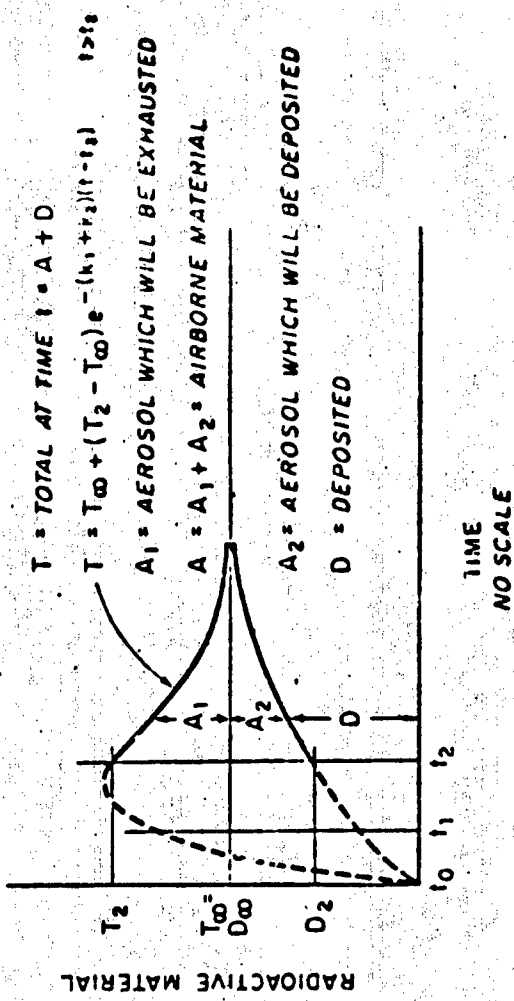


Figure 1.1. Hypothetical curve for the ingression of radioactive material, showing a relation between airborne and deposited material.

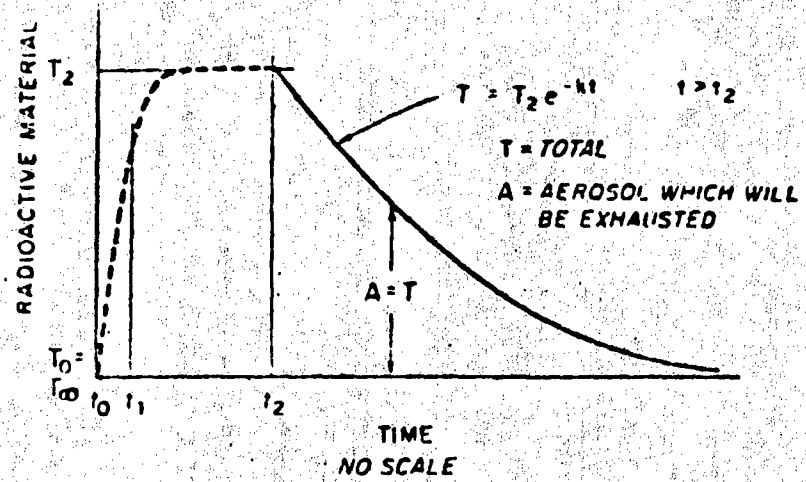


Figure 1.2 Hypothetical curves for the ingress of radioactive material, assuming all material to be airborne.

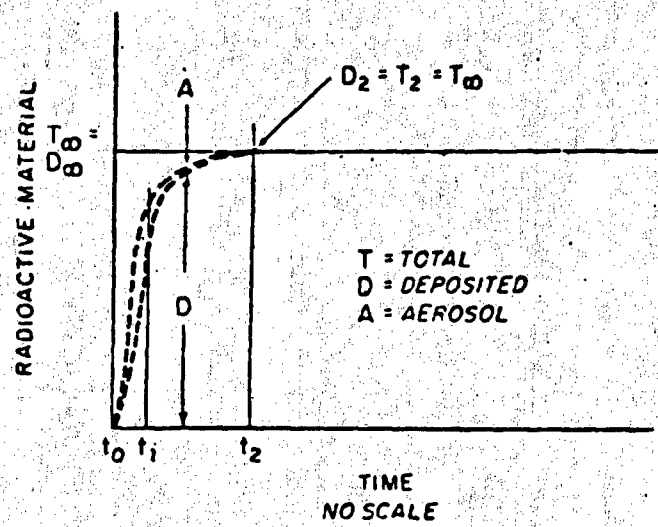
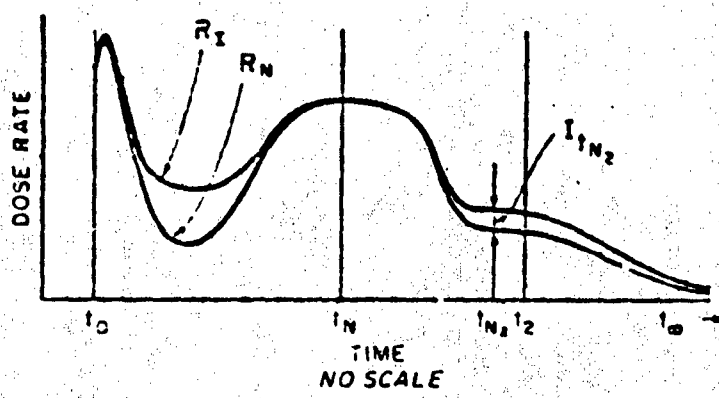
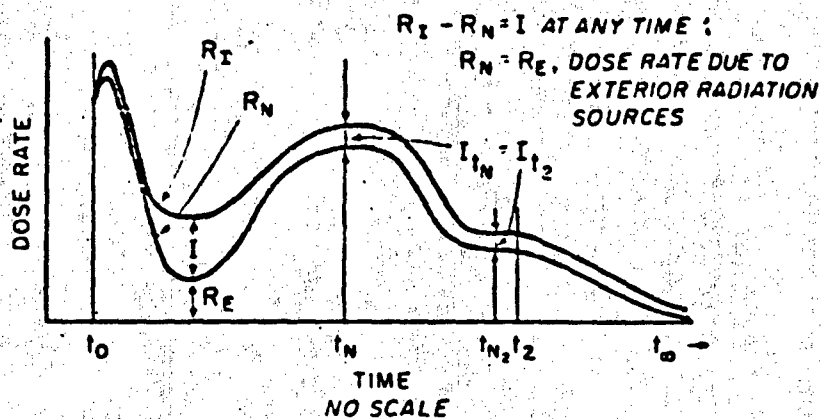


Figure 1.3 Hypothetical curve for the ingress of radioactive material, assuming all material to be deposited.



a. FIRST NORMALIZATION



b. SECOND NORMALIZATION

$R_I - R_N = I$ AT ANY TIME ;
 $R_N = R_E$, DOSE RATE DUE TO
 EXTERIOR RADIATION
 SOURCES

$I_{t_N} = I_{t_{N2}}$

$I = I_{t_N} - I_{t_{N2}}$

$I = I_{t_{N2}} - I_{t_N}$

Chapter 2

PROCEDURE

2.1 INSTRUMENTATION

2.1.1 **Gamma-Intensity-Time Recorders (GITR's).** These instruments consist of two receiving concentric ionization chambers with electrometers, connected by a cable to a battery-powered electronic data-logger unit that includes a timer device. Pulses for a given gamma dose rate, or the reciprocal of the dose rate, information on two logic channels, and timing pulses are recorded on a third channel. Thus the time between pulses or pulse frequency is a measure of dose rate. The nominal dose rate range is 0 milr/hr to 67,000 r/hr.

These units were shock-mounted with the center of the chamber sensitive volume 3 feet above the deck. Cooling coils were provided around the electrometer case when units were installed in high-temperature compartments (Figure 2.1).

A detailed description of these units and the calibration techniques used is available in Reference 18.

2.1.2 **Total Air Sampler.** The sampling head (Figure 2.2) for this instrument contained a 12-inch-diameter filter unit. A pre-filter of Hollingsworth and Vose No. 70 filter paper and Mine Safety Appliance 1109 filter paper, backed by a Millipore filter, and supported on a wire screen, was used. An airflow of $10 \text{ ft}^3/\text{min}$ (cfm) was maintained by an NRDL constant-flow suction unit (Figure 2.3) developed for use during Operation Castle and described in Reference 6. This sampler was intended to operate continuously from H-5 to H-65 minutes.

Airflow calibration was accomplished by adjustment of the constant-flow control valve and using a calibrated Flowrator to measure airflow. The Flowrator is a metering device designed to measure fluid flow rates (Stabi-Vis Flowrator, Fisher-Porter Co.).

The total air sampler was not shock-mounted. The suction unit was mounted in a nearby convenient location and was connected to the sampling head by Pressureflex hose. The sampling head was mounted on a pipe stand, with the orifice approximately 2 feet above the deck.

2.1.3 **Incremental Air Samplers.** These consisted of three basic units: (1) a constant-flow suction unit, (2) a Ledex solenoid-operated indexing head connected to a valve in a 10-port manifold, and (3) a group of 10 Andersen sampling heads. The solenoid was controlled by a timing circuit to sequentially open the 10 ports in the manifold at preset time intervals. By this means, one suction pump pulled air in turn through each of the 10 Andersen sampling heads. A timing circuit failure resulted in the use of only one sampling head at each installation; therefore, this description will be confined to the Andersen sampling head and suction unit, though the name "incremental sampler" will be used throughout the report to identify this air sampler.

The Andersen sampling head, as modified for Project 2.2, consists of five stages with an elbow added above the entrance orifice to prevent material from falling into the first stage (Figure 2.4). Each of the first four stages consists of a perforated metal plate. The particle-laden air is drawn through the holes, producing a jet of air against a filter paper on a plate below. Deposition of the particles on the filter is dependent upon the size, density, and velocity of the particle. The air then passes over the edge of the collection plate and into the next stage. The hole size in the perforated plates is smaller in each succeeding stage, producing

2.1.2.2. Wall losses were used as a method to collect a sample of wall losses that can be obtained in the airstream.

The collection characteristics of the sampling head were determined by adjusting the airflow through the head to 1.0 ft^3/min and exposing it to aerosols of dioctyl phthalate for several narrow ranges of particle size (Figure 2.5). Wall losses were determined by exposure of the sampler to an aerosol having a wide range of particle sizes and tagged with radioactivity. These wall losses were found to be approximately 4 percent of the total activity passing through a sampling head. In order to maintain air velocities through each stage equal to the calibration velocities, it was necessary to use a suction unit that would maintain the calibration airflow of 1.0 ft^3/min over the range of pressure drop caused by filter loading. The A. C. Schmidt 2-APR constant-flow suction unit with a capacity of 1.5 ft^3/min (Figure 2.6) was used for this purpose. The suction unit was adjusted prior to shot time to pump 1.0 ft^3/min as measured by a Flowrator, which was previously calibrated with a wet-test meter. The principle of operation of the Schmidt constant-flow unit is the same as that of the NRDL 10- ft^3/min constant-flow suction unit (Figure 2.3).

A typical incremental air sampler station is shown in Figure 2.7. The 12 liter/min pump and battery-powered sampler shown were installed but did not operate. The supporting framework for each station was shock-mounted, and sampling orifices were approximately 4 feet above the deck.

2.1.4 Animals. Guinea pigs and mice were used for the inhalation studies. The animals were approximately 3 months old at the time of exposure. The average weight of the guinea pigs was approximately 400 grams. The average weight of the mice was approximately 25 grams. A total of 148 guinea pigs and 146 mice were shipped by air to the test site, where they were housed in a portable facility (7- by 7- by 7-foot instrument huts) under controlled conditions of temperature and humidity. A similar unit was used to house the contaminated animals after recovery.

Each animal station (Figure 2.8) consisted of three cages, each partitioned into four sections. A guinea pig was placed in each of 10 sections, five mice in each of the remaining two sections. The cages in the four closed compartments were equipped with a cooling system designed to pass chilled water through tubing installed on the two solid-side panels of each cage. A temperature-sensing element was mounted in the center cage of each station to control the water circulation. Figure 2.9 is a schematic diagram of the cooling system, which also served all GITR cooling coils. This method of cooling was adopted so as to permit the animals to lose body heat by conduction, eliminating the need for undesirable air movement. Drip-type water bottles, which required the animals to lick each drop from the end of a small tube, were installed in each cage in such a manner as to minimize contamination of the water supply. To ensure that internal contamination could result only from inhalation, no food was provided for the animals. The animal cages were mounted approximately 4 feet above the deck. This height was dictated by practical mounting considerations.

2.1.5 Surface Samplers. Strips of salt-water-sensitive film ($\frac{1}{2}$ by 1 inch) were affixed to metal plates the size of microscope slides (1 by 3 inches). Two $\frac{1}{2}$ -inch circular holes were cut in each plate to permit examination of the film under a microscope. The plate-and-film units were attached to deck, bulkhead, and overhead surfaces with tape. The sampling area was approximately 2 in^2 . Details of film preparation and calibration for drop size determination are given in Reference 19.

2.1.6 Temperature-Humidity Recorder and Counting Apparatus. Bendix Fries hygrometerographs, with a temperature range of 10° to 110° F and a relative humidity range of 0 to 100 percent were installed in each test compartment. These are stock instruments requiring no power; the recorder drum is driven by a 7-day clock mechanism.

The animal tissue counter was a Nuclear-Chicago DS 5-1 scintillation detector, with a detector and scaler. It was calibrated with Cs^{137} , Sr^{90} , and Ce^{141} sources.

Air and surface sample activity was counted with a Radiac AN/UDR-9 scaler using a NaI crystal scintillation-detecting unit. Activity determinations of air samples whose count rate was too high for the UDR-9 were made in a 4-8 ionization chamber. This unit used a vibrating reed electrometer and was calibrated against a Cs^{137} and a radium source. Laboratory-determined conversion factors were used to convert 4-8 ionization chamber measurements to equivalent UDR-9 measurements.

2.1.7 Test and Instrument Installations. The instruments described above, with the exception of the counting equipment, were installed on the USS Howorth (DD-592) at locations shown in Figure 2.10. The complete GITR array is shown in Figure 2.11. Three spaces were utilized for studies of contamination ingress via ventilation systems: the galley, the after (at) crews quarters, and the after (at) the room. Figures 2.12 through 2.14 show the arrangement of these spaces and a schematic drawing of the air systems. A blower was installed in each exhaust system to induce 20 percent of rated airflow. The galley and crews quarters were stripped of most equipment to provide room for instrumentation and to eliminate possible contamination of the equipment. Although inoperative, the after engine room was not stripped.

One boiler and the associated combustion air system, located in the after fireroom, was utilized for studies of ingress via boiler combustion air (Figure 2.15). Nos. 5 and 6 forced-draft blowers were operated at full-power capacity (approximately 24,000 ft^3/min each, totaling 48,000 ft^3/min), forcing air through No. 3 boiler, which was unfired. All fireroom openings and fittings were secured or blanked so that the only source of contamination into the working areas was the leakage from the combustion air system. Figure 2.16 shows the general arrangement, including the location of instruments in the after fireroom.

Instrumentation in each of the test spaces was similar, consisting of a GITR, two or three incremental air samplers, one total air sampler, surface samplers, an animal station, and a hygrothermograph.

Additional incremental air samplers were installed to sample air in ventilation-intake housings (Figures 2.17 and 2.18), in the after uptake space (Figure 2.19), and on an instrument platform constructed atop the forward gun director. An additional animal station was also located on this platform.

Surface samplers were taped to decks, bulkheads, and overheads in the four test compartments, compartments containing ventilation-intake housings, and the after uptake space. Eighty surface samplers were installed for each shot at locations shown in Figure 2.20.

Two instrument-starting circuits were installed, one for all GITR recorders aboard the ship (Reference 18) and one for the air samplers, an integral part of the incremental air sampler timing circuit. Each starting circuit was composed of a relay system activated by a master relay connected to the Edgerton, Germeshausen and Grier, Inc. (EG&G) H-5 minute radio timing-signal receiver relay.

Power for the air samplers was supplied by the ship's emergency diesel generator.

2.1.8 Test Compartment Airflow Characteristics. Pertinent compartment and airflow data is given in Tables 2.1 and 2.2. The data demonstrates the gross differences in volumes, flow rates, and consequent rates of air change that led to the selection of these compartments. Influential to this selection was a variety of air distribution patterns. Sections of both the galley and engine room were relatively dead airspaces, whereas the crews quarters had a relatively uniform distribution of air. Each space had a different air delivery pattern: in the galley, through three openings in the overhead across the compartment, the air delivery was vertically downward; in the crews quarters, air was delivered vertically downward about a foot above the deck from six ducts; and in the engine room, air was delivered via three ducts to the upper level and one to the lower level at an acute angle to the horizontal. In this latter case, all ducts

each compartment (Figures 2.12 through 2.14). No survey of air distribution patterns was feasible (though planned), and air samplers were located in what were judged to be primary airpaths. It can only be qualitatively stated that dilution and diffusion effects were nonuniform in both the galley and the engine room, based on the rate of change of air and the variation in distances between supply and exhaust terminals (Table 2.2).

In the after fireroom, the only air movement would be due to the pressure created by the forced-draft blower (8 to 16 inches of water) forcing air out through hatch and ventilation seals. This would be expected to produce a rather slow movement of air to the overhead.

Although the after fireroom (Table 2.2) was the only fireroom designated as a test space for this project, GITR's for Project 2.1 were installed in the forward fireroom. This GITR data was also useful to Project 2.2. In the forward fireroom, No. 1 boiler was fired to supply steam to operate machinery in the forward engine room. Combustion airflow was about half of the airflow through the unfired boiler in the after fireroom. In both firerooms, hatches and ventilation openings were closed and sealed against the ingress of contaminants.

2.1.9 Air Sampler Efficiency. In all sampler installations in compartments and ventilation intakes, the sampler opening faced at 90° to the estimated direction of air movement. In these cases, the average face velocity at the sampler intake was estimated to be equal to or greater than the airstream velocity. However, in the uptake space, airstream velocities were probably higher than sampler velocities. Further, the sampler locations were dictated by space requirements and may not have been in the principal airpath. On the instrument platform above the gun director, the sampler openings faced downwind. Any wind velocity above 2 knots would reduce the efficiency of sampling.

2.2 OPERATIONS

Contamination-ingress studies were conducted aboard the DD-592 during Shots Wahoo and Umbrella. This destroyer was moored downwind from, and starboard side to, surface zero at a nominal standoff distance of 4,900 feet for Wahoo and 3,000 feet for Umbrella. Early on shot day, animals were placed in their cages and instruments were checked. Personnel debarked at H-5 hours for Wahoo and at H-2 hours for Umbrella, leaving the ship unmanned and completely closed, except for air-intake openings for the following systems: (1) test ventilation, (2) combustion air systems for test boiler and operating boiler, and (3) combustion air systems for operating diesels. The operating boiler supplied steam to drive the main propulsion machinery, which was being operated for shock-damage evaluation. The diesels were prime movers for generators furnishing power for instrumentation. A washdown system, activated several hours prior to shot time, washed the entire weather surfaces of the ship, with the exception of the instrument platform atop the forward gun director. The washdown continued to operate until approximately H-19 hours after Wahoo and H-23 hours after Umbrella. The wind speed was 15 knots during Wahoo and 20 knots during Umbrella.

2.2.1 Shot Wahoo. Following Shot Wahoo, the upwind mooring barge broke loose and, subsequently, struck the starboard side of the stern of the DD-592, leaving the ship moored by the bow only. The ship changed position, heading into the wind, but maintained its approximate distance from surface zero.

Project 2.2 recovery operations were accomplished on the day after the shot. The recovery party boarded the ship at H-21 hours 55 minutes (1125) to recover samplers, instruments, charts, and Project 2.1 film badges, which had been installed in Project 2.2 test spaces. Recovery was completed in 45 minutes. No pocket dosimeter reading exceeded 150 mr.

2.2.2 Shot Umbrella. Preshot operations differed from those for Wahoo in that the majority of GITR recorders were manually started, timed by an H-3 hour radio voice signal. Only two

less than 100 ms. The post-arrival data analysis was part of Task 2.1.

Postshot operations started at H+2 hours, at which time the recovery party boarded the ship and deactivated the washdown system. Recovery was completed, the washdown reactivated, and personnel debarked by H+2 hours and 45 minutes. No pocket dosimeter reading was greater than 200 mr.

2.2.3 Postrecovery Operations. Dissecting and counting of animal tissues was accomplished in the Eniwetok Marine Biological Laboratory. The sacrifice schedule is given in Table 2.3. Counting of all other collection media was accomplished in the project laboratory.

2.3 DESCRIPTION OF REQUIRED DATA

2.3.1 Data Obtained and Data Available from Other Projects. Animal data was obtained during Project 2.1. All GITR data, including air sampler data as a function of several ranges of particle size, total air sampler data, and surface sampler data were obtained during Shot Umbrella. All sample collections were total collections made over a period of time from some unknown time of arrival of radioactive material to H+2 hours. Many of the surface samples showed no activity above background. No determination of particle size was possible, because the salt-water-reagent film was fogged due to the humid salt atmosphere and high temperatures.

Additional data was available:

(1) From Project 2.1 (Reference 18): all GITR data throughout the ship and gamma ionization decay data starting at H+6 minutes, obtained on the DD-592 (Shot Umbrella); some GITR data for the forward firerooms of the DD-474 (Umbrella only) and the DD-593 (Wahoo and Umbrella); and film badge data from the three ships for both shots.

(2) From Project 2.3 (Reference 20): radiochemical analysis of a DD-592 fallout sample for converting this project's total air sample data to equivalent fissions, reduced photography data of the base surge, and data from incremental fallout collectors and an air filtration instrument, which were installed on the DD-592 instrument platform above the forward gun director (generally referred to as director platform).

2.3.2 Reduction of Gamma-Intensity-Time Data. The reduction of all GITR raw data to final corrected data was accomplished by Project 2.1 assisted by Project 2.2 personnel and is described in detail in Reference 18. The GITR magnetic tape pulse recordings were initially converted to dose or dose rate histories by means of an analog data reduction apparatus supplied and operated by Project 2.3 (Reference 20). To obtain a more accurate readout during the periods of rapidly changing radiation intensities, the IBM-704 computer at the Eniwetok Proving Ground (EPG) was utilized. Magnetic tape data pulses were entered into the IBM-704 via an auxiliary special-purpose magnetic tape unit and gate chassis connected to the computer. Corrections for calibration shifts, radiation source geometries, detector geometries for various assumed gamma energies, and timing corrections were calculated or estimated and applied to the raw data. The manually started GITR records had to be time-correlated with data from the radio-started GITR's. This was accomplished by lining up times of those prominent curve features (such as maxima, and the like) that should have occurred at the same time for all stations aboard one ship.

On the DD-592, radiation intensities at exterior locations were high enough to saturate the GITR detectors, resulting in gaps in the data. An average weather deck dose rate history for this period was estimated by normalizing data from appropriate interior locations to average weather deck data in the time periods just prior to and after saturation. The only interior station where saturation was encountered was in the gallery where the dose rates during the saturation (between 27.9 and 31.7 seconds after shot) were estimated in a similar fashion.

radiation the range of the relative uncertainty in the dose rate data. (2) limits for correction factors calculated for a broad range of assumed radiation source geometries and gamma energies; (3) estimated effects of timing errors; and (4) the variance of data from calculated averages where appropriate. In general the precision of these data was estimated to be within ± 20 percent. This pessimistic estimate of precision resulted from the manual starting of most of the GITR's which created some uncertainty in the timing of various GITR records (Reference 18).

The GITR dose rate data was corrected for decay. The curves were examined for features that might indicate the beginning and end of envelopment, the beginning and end of the ingress of radioactive material, and the magnitude of decay-corrected dose rates that were due to deposited material. The decay used was based on preliminary experimental data of ion chamber decay of U^{235} fission products by J. Mackin of NRD (report in preparation) prior to $H + 6$ minutes and the Project 2.1 decay data normalized at $H + 6$ minutes.

The normalized techniques described in Section 1.3.3 of Equation 1 were utilized to estimate the dose rates due to the ingress of radioactive material. Two estimates of dose rate's were made for each ingress compartment GITR location(s). The two dose rate histories, which were normalized to the ingress compartment dose rate histories, were selected because integration of the dose rates so obtained gave near maxima and minima doses for the data available. No limits of probable error can be assigned to the estimated ingress dose rates and doses. Although limits can be assigned to uncertainties in the basic data used, this is not true for the normalizing factor or the implicit assumption that this factor (or shielding factor relationships) were constant. The range of estimated doses is indicative of uncertainty of the estimates.

2.3.3 Reduction of Air and Surface Sample Data. Incremental air sampler data in counts per minute were decay-corrected to a common time from the time of counting, and the percentage of activity in each particle size range (sampler stage) determined. The total air sampler data was decay-corrected to the same time for comparison of total activities collected by the incremental and total air samplers. Upon return to the laboratory, the total air samples were counted again (the incremental samples had decayed to very low values by this time) and the counting data converted to fissions per sample by comparison with a Project 2.3 fallout sample from the DD-592, Shot Umbrella.

No time history of material collection was deducible from the gamma dose rate estimates. The simplest assumptions were used therefore and dose rates estimated at the center of a spherical volume using Equation 1.2 and integrated to estimate the dose due to airborne radioactive material in the ventilated test compartments. Equations 1.3 and 1.4 were used to estimate airborne concentrations of activity.

Surface samples were counted and, for the only significant case of deposition, the highest sample activity was used to estimate dose rates and the dose due to deposited material.

No limits of probable error can be assigned to estimates based on sampler data. The approximations and assumptions were made in such a manner as to provide maximum dose estimates for the data obtained.

2.3.4 Film Badge Data. The data was used in lieu of GITR data and to supplement GITR data in some instances, to estimate ingress doses, or to establish the relative magnitude of doses between various shipboard locations, between ships and shots. Ingress doses were estimated by the differences in doses between ingress and the most nearly physically similar noningress compartments. No limits of probable error can be assigned to such estimates for the same reasons given for GITR-based ingress dose estimates. The film badge data has been assigned standard limits of error by Project 2.1 (Reference 18) of ± 20 percent.

2.3.5 Animal Tissue Dose. Animals were sacrificed, tissues counted, and activity totaled at various times. The sacrifice schedule for both shots is given in Table 2.3. Because of

radiological decay and biological elimination as a function of time.

Because of the late recovery following Shot Wallou, only the middle section of the radiobiological decay curve (turnover curve), from 40 to 185 hours after detonation, could be determined. After Shot Umbrella, recovery was made at $W + 2$ hours, and sacrificing started immediately. Thus, an early portion of the curve was determined. Both sections of the curves thus determined fitted well with the curve for similar times developed in experimental studies with mice at NRDL by the use of an ionic type of simulant (Reference 17). Complete total-body curves for the director platform animals were constructed by normalizing the laboratory experimental curves to best fit the field data. Based on similar curves drawn for each test animal, total tissue activity was calculated for the following postshot periods: the first 2 days, the first week, the second week, and the third week.

Integrating under each curve for the various time intervals given above provided values for the expression

$$\frac{1}{W} \int_a^b Qdt$$

which were substituted in Equation 1.6 to determine the average whole-body internal dose in rads.

Turnover curves were similarly developed for individual organs: the gastrointestinal tract, liver, thyroid (in Shot Umbrella only), skeleton (as represented by the tibia), and the respiratory tract. Individual organ doses were calculated in the same manner as described above for whole-body internal doses.

3.3.6 Correlation of Data. Ingress dose estimates obtained by the various methods outlined were compared in an attempt to determine whether they were over- or underestimates and whether they were influenced by the inclusion or exclusion of dose rate components due to ingress in adjacent compartments.

Exterior, intake housing, and test compartment air sample data were compared for gross differences in particle size and total collections as a function of location.

Internal doses based on animal data were also compared to demonstrate gross differences as a function of location and the relative magnitudes of whole-body doses compared with the relative magnitudes of air sample total collections at the same locations.

Estimates of airborne activity concentrations were compared to a maximum permissible concentration, and estimated internal doses were compared to existing dose damage criteria.

Ingress external and internal dose estimates and total dose estimates were compared to demonstrate their relative magnitudes and hence their relative importance.

TABLE 2.1 TEST COMPARTMENT VOLUMES AND SURFACE AREAS

Compartment	Volume ft ³	Deck Area ft ²	Forward or After Bulkhead Area		Port or Starboard Bulkhead Area ft ²
			ft ²	ft ²	
Galley	1,670	235	110	10	840
After engine room	17,000*	1,218†	610	—	—
After crew's quarters	4,000	570	245	147	—
After fireroom	8,000*	1,200*	250	110†	—

* Excluding approximate machinery volume.

† Including approximate machinery surfaces.

TABLE 2.2 TEST COMPARTMENT AIR VOLUMES AND AIRFLOW DATA SHOT UNNECESSA

Compartment or Air System	Nominal Flow Rate (20 percent of rated capacity) ft ³ /min	Nominal Time for One Air Change seconds	Distance from Air to Traverse Supply to Exhaust Terminals feet		
			Supply feet	Exhaust feet	Exhaust feet
Galley	1,670	100	64	210	210
After engine room	17,000	4,636*	255	2 to 4	6 to 18
After crew's quarters	4,000	300†	800	8 to 10	17
After fireroom	8,000	5	—	—	—
No. 3 boiler air system	4,000	49,000*	5	—	—
No. 1 boiler air system	4,000	24,000*	10	—	—

* Port and starboard lower each supplied half of the total.

† This system normally served several other compartments and had a total (60 percent of rated capacity) airflow of 1,100 ft³/min. For this test, 300 ft³/min were supplied to the after crew's quarters while 70 ft³/min were exhausted via bypass ducting in lieu of entering the other compartments.

† The only airflow was due to boiler air causing leakage.

TABLE 2.5 SACRIFICE SCHEDULE

All animals in hecate tanks		After defecation		After		After		After		After	
Interval	Defecation	Defecation	Defecation	Gastric	Defecation	Gastric	Defecation	Gastric	Defecation	Gastric	Defecation
	Platform	Quarters	Engine Room	Forecabin	Platform	Quarters	Engine Room	Forecabin	Platform	Quarters	Engine Room
Shot Wahoo											
First	59	15	47	31	13*	36	52	31	56	13*	
Second	74	30	121	73	—	69	81	91	91	—	
Third	95	117	117	120	—	115	129	129	129	—	
Fourth	115	—	—	—	—	115	—	—	—	—	
Fifth	165	—	—	—	—	155	—	—	—	—	
Shot Umbrella											
First	—	—	2.5	—	—	—	—	2.5	—	—	
Second	—	—	20	—	—	—	—	20	—	—	
Third	—	—	91	—	—	—	—	91	—	—	
Fourth	—	—	162	—	—	—	—	162	—	—	

* The time of death of gallay animals was estimated in the following way. Recovery was made at H+22 hours.

Although all animals were not quite stiff, indicating that the time of death were at about H+21 hours. In all animals analyzed, the activity in the gastrointestinal tract had the greatest concentration in the large intestine, the most highest concentration in the small intestine, and the lowest concentration in the stomach.

Thus means that all animals lived until at least H+1 hours. Thus, because all animals recovered at H+8 hours and all were dead at H+21 hours, the average time of death was H+13 hours.

1 Animals from all compartments were sacrificed simultaneously.

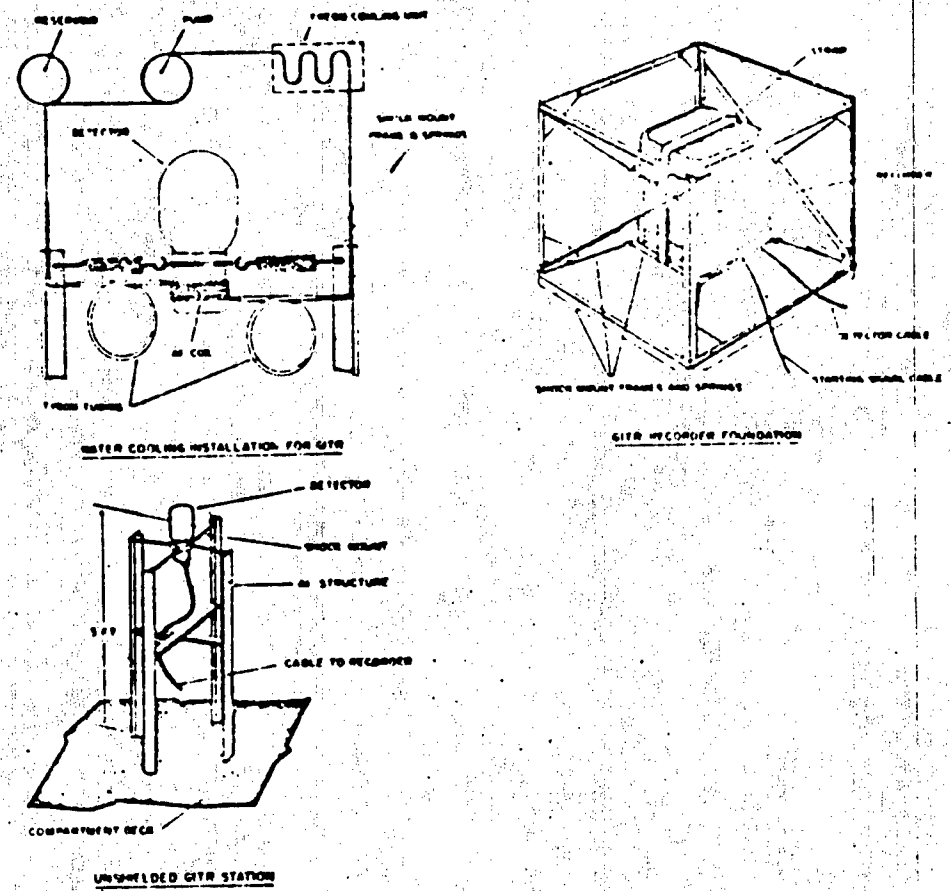


Figure 2.1 Typical GITR station.

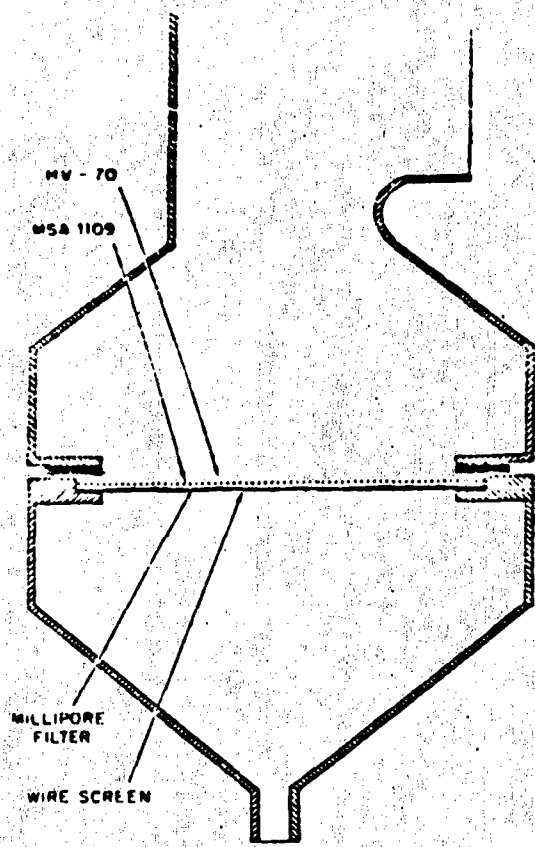


Figure 2.2 Total air sampler sampling head.

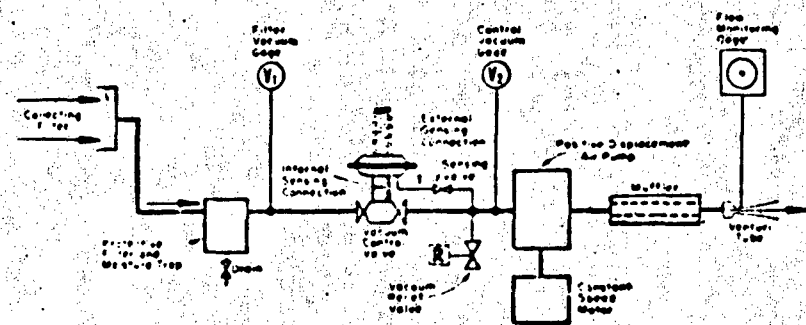


Figure 2.3 SRDE 10 cfm suction unit schematic.

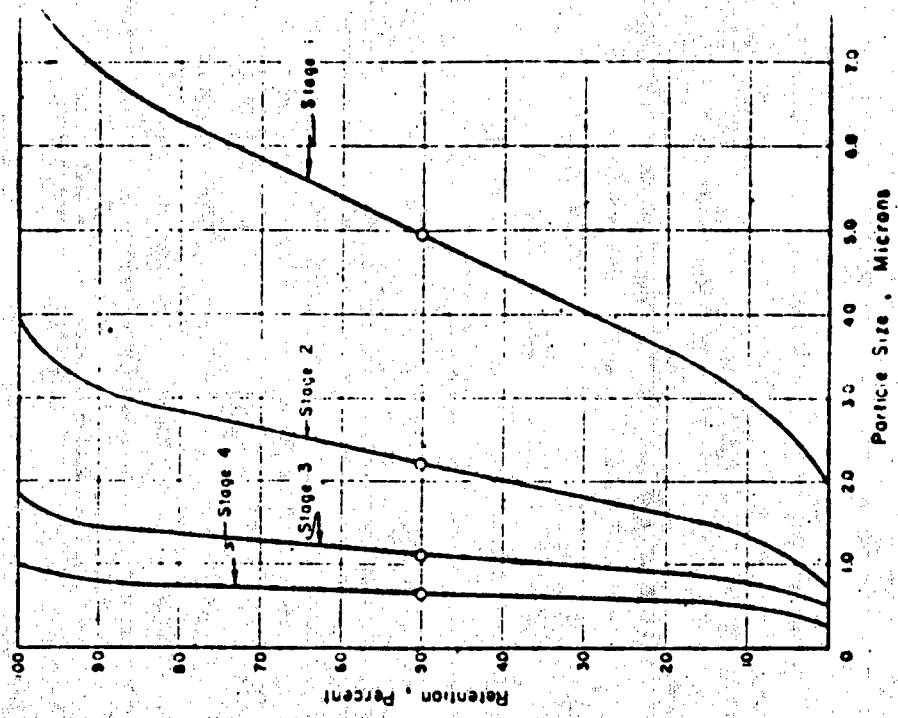


Figure 23 Andersen sampler calibration curves.

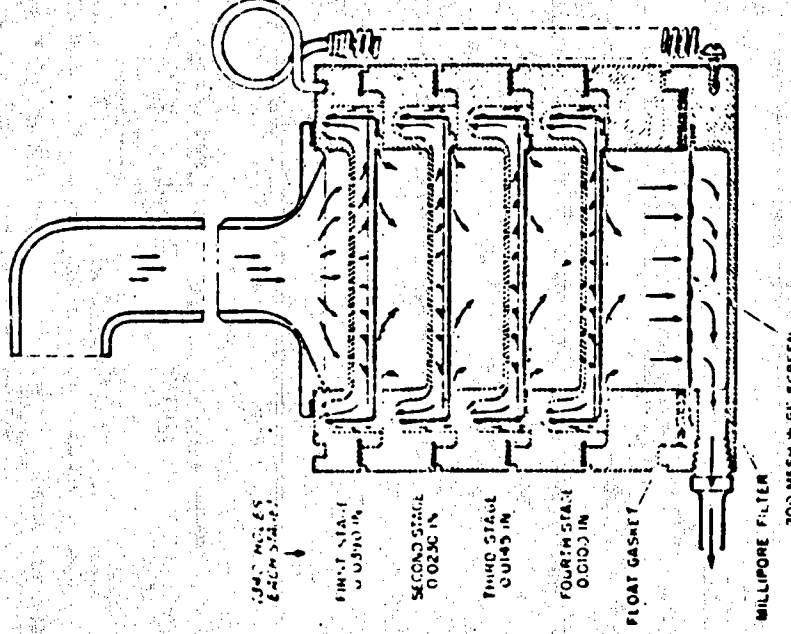


Figure 24 Andersen sampling head.

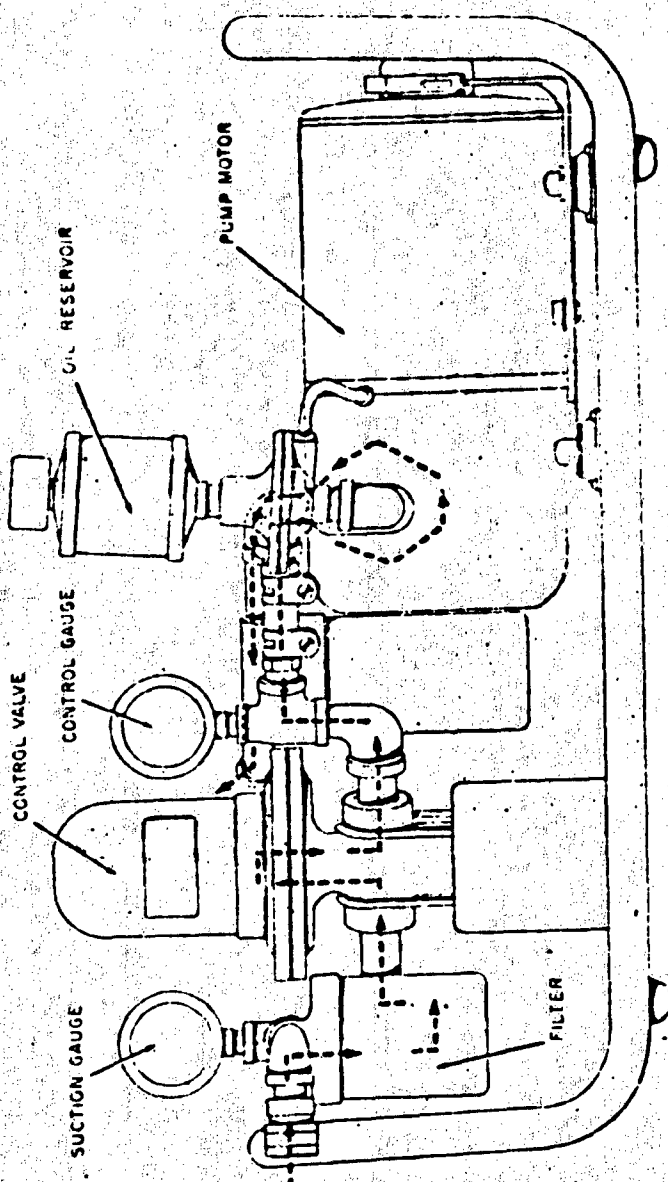


Figure 2.6 A.C. Schmidt 2-AMP Constant-flow suction unit.

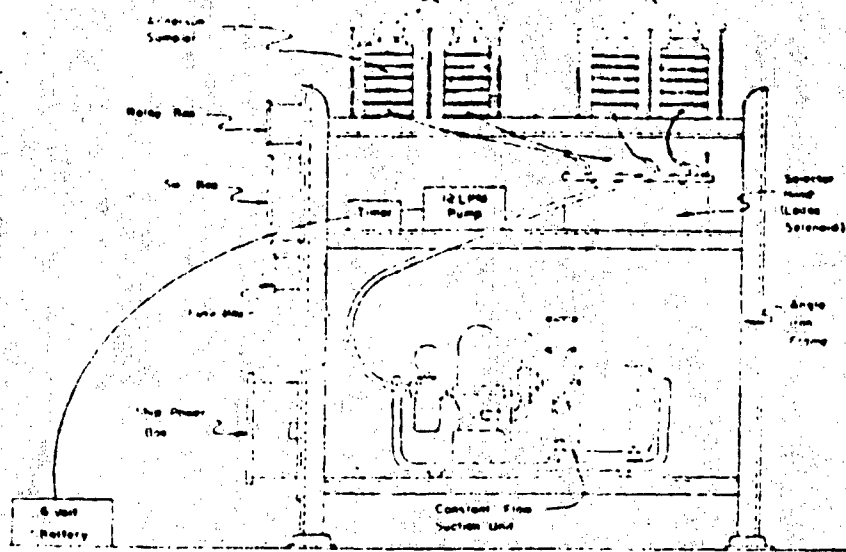


Figure 2-7. Typical incremental air sampler station, DB-592.

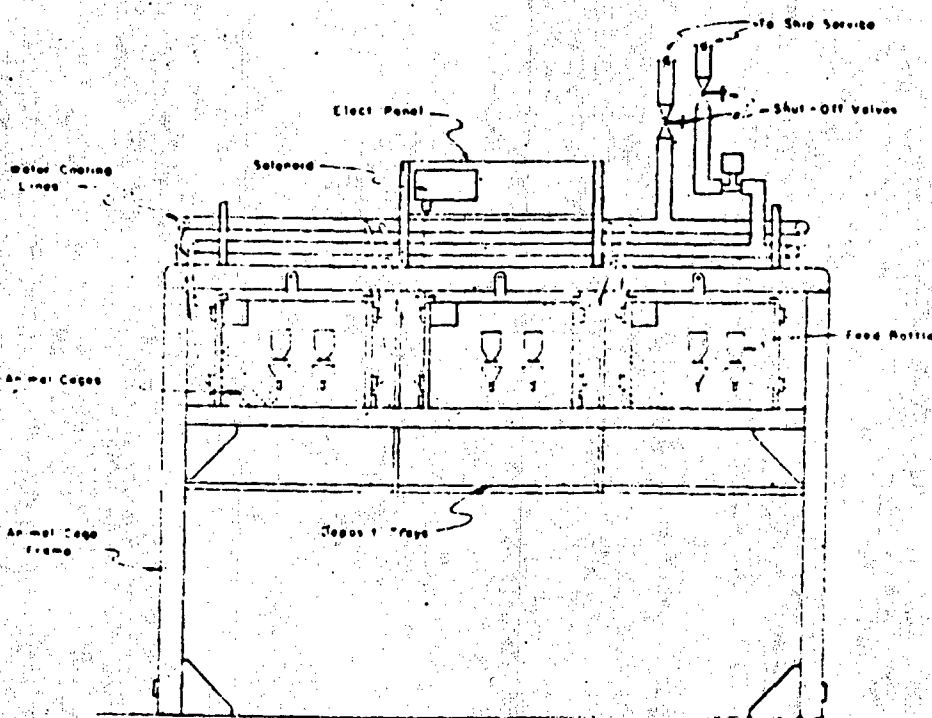


Figure 2-5. Typical animal station, DD-542.

CONFIDENTIAL

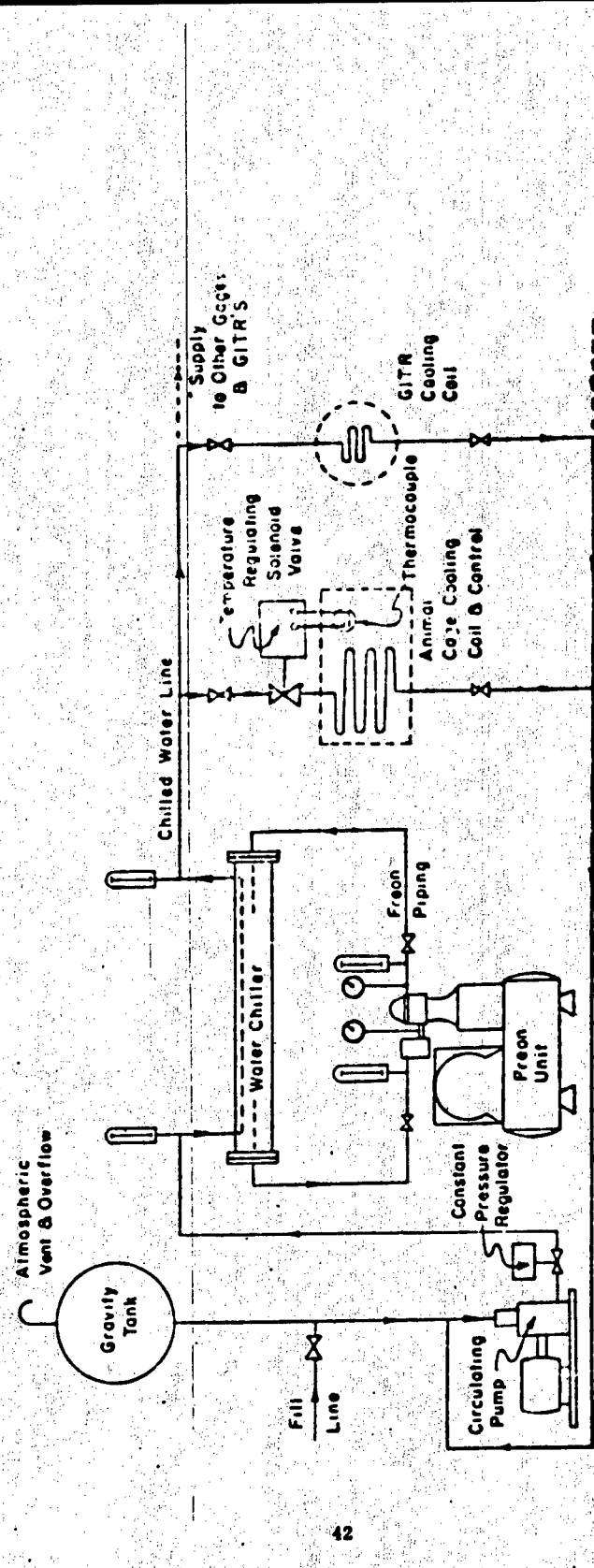


Figure 2-9 Cooling system on DD-592.

CONFIDENTIAL

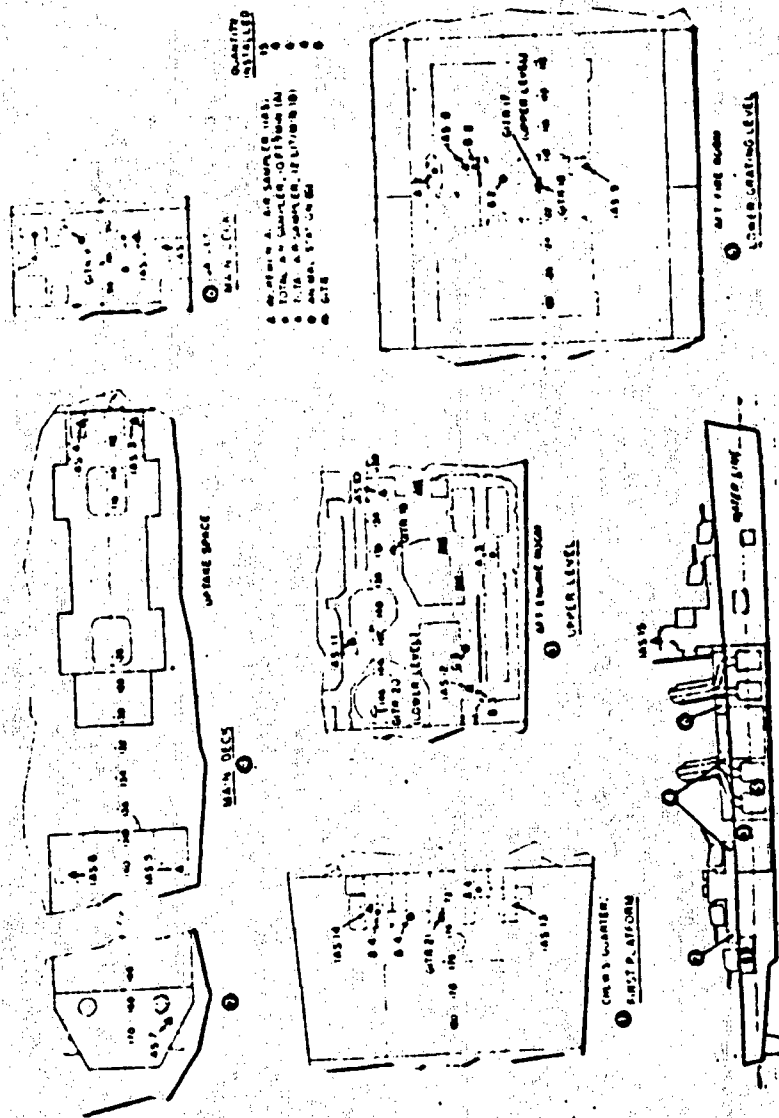
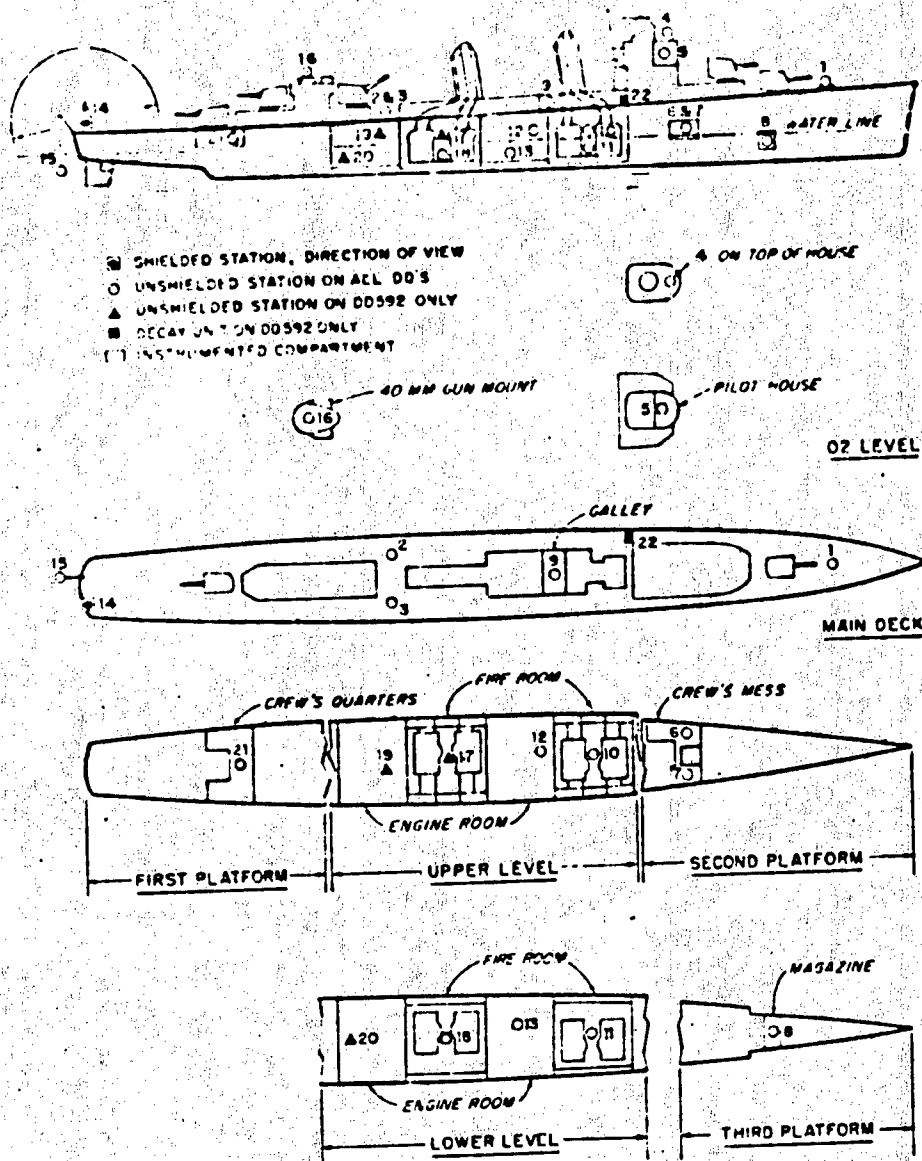


Figure 2.10 Instrument locations on B11-B12.

CONFIDENTIAL



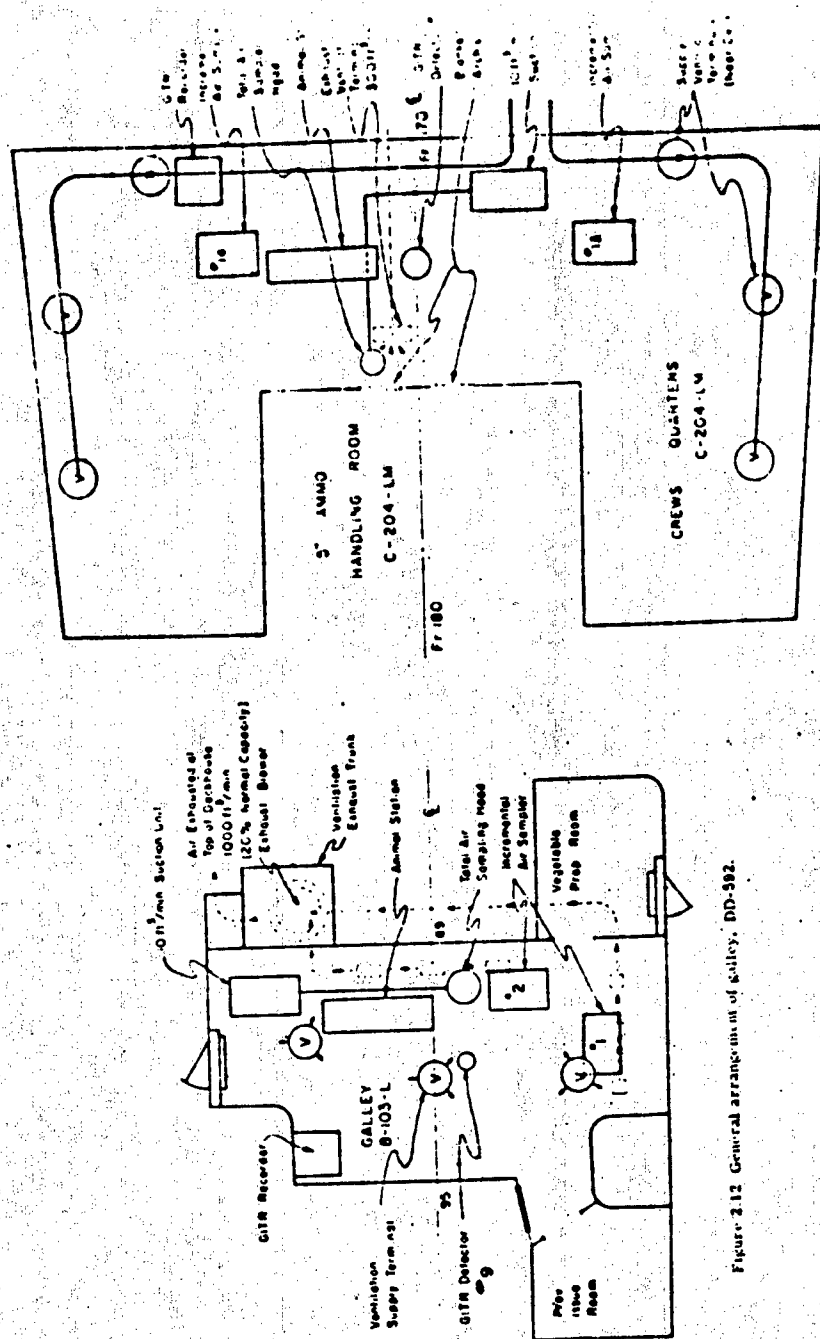


Figure 2.12. General arrangement of Valley, DD-382.

Figure 2.13 General arrangement of cross quarters, DD-393.

CONFIDENTIAL

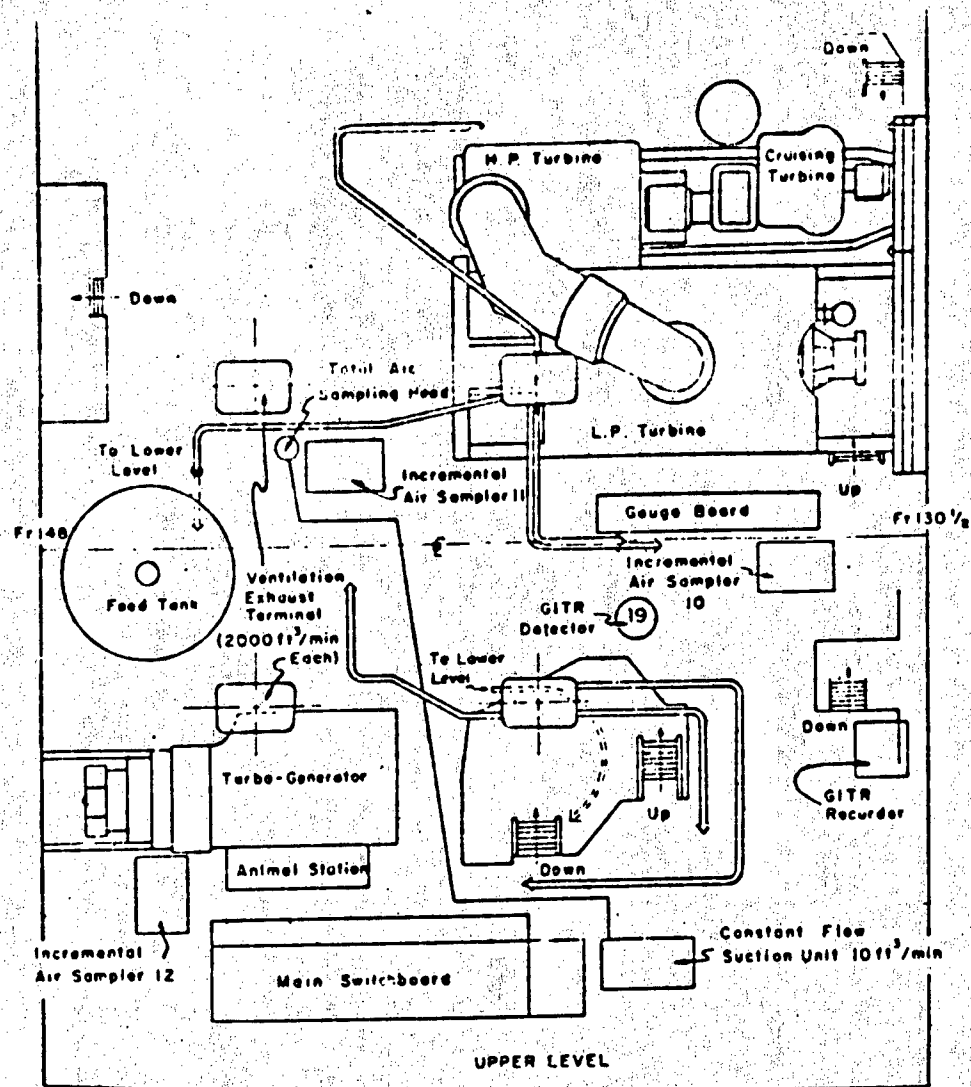
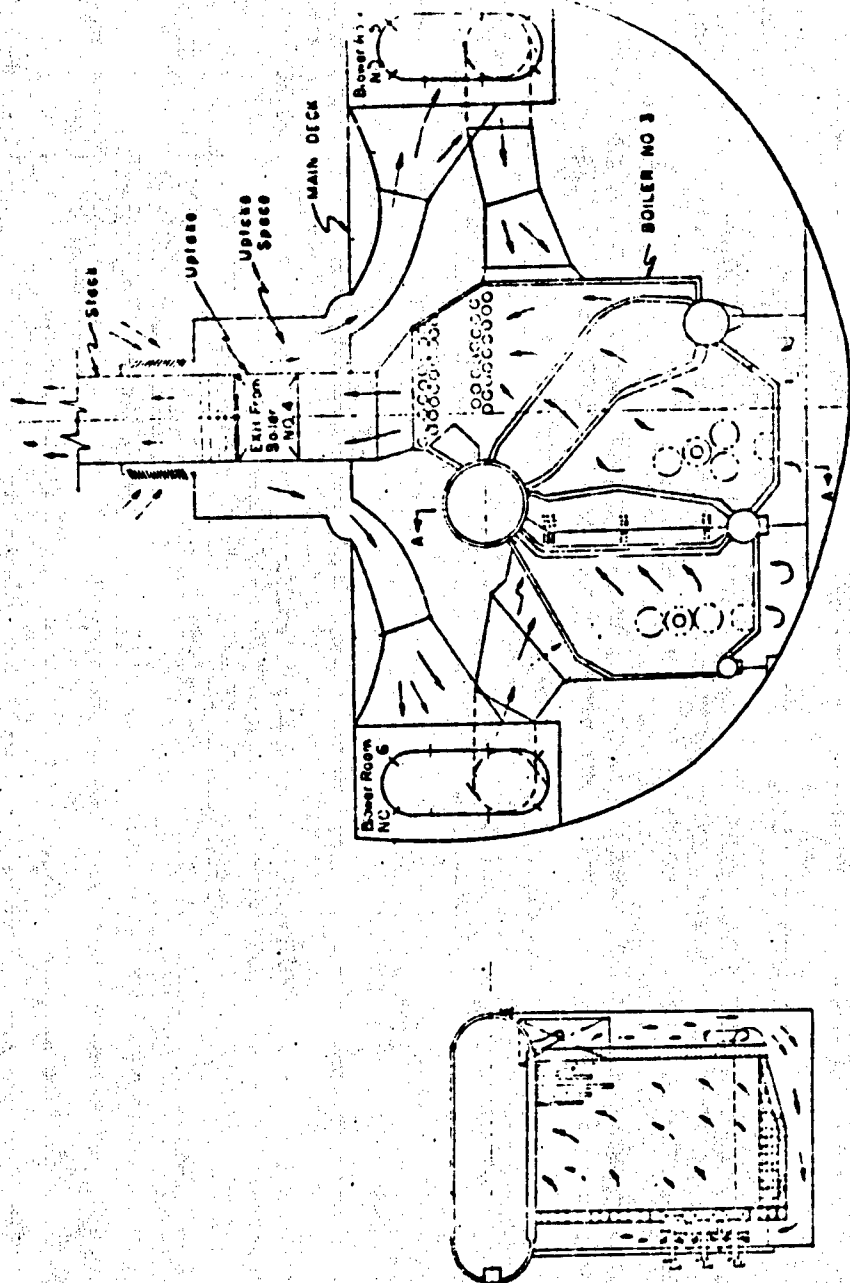


Figure 2.14 General arrangement of after engine room.



EECTICIN TURMUS : OMAARD

Figure 2.15 Boiler combustion air system, Boiler No. 3, BP-592.

CONFIDENTIAL

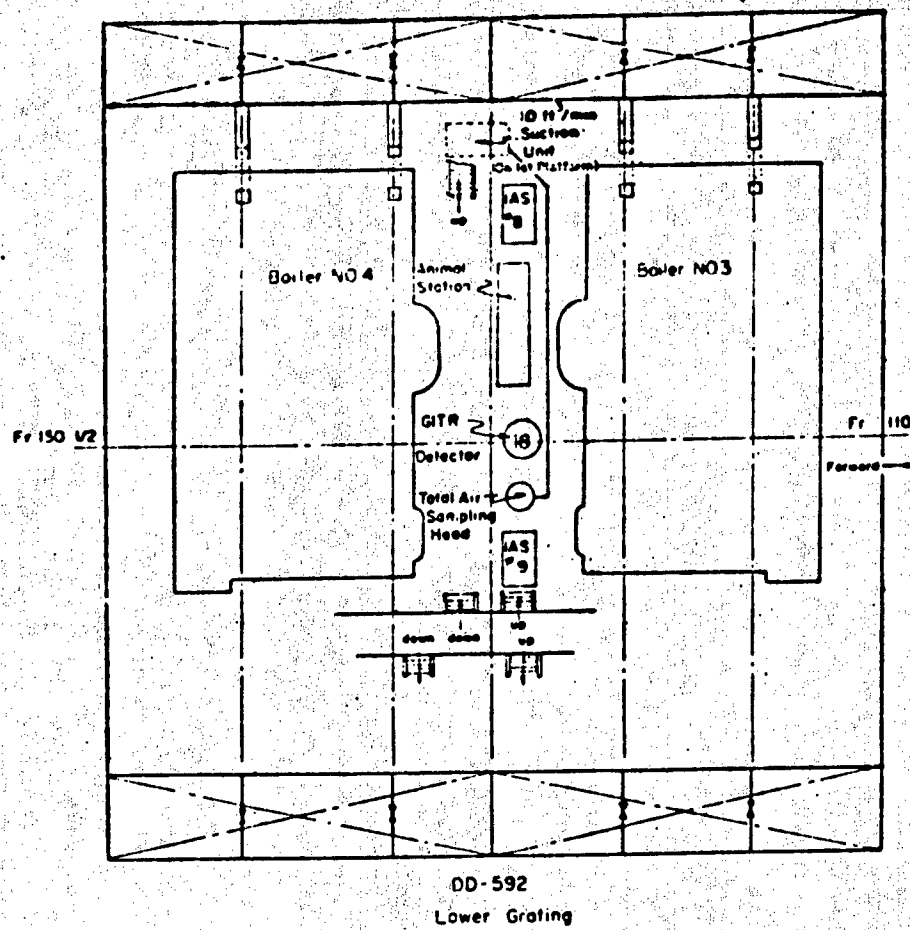


Figure 2.16 General arrangement of after fireroom.

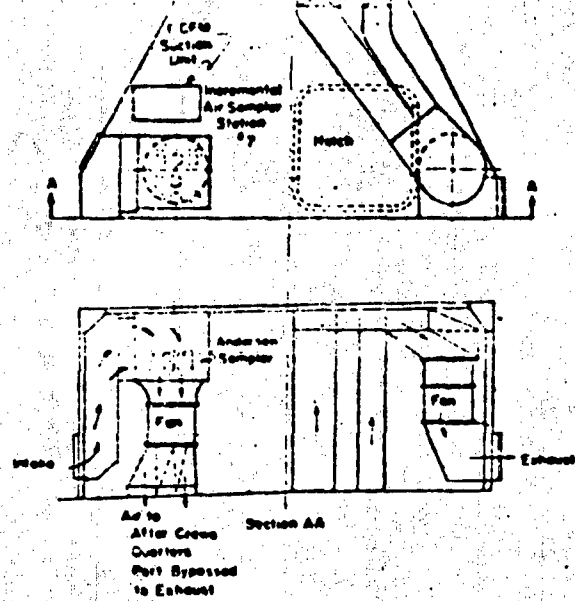


Figure 2.17 General arrangement of fan space, DD-592.

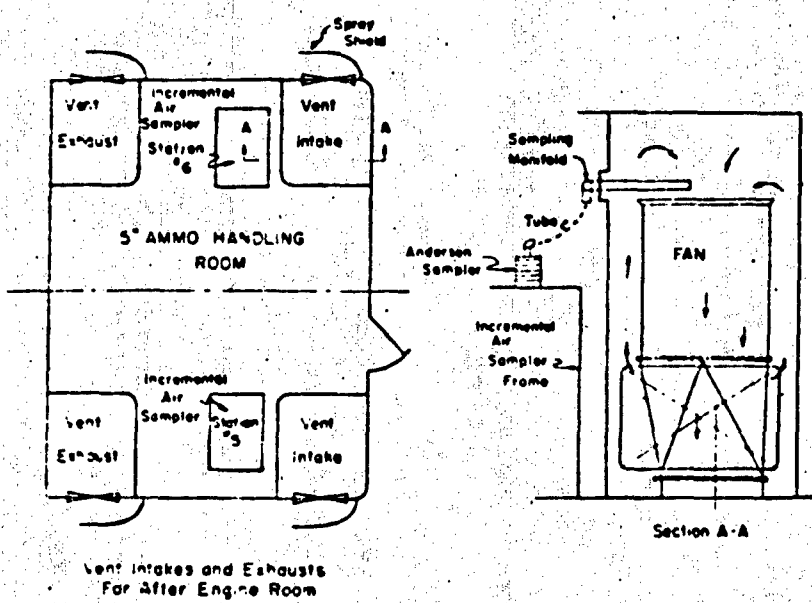


Figure 2.18 General arrangement, 5-inch-ammo handling room, schematic, DD-592.

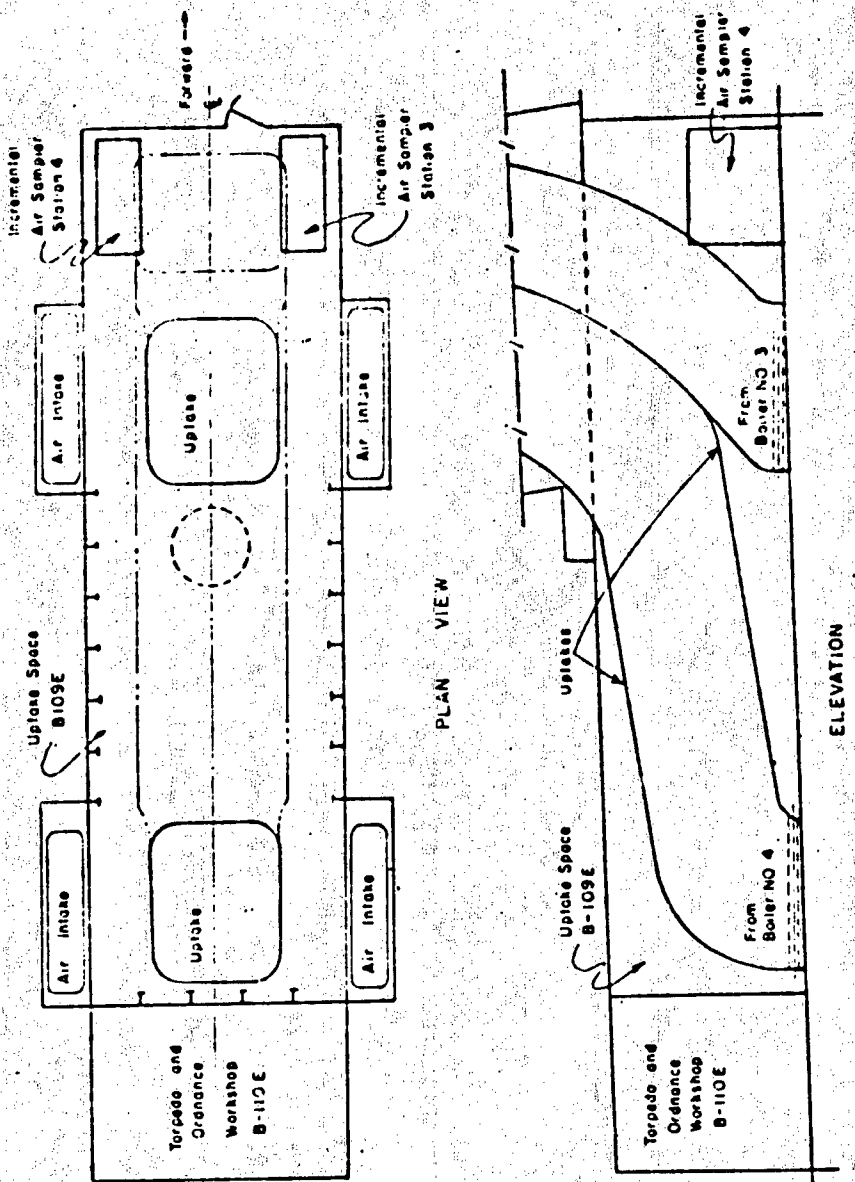


Figure 2.19 Update aspects. DD-592

CONFIDENTIAL

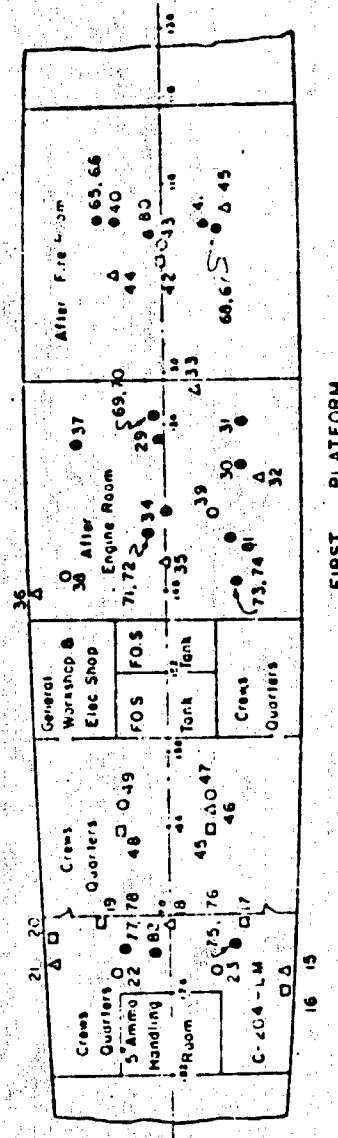
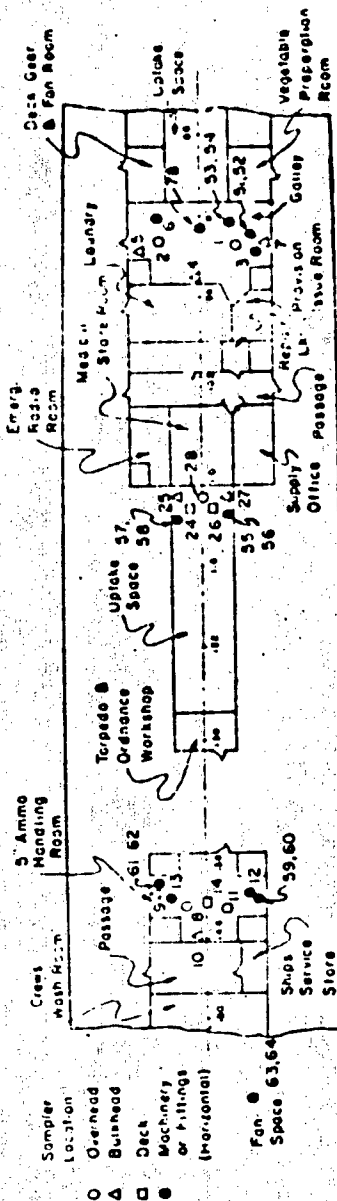


Figure 2-20. Surface sample locations. Sample numbers shown are for Shot Wahoo. Add 100 to each sample number for Shot Untrellis.

CONFIDENTIAL

Chapter 3

RESULTS AND DISCUSSION

During Shots Wahoo and Umbrella, there were power failures on the DD-592 and also some deviation from the designed test conditions.

During Shot Wahoo, GITR's and air samplers were not in operation nor were ventilation fans running. Consequently airtight through ventilation test spaces is unknown. Test conditions in the fireroom were as designed. Main deck test spaces had approximately 4 inches of water on deck. All test intervals in the galley were prior to recovery at H + 24 hours. In this space, the temperature exceeded 110° F and was estimated to be near 120° F. Temperature in the after crews quarters was constant at 76° F and in the after fireroom at 86° to 87° F.

During Shot Umbrella, a short in the air sampler timing circuit resulted in the collection of 2-hour air samples instead of a series of incremental samples. Only two GITR recorders were started by the radio starting relay at H - 6 minutes. All other GITR recorders were manually started based on a H - 3 hour radio voice signal. The poorer timing accuracy of a manual start several hours before shot time was considered a lesser risk than the possible loss of all data in case of a power or starting circuit failure. With these exceptions, test conditions and instrument operation were as designed. Recorded temperatures in test spaces were 82° to 84° F except in the galley where the temperature was 90° F. Relative humidities were about 90 percent.

Data was obtained principally for Shot Umbrella and, where not otherwise specified, results and discussions refer to the DD-592, Shot Umbrella. Before presenting estimates of external and internal doses, it is pertinent to present all information that is available with respect to the radiation environment as a function of time and to note those features that relate to the ingress of contaminants. (Throughout this report the terms "external" or "internal" will be used with reference to a person or animal, and the terms "exterior" or "interior" will be used with reference to a ship.)

3.1 RADIATION ENVIRONMENT, SHOT UMBRELLA

3.1.1 Total Gamma Radiation as a Function of Time. These results, as determined from GITR measurements on the DD-592, are given in Figures 3.1 through 3.10 for total gamma dose rates and in Figures 3.11 through 3.18 for total gamma doses. (The word "total" is used to indicate the combined contributions of all radiation sources that affect the radiation detectors.) These curves show the rapidly changing radiation environment for the instrumented areas of the ship. All of the dose rate curves have the same general shape, and similarly, all dose curves have the same general shape. An example of the rapid accumulation of dose can be seen from the weather deck data (Figure 3.11). Approximately 90 percent of the weather deck average dose was accumulated between H + 16 and H + 60 seconds. During this period, the maximum peak intensity (Figure 3.1) occurred at a nominal time of H + 30 seconds with near-peak intensities nearly constant from H + 30.5 to H + 33 seconds. Approximately 8 percent of the dose was accumulated from H + 190 to H + 600 seconds during the subsequent peak.

In Reference 13, it was estimated that transient radiation sources contributed more than 95.5 percent of the weather deck dose on the DD-592. No significant dose was accumulated after H + 10 minutes at the various deck locations. The probable sources contributing to the radiation after this time were deposited contaminants on the weather surfaces, within the ship.

the period between 10 and 100 minutes after Shot Umbrella was out, about 1/3 of the total dose received prior to this time period, and less than 1 r was received during the subsequent 24 hours.

At H + 2 hours, radiation readings at the rail of the recovery tug, during its approach to the DD-592 for sample recovery operations, were 40 to 60 mr/hr; and at H + 22 hours, during an approach for a second boarding, readings at the rail of an LCM were 20 mr/hr. From various observations, the ship was in contaminated water from sometime shortly after detonation to a time beyond the period covered by data available or of interest in this report.

The dose rate histories throughout the ship, while all generally similar because of the dominance of the exterior transient radiation sources, have distinctive characteristics which separate them into two groups—ingress and noningress compartments. During the period between major dose rate peaks at H + 120 to H + 140 seconds, the galley and after engine room dose rates are the highest aboard ship, respectively 1.8 and 3 times the average weather deck dose rates (Reference 10, compartment to deck dose rate ratios), whereas the fire room dose rates are 0.5 to 0.8 times the weather deck dose rates. At late times (after 2,000 seconds), the highest dose rates are found in the lower level of the forward fireroom, after fireroom, and galley, respectively: 2, 1.8, and 1.5 times the weather deck dose rates. At these times, the after engine room dose rates are but little higher than in noningress compartments.

This evidence is indicative of the presence of deposited activity in the galley and boilers or boiler air systems and a radioactive aerosol in the after engine room, which had been exhausted by ventilation airflow at later times.

No distinctive evidence of dose rate components due to the ingress of contaminants can be found in the crews quarters dose rate history. However, in the lower level of the forward engine room, a noningress compartment, there is evidence of a contribution to dose rate from an interior source that was not seen in the upper level. The high dose rates in the lower level between the major dose rate peaks suggest the possibility that radioactive material in the main circulating water (or deposited in condenser, pumps, or piping) may have been the principal radiation source at this location.

3.1.2 Estimates of Some Characteristics of the Enveloping Base Surge. In Reference 20, it was suggested that a correlation existed between the shipboard gamma radiation histories and the base surge transit. Aircraft photography data (Reference 20) shows the base surge to be toroidal in shape. During and after formation, the toroid expanded radially at high speed. It eventually reached a maximum diameter, after which it was windborne and moved downwind. The downwind segment of the base surge passed the DD-592 during its initial expansion and is presumed to contain the principal radiation source of the maximum dose rates measured aboard the ship. The passage of the initially upwind segment of the base surge, driven downwind by the 20-knot surface wind following the initial base surge expansion, is presumed to contain the principal radiation source of the subsequent and broader dose rate peak.

Several estimates of the transit time of the base surge can be made. Based upon visual observation from a tug at several miles from surface zero, the sample recovery party estimated that the DD-592 was engulfed in the base surge at H + 30 seconds and became visible through a haze at H + 6 minutes. The H + 30 second estimated time of start of envelopment coincides with the approximate time of the first major dose rate peak and the H + 6 minute time is in the middle of the subsequent dose rate peak. Turning again to Project 2.3 data (Reference 20), at H + 30 seconds the estimated speed of advance of the base surge is about 60 knots (100 feet per second) and the downwind toroidal section of the base surge is roughly estimated to be 1,200 feet from outer edge to inner edge. Based on these estimates, the DD-592 would have been enveloped for approximately 12 seconds. This, of course, assumes the absence of an invisible aerosol following the trailing edge of the base surge.

A second estimate is available from Project 2.1 data (Reference 18). If the base surge is considered as a semi-infinite radiation source at the instant of envelopment, an infinite source

11. In the dose rates at the beginning of envelopment and at $t = 0$, one would be half of the peak dose rate if radiological decay is eliminated. From the decay-corrected plot of the weather deck average dose rates, the times at which the dose rates are half of the maximum value are $H + 29$ and $H + 35$ seconds. If a fourth of the peak value were used instead of a half, assuming that the source was something less than semi-infinite, then the times would be $H + 28$ and $H + 40$ seconds.

Similar treatment would place the time of envelopment by the initially upwind segment of the base surge at $H + 285$ and $H + 435$ seconds, respectively. This segment of the base surge was greatly dispersed and diluted at this time compared to the downwind segment at the time of its passage over and around the DD-592.

Project 2.3 had two types of collectors on the gun director platform of the DD-592, which yielded time-dependent information (Reference 20). Their incremental fallout collectors (IC) and air filtration instrument (AFI) obtained 1-minute and 2-minute incremental samples, respectively, at $H + 1$ to $H + 2$ minute IC samples and the 2 to $H + 2$ minute AFI sample contained more radioactivity than subsequent samples (all corrected for decay to a common time) by an approximate factor of 30 for starboard IC, 15 for port IC, and 8 for AFI. The $H + 2$ minute AFI sample included sea water in such quantity as would be delivered by a heavy rain. To review and summarize: it is estimated that the DD-592 was enveloped by the base surge sometime between $H + 28$ and $H + 30$ seconds and emerged from envelopment at about $H + 40$ seconds. At $H + 30$ seconds, the base surge was moving at an estimated speed of about 60 knots, and during or immediately subsequent to the envelopment, there was probably a heavy rainfall of sea water. Fallout collections were considerably greater during the period $H + 1$ to $H + 2$ minutes than during any equal subsequent time period.

At about $H + 285$ seconds, a second envelopment occurred because of the passage of the upwind segment of the base surge. This was windborne and therefore moving at the speed of the surface winds, about 20 knots. This envelopment ended at about $H + 435$ seconds. The outline of the ship was visible at about $H + 360$ seconds, an indication of the dispersed and dilute nature of this segment of the base surge at this time.

It seems most probable that radioactive aerosols were drawn or forced into open ventilation and boiler air systems in the greatest amounts during or immediately after passage of the visible base surge.

3.1.3 Air Sample Data. Results from the incremental air samplers are presented in Table 3.1 as total activity collected in each sampler and the percentage of this total that was found in the five stages of each sampler. The data was corrected for decay (Project 2.1 decay data) from time of counting to $H + 10$ minutes for comparison at a common time. The total air sample data is presented in Table 3.2, decay-corrected on the same basis as the incremental sample data, and also in terms of fissions as determined after return to NRD.

The activities of the total air samples and the adjacent incremental air samples are approximately proportional to their flow rates (10 to 1). In the crews quarters where they were not adjacent, the activity of the total air sample (taken in the center of the compartment near the exhaust terminal) was equal to the average of the port and starboard incremental air sample activities (corrected for differences in sampler flow rates).

The data from the incremental air sampler shows that 98 to 99 percent of the activity sampled was associated with particles equal to or less than 1 micron in size and hence readily airborne and respirable. The principal exception is the starboard side of the uptake space where approximately 15 percent of the activity was associated with particles greater than 1 micron in size.

Inspection of Table 3.1 reveals that starboard side ventilation intake and uptake space collections were all greater than port side collections and that within the galley the opposite is true. Considerations of airflow effects due to a 20-knot wind from starboard to port and the initial passage of the base surge at 60 knots when high concentrations of activity may have been

on the windward side of a structure and a low-pressure region to leeward. If it is assumed that sampling times were uniform (a reasonable assumption because the 20-knot wind would uniformly clear airborne material from the vicinity of the ship), then average activity concentrations for the time of sampling would be proportional to the total samples collected. The high- and low-pressure regions to starboard and port could cause differences in airborne concentrations, which are reflected by the differences in starboard and port total sample collections.

Similar circumstances apply to the galley ventilation. Here the starboard mushroom ventilation inlet may have been in the low-pressure region, which is created by a wind on top of a structure near the windward edge, thus delivering lower concentrations to the starboard side of the galley. This air current would have little opportunity for mixing with air from other inlets. A second possibility is that the starboard sampler was not in the principal airpath and, because of this, sampled relatively dilute concentrations of airborne material.

Total air delivery comes to us from the starboard side of the uptake space and from the interior port side. It is possible that those from the starboard ventilation inlets is this may be the result of low sampling efficiency, and also, in the case of the uptake space, the principal airpath may have bypassed the samplers.

In the engine room, the three samplers collected approximately equal amounts of activity. However, it seems unlikely that this was the result of uniform concentrations of activity but rather the effect of sampling different concentrations for compensating times of sampling. Sampler Number 10 sampled air delivered by the port supply system, and the total collection was approximately twice that of the intake sampler. Sampler Numbers 11 and 12 sampled air delivered by the starboard supply system, and sample activity collections were slightly higher than for the intake sample.

The activity in the crew's quarters air samples (Stations 13 and 14) were much less than the activity in the intake air sample (Station 7). This difference might be due to a combination of the following: (1) dilution due to mixing with clean air in the compartment, (2) a short sampling time period due to the diffused shape of the volume of contaminated air carried past the air sampler, and (3) loss of airborne activity due to deposition in ducts and/or compartment.

An inspection of the ventilated compartment airflow characteristics given in Table 2.2 indicates that radioactive material would be introduced into test compartments from immediately to within 5 to 10 seconds after it was available at ventilation intake openings. The estimated times of visibility for the highest concentrations are short with respect to the time to change air in a compartment; hence, the volume of such activity concentrations is some fraction of the total room volume. The short time of introduction, the small volumes with respect to room volumes, and the delivery of these total volumes as smaller volumes by the ventilation distribution systems at varying distances from exhaust terminals would lead to the conclusion that there was little opportunity for uniform activity concentrations throughout a test compartment. It seems most probable that samplers were sampling discrete volumes of contaminated air, and that there was little opportunity for mixing except near the exhaust terminals. If samplers did sample discrete volumes of contaminated air, it is probable that the contaminated air contributed to the dose rates in the compartment for a time period both before and after the sampling period. In this case, a sample collection is something less than necessary for conversion to dose rates and may compensate to some unknown degree for the assumption of uniform distribution of radioactive material, which should provide an overestimate of dose rates.

3.1.4 Surface Sample Data. The data is presented in Table 3.3 as the count rate at the time of counting. The uptake space, galley, and compartment housing the trunk for the ventilator intake to the crew's quarters were locations for which the highest sample counts were obtained. Although the surface samplers represent a very small sampling of the total surface in each compartment, they are adequate to show the localized nature of deposition. In all spaces except the uptake space, the samples showing significant deposition were located on obstructions or fittings such as air sampler frames. The data indicates little deposition on decks or bulkheads except in the uptake space.

over, leakage from ventilator trunks, or air sample exhaust. Ventilator trunks were normally under negative pressure due to induced flow, and leakage from these trunks could only have occurred if pressures were raised by wind or base surge passage. The source of these activity collections cannot be determined.

3.2 EXTERNAL IRRADIATION

3.2.1 Estimates of External Radiation Doses Due to the Ingress of Contaminants, Based on GITR Data. All DIP-502 GITR dose rates were corrected for decay (decay factors used are given in Appendix B) to r/hr at $H = 30$ seconds. Stations 2 and 3 were used for exterior dose rates, because these stations are in the same section of the ship as the ingress test compartment(s). However these detectors were saturated prior to $H = 50$ seconds. The synthesized storage reactor deck dose rates were used for this period.

The dose rates at the stations 2 and 3 and for stations 6 and 7 were averaged to represent dose rates for ship outline locations in their respective area or compartment. Decay-corrected dose rates for the average of stations 2 and 3 and the average of stations 6 and 7 are shown in Figures 3.19 and 3.20. Figure 3.21 shows all of the noningress compartment decay-corrected dose rates normalized to the average of stations 2 and 3 at 360 seconds. This time was selected for normalization, because it is the time of maximum dose rates during the second envelopment at nearly all of the stations on the ship. Figure 3.21 shows on a comparative basis those dose rates that are available for use in the normalizing technique described in Section 1.3.1 for estimating dose rates due to ingress. Numerous attempts at using this technique demonstrated that the period prior to $t = 50$ or 60 seconds was the most sensitive in dose determinations, and in Figure 3.21 it will be noted that the averages for stations 2 and 3 and stations 6 and 7 represent the extreme range of noningress dose rates during this period. As previously indicated for station 13, the lower level of the forward engine room, the presence of a local radiation source is apparent starting at $t = 60$ seconds and eliminates this station for use in the normalization technique.

The averages for Stations 2 and 3 and Stations 6 and 7 were normalized to the total ingress-compartment data, as explained below, to simulate the decay-corrected dose rates, which would have been observed had there been no ingress of contaminants into the ship. Figures 3.22 through 3.29 show such noningress curves and also the total decay-corrected dose rates in various compartments.

The successive steps in determining the normalization factor assume that the decay-corrected in excess dose rates, i.e., the difference between the total decay-corrected dose rate and the normalized decay-corrected noningress dose rate in the compartment, were the same at 300 seconds and 320 seconds when the averages of Stations 2 and 3 were used as normalized decay-corrected in excess dose rates, and that decay-corrected in excess dose rates were the same at 300 and 320 seconds when the averages of Stations 6 and 7 were used as normalized decay-corrected in excess dose rates. Normalization factors determined by successive approximations to π_0 if these assumptions are given in Table 3.4. Average decay-corrected dose rates for Stations 2 and 3 and 6 and 7 were multiplied by the appropriate normalization factor to obtain normalized decay-corrected dose rates, which, when subtracted from the observed ingress compartment data, leave remainders that are the derived estimates of decay-corrected dose rates due to ingress.

As is evident from Figure 3.21, the use of Stations 2 and 3 and 6 and 7 for these normalizations should result in the widest range of decay-corrected ingress dose rate estimates to be derived from the available data. Curves of these two sets of estimated decay-corrected ingress dose rates are presented in Figures 3.30 through 3.37. Note that numerous instances of negative dose rates are found. This result must be accepted as one of the inaccuracies in using the

CONFIDENTIAL

1.4.2. The dose rates estimated for the machinery spaces are relatively constant without imposing a severe bias for which there is no rationale in the selection of a normalization factor.

As expected, the best agreement between the two sets of estimated dose rates and the fewest negative values are found in the best shielded compartments—the lower level of the machinery spaces.

Decay-corrected ingress dose rates are all relatively constant by H + 1 hour, the end of most of the available data. At this time, it is assumed that these dose rates are principally due to activity deposited as the result of ingress. Lacking any data, it was assumed that this activity was deposited prior to H + 60 seconds and that the buildup occurred between H + 30 and H + 60 seconds. The dotted lines in Figures 3.30 through 3.37 represent approximations of the decay-corrected dose rates due to deposited activity based on the above assumptions. Single values were obtained for the machinery spaces, but in the valley, the upper dotted line was derived from the upper set of stations based on the normalization for Stations 6 and 7 and the lower curve from the lower set of stations based on the normalization for Stations 2 and 7. The opposite is true for the crews quarters.

Decay-corrected dose rate curves provide little additional information on the times of beginning and end of ingress or envelopments. They appear to confirm the initial time as being between H + 28 and H + 30 seconds, and that the highest concentrations of activity were associated with the base surge front. All curves break at about H + 60 seconds, and at this time the influence of local radiation sources are apparent. Ingress decay-corrected dose rates all reach a minimum at H + 220 seconds prior to the second development and, as assumed by Project 2.1, this envelopment appears to have ended not later than H + 600 seconds. At about H + 1,200 seconds, an intense radiation source was off the starboard bow or beam, presumably waterborne and perhaps a patch of foam as discussed in Reference 20, and contributed most heavily to dose rates in the starboard side of the crews mess, starboard weather deck, and the weather deck bow station. Although all of these peaks are not shown, the peak decay-corrected dose rate was about equal to the maximum decay-corrected dose rate at these stations during the second envelopment.

The decay-corrected dose rates estimated to be due to the ingress of contaminants (both total and due only to deposited activity, Figures 3.30 through 3.37) were divided by the decay factors given in Appendix B to obtain estimates of the dose rates due to ingress. These dose rate estimates (including negative values) were numerically integrated to give dose estimates which are presented in Table 3.5. Regardless of the uncertainties and the wide range of these estimates, it is to be noted that a large portion of each dose was accumulated prior to the second envelopment. Some of the differences between the dose estimates at each location may be due to radiation from adjacent ingress spaces. Stations 6 and 7 were remote from all ingress sources, whereas Stations 2 and 3 were above the after fireroom and near the after uptake space. However, this rationalization cannot be applied to the dose estimates for the crews quarters, because this compartment was not near any of the other ingress test compartments.

3.2.2 Estimates of External Gamma Radiation Dose Due to Airborne Activity and Airborne Activity Concentrations Within Test Compartments, Based on Air Sample Data The estimates of GFR-based decay-corrected dose rates due to the ingress of contaminants are too indeterminate to be used to apportion the air sample collections as a function of time. Therefore, it was assumed that: (1) at H + 30 seconds, there was an instantaneous influx and diffusion of airborne activity, which was uniformly distributed throughout the test space; and (2), airborne activity concentrations due to ingress were reduced thereafter only by the effects of dilution, convection, and radioactive decay, reflecting all subsequent ingress.

A determination of the number of fissions for each total air sample was made at NRDI after completion of the field work, because the total air samples were the only ones whose activity at this late time was high enough for counting purposes. To determine the number of fissions per sample, a Project 2.3 sample, AOC 592 FUM (Reference 20), was used as the reference.

tokens at 1 minute and 15 minutes of 10 samples determined for the sample. The sample was counted and a fission-to-count-rate ratio was determined. The total air samples were counted in the same counter, and using the above-mentioned relation of fissions to count rate (correcting for decay), the total air sample count rates were converted to fissions and are given in Table 3.2. The collection of these numbers of fissions as a function of time was determined and converted to dose rates and airborne concentrations using Equations 1.2, 1.3, and 1.4 as appropriate. The estimated dose rates and concentrations for the first 10 minutes after shot are given in Tables 3.6 through 3.9. Doses estimated from these dose rates are presented in Table 3.10 (omitting the fireroom, because this dose estimate was too low to be significant). For the fireroom, it was assumed that radioactivity from boiler casing leakage was introduced into the fireroom at H + 30 seconds and remained throughout the sampling period. The air sample then represents a collection at a constant rate (constant concentration) for the total sampling period of 120 minutes. The compartment had been sealed, and no basis for estimating airflow characteristics was available.

3.2.3 Estimates of External Radiation Dose Due to Deposited Activity Within Test Compartments. To estimate the dose rates due to deposited activity, the highest surface sample count rate for the film slide collectors in each compartment was used as the count rate for both the decks and the bulkheads in the compartment (all bulkhead count rates were below background at time of counting). These count rates were substituted in Equation 1.5, and the H + 10 minute dose rates so estimated are presented in Table 3.11. Comparison with the dose rates estimated for airborne contaminants at H + 10 minutes in Tables 3.6, 3.7, and 3.9 show that only in the galley could deposited activity be considered significant.

The dose rate estimated for the galley at H + 2 minutes from Table 3.11 was corrected for decay to obtain estimates of dose rates from H + 1 to H + 10 minutes and at H + 120 minutes assuming all material deposited by H + 1 minute. (Decay data from Reference 19 was utilized for the time period H + 6 to H + 10 minutes and extrapolated (a slope of about -1.8) for H + 30 seconds to H + 6 minutes.) The dose rate estimates and the dose to H + 10 minutes are presented in Table 3.12.

3.2.4 Summary of External Gamma Dose Estimates Due to the Ingress of Contaminants. The total gamma dose measured in each test compartment and the various estimated gamma doses due to the ingress of contaminants are presented in Table 3.13; film badge doses are 24-hour doses (Reference 18), GITR doses vary from approximately 1- to 2-hour doses. The ingress dose estimates are round figures, adequate to represent these estimates for 1 to 24 hours. The uncertainties inherent in the basic data and in the assumptions and approximations used in the estimating techniques have resulted in a wide range of values for the ingress dose estimates at each location.

Comparison of the forward and after fireroom ingress dose estimates indicates that full-power operation of a boiler would result in higher dose estimates than those presented here, because combustion effects would cause greater deposition of material than for either of the two conditions in these tests. During the tests, the operating boiler was fired with diesel oil to achieve unmanned operational reliability. The use of regular boiler fuel would result in greater soot deposits and therefore also increase the probability of larger deposits of radioactive material. No estimate of the magnitude of these effects can be made, but it is most probable that an increase in dose would result.

Comparison of ingress dose estimates and total doses indicates that even the highest ingress dose estimates are only a half to a third of the total dose for the best and least shielded compartments respectively. The relative importance of the ingress dose is therefore a function of the shielding provided by the ship's structure. For a destroyer operating under the circumstances encountered in these tests then, even the maximum ingress dose estimates are secondary to the high doses which were measured in lightly shielded compartments.

Wahoo, consists of recovery party radiological survey dose rates and Project 2.1 film badge doses. The postshot survey readings for Shots Wahoo and Umbrella are presented in Table 3.14. Comparison of the Shot Wahoo data with the Shot Umbrella data (corrected for decay to H + 22 hours) gives an indication of the relative magnitudes of deposited radioactive material. In ingress test compartments, dose rates were at least 3 to 4 times higher and weather deck dose rates were generally about 10 times higher after Shot Wahoo than after Shot Umbrella.

Twenty-four-hour film badge doses (the average from all film badge arrays in each compartment) are presented in Table 3.15 for the DD-592 for both shots, together with the ratios of Wahoo doses to Umbrella doses. These ratios vary from 1.5 to 2.9 but reveal no information with respect to ingress.

In order to make some comparison of the effects of ingress, the film badge data has been utilized. Noningress controls—dose data from a compartment whose shielding approximates that in the ingress test compartments—were selected and their dose data subtracted from ingress compartment doses to obtain an estimate of the dose due to the ingress of contaminants. These dose estimates are presented in Table 3.16 for the DD-592, Shots Wahoo and Umbrella. Similar dose estimates for the forward fireroom (in operation and instrumented with film badges and GITR's) are presented in Table 3.17. Considering the uncertainty in these estimates, it would appear that, for Shot Umbrella, there is a decrease in ingress dose with distance from surface zero; for Shot Wahoo, there is a decrease from the DD-474 to the DD-592; but both the DD-592 and DD-593 ingress doses are approximately equal to or greater than those for the DD-592, after Shot Umbrella.

The magnitude of the dose in the fireroom, DD-593, after Shot Wahoo is evident in data presented by Project 2.1 (Reference 18). During the period after the ship emerged from envelopment by the base surge or cloud and prior to the time that the ship presumably became surrounded by contaminated water, i.e., between 17 and 50 minutes after Shot Wahoo, the dose rates in the fireroom were on the order of 10 times higher than dose rates on the washed weather decks and about 100 times higher than the dose rates in the adjacent engine room. The fireroom dose rates approximate decay during this period and appear conclusively to be due to deposited radioactive material in the boiler or boiler air system. The dose for this period, approximately 35 minutes, was 5 r. The dose for the equivalent period in the fireroom of the DD-592 after Shot Umbrella was 1.6 r. The dose in all other compartments of the DD-593 for this period was less than 1 r.

After Shot Umbrella, when the ships had emerged from envelopment, the fireroom dose rates were 1.5 and 8.5 times the average weather deck dose rates for the DD-474 and DD-593, respectively.

The locations of the three ships for Wahoo were: DD-474, 2,900 feet; DD-592, 4,800 feet; and DD-593, 8,900 feet downward from surface zero. For Umbrella, the locations were: DD-474, 1,000 feet; DD-592, 3,000 feet; and DD-593, 7,900 feet downward from surface zero.

The dose estimates for the firerooms are for 1-boiler operation. Realistic operating conditions would include operation of both boilers at full power and with ventilation systems open. For these conditions, the fireroom external ingress dose would be more than twice the dose estimated for 1-boiler operation and sealed ventilation openings.

3.3 ANIMAL TISSUE DOSE

Complete total-body radioactivity curves for the platform animals were constructed from the field and laboratory curves (Figures 3.38 through 3.41). These have shapes typical of the curves for all test animals. Turnover curves were similarly developed for individual organs: gastrointestinal (GI) tract, liver, thyroid (Shot Umbrella only), skeleton (as represented by the tibia), and respiratory tract. The individual organ turnover curves for the guinea pig and mouse tissues are shown in Figures 3.42 through 3.45. Total tissue activity was calculated by

first week, 12.5% on the second, and 16.0% on the third week. The dose to the whole body is presented in Table 3-18 and individual organ doses are presented in Tables 3-19 through 3-23. Of these organs, the GI tract, the skeleton, and the thyroid may be considered critical radiosensitive organs. A critical organ may be defined as: (1) an organ with the greatest accumulation of radioactive material, (2) an organ that is essential or indispensable to the well being of the whole animal, or (3) an organ that can be damaged with a low dose (Reference 3).

3.3.1 Internal Dose to Animals—General Trends. Inspection of both the whole-body (Table 3-18) and individual organ dose (Tables 3-19 through 3-23) reveals that the predominant dose from internal contamination is accumulated during the early exposure period (0 to 50 hours). The only long-term exposure dose of importance is the dose resulting from the exposure for 0 to 7 days, a major part of which was accumulated during the early period. After the third week, the activity level was essentially background.

The dose to the liver is lower than the dose to certain critical organs—GI tract, thyroid, and skeleton (bone marrow). The higher activity of these critical organs is diluted by tissues containing low levels of radioactivity, primarily muscles and connective tissues.

Among the various organs listed in the dose tables, the skeleton (which contains the marrow), GI tract, and thyroid are the most sensitive to internal contamination. The liver contains less contaminants and, in addition, is the least radiosensitive of the organs analyzed in this study. The tibia of the animals from the test compartments generally received the highest dose and the liver the least. Of the director platform animals, either the GI tract or respiratory tract doses were equal to or greater than the tibia dose. It will also be noted that in nearly all cases, the dose to the GI tract is greater than the dose to the respiratory tract. This suggests that the main pathway by which the activity enters the blood is by intestinal absorption rather than from the lung alveoli. This concept is supported by experimental investigation where it was found that animals exposed to young fission products showed a rapid uptake and a rapid decline in activity. Buildup of activity in the GI tract coincided with the decline of activity in the lungs (Reference 16).

Finally, it will be noted that the doses to the mice are higher than those to the guinea pigs. However, this general discrepancy can be explained by the difference in tidal volume of required air, as will be demonstrated presently.

3.3.2 Estimates of Internal Dose to Man. As previously stated, the guinea pig was chosen for this study because its alveolar retention of 1-micron-size particulates is quantitatively similar to that of man. However, the results of the studies of the individual organs of the animals used during Shots Wahoo and Umbrella indicated that, in nearly all cases, the main portal of entry of the radioactivity was probably the intestine rather than the lungs. Initially, the animal inhaled the airborne radioactivity into the nasal and oral cavities. The inhaled activity can either be caught or settle out on the walls of these cavities or continue moving in the trachea down toward the bronchi. The activity that cannot penetrate the alveoli is largely caught by the mucus of these membranes and by means of theiliary action of the epithelium of this part of the respiratory system swept up into the pharynx and subsequently swallowed. The transient time of radioactivity in the lungs was very short, with a great part of the activity going in and out of the lungs well within 1 hour (Reference 16). Once in the GI tract, the amount of radioactivity absorbed into the circulatory system depends upon the solubility of the material ingested and whether or not the soluble material can penetrate the intestinal wall. Thus, the amount of soluble and penetrable material present in the GI tract determines the degree of internal contamination (References 22 and 23). This is equally true for man, guinea pig, and mouse, because the physiological mechanisms of each is similar.

Thus, the degree of internal contamination is dependent upon the volume of contaminated air circulated in and out of the nasal, oral, and upper respiratory systems. The volumes of air

was estimated by taking one-sixth of the mouse dose values and one-half of the guinea pig dose values. The results of these calculations for the individual organ doses for the early period (0 to 50 hours) and the significant long-term period (0 to 7 days) are presented in Tables 3.24 and 3.25. Estimated doses for man derived from the guinea pig and mouse data are in close agreement. This can be taken as supporting evidence for the theory that the inhaled volume of air per minute per gram of tissue is an important determinant of the internal contamination in the animals studied. The differences that do exist between doses to man, calculated from the mouse and guinea pig data, may have been due in part to the varying amounts of self-licking by these animals (although the skins of these animals were not included in any of the calculations, they were found to be highly contaminated with radioactivity).

3.3.3 Assessment of the Internal Hazard to Man: Whole-Body Dose versus Dose to Critical Organ. Radiation syndrome and effective dose are based on consideration of the whole animal. Dose to the whole animal, however, is not a direct measure of white blood cells. The effects of 50 r to a given organ cannot be described in terms of white blood cell level. Similarly, such descriptions as "generalized malaise, erythema and vomiting" for other whole-body doses would be meaningless when applied to individual organs such as the bone marrow, GI tract, and thyroid. Thus, in considering the effects of an early dose (whether it be external or internal) that would lead to an immediate biological effect discernible as radiation syndrome, the dose to the whole body is more meaningful.

However, as expected, the data indicates that the radioactivity is concentrated in certain organs and that some of these organs are considerably more radiosensitive than others. Thus, the use of the dose to the whole body (total radioactivity divided by the whole-body weight) to determine the early radiation syndrome would ignore the fact that certain highly radiosensitive organs, i.e., critical organs, are absorbing a greater part of the absorbed energy.

This problem can be resolved by treating the dose absorbed by the critical organ as if it were the dose to the whole body, i.e., a dose of 50 r to the skeleton then would be considered as a dose of 50 r to the whole body. In this way, the hazard would be overestimated, allowing a safety factor to be incorporated into the calculated values.

Internal Dose to Man, Calculated on the Basis of Critical Organs. Prior to the consideration of the internal dose, it should be noted that adequate shielding would be necessary to reduce the external gamma doses, which range from 1,130 to 51 r for Wahoo and 549 to 22 r for Umbrella, before ingress external or internal body exposures would be limiting factors in operational conditions. However, it is with this ingress radioactivity, which can irradiate personnel from the outside or, when absorbed into the body, irradiate an internal emitter, that the present study is concerned.

The results of the conversion of animal dose to dose to man, are given in Tables 3.24 and 3.25. Several doses on the director platform exceeded 25 to 50 rads, the dose level that would result in first signs of hematologic changes. The highest value, 174 rads, would not result in any deaths, but generalized malaise, changes in blood picture, and vomiting could result. However, these internal doses were not a result of ingress radioactivity but were due to local fallout and probably water of the base surge.

3.4 CORRELATION OF AIR SAMPLE AND ANIMAL DATA

The data obtained was inadequate to provide any true correlation between air sample and animal data. The only evidence that such a correlation might be possible is presented in Table 3.26. Early whole-body internal doses have approximately the same relation to each other as do the adjacent air sample activities for the various test compartments. Director platform data does not follow this general trend, indicating a severe bias between animal and air sampling. Animals and air samples were located on opposite sides of the platform and may have

CONFIDENTIAL

sampled, the sample air velocity was assumed to be greater than sampling intake velocities. Animal self-licking is a possible source of bias in the animal data.

To utilize the air sample data as measurements related to internal dose, the air sample activity was converted to average microcuries per unit volume of air samples, based on several assumptions. These average concentrations are also presented in Table 3.26, and it will be noted that there is no correlation with animal doses, an indication that the assumptions were inadequate for the purpose of determining an average concentration.

3.5 SUMMARY

3.5.1 External and Internal Doses. Estimates of external and internal doses due to the ingress of contaminants on the DD-592 are presented in Table 3.27. The estimates of external dose resulted in a wide range of values (and quite a bit of uncertainty). For each ventilated compartment, the lower external dose estimates (0.5 to 2 r) represent less than 1 percent of the total dose, and in the firerooms (3 to 4 r) about 3 and 15 percent of the total dose. The higher dose estimates for a fireroom (15 r) and ventilated engine room (31 r) represent approximately 50 percent of the total dose in these compartments. Note that for full-power 2-boiler operation, with ventilation systems open (a normal operating condition) the fireroom estimates should be multiplied by a factor of 2 or 3. The higher dose estimates for the two ventilated nonmachinery compartments, though quite unreliable, are less than 30 percent of the total dose in these lightly shielded compartments.

The external ingress dose estimates are for an exposure of 1 hour, but a large portion of these doses were accumulated during the first envelopment by the base surge after Shot Umbrella. The highest external doses due to ingress would result in a transient slight lowering of white blood cells in individuals exposed to these doses. However, exposures in this range would not cause any casualties or any reduction of combat effectiveness to personnel. The lower estimates of external dose and the absorbed dose in various critical organs would not cause any reduction in combat effectiveness, nor any major changes in hematology. Internal doses due to deposition of contaminants inside the body are for a 7-day exposure and generally are small compared to doses from external sources.

3.5.2 General Considerations. The doses due to transient exterior radiation sources reported by Projects 2.1 and 2.3 are considerably higher than the highest doses estimated to be due to the ingress of contaminants. The transit dose is, therefore, the dose of primary concern to a weapon-delivery ship, and reduction of this dose should be attempted. If this reduction is accomplished by maneuvering to avoid the base surge or cloud, then the ingress of contaminants should no longer require consideration. If the dose reduction is accomplished by shielding and the ship operates within the base surge or cloud, then the dose due to the ingress of contaminants could be the principal dose in some compartments. If the ship operates within the confines of the base surge or cloud without additional shielding, the relative contribution to the total dose by the ingress dose would determine whether reduction or elimination of the ingress dose should be attempted. In any case the internal dose will seldom, if ever, be significant with respect to other sources of dose delivery.

It seems probable that personnel on a weapon-delivery ship may suffer repeated exposures during a mission or consecutive missions and that some system of dose limits together with operational requirements will determine necessity and amount of shielding required to meet these limits. Such judgment would also require consideration of the dose due to the ingress of contaminants, particularly in the case of firerooms and compartments with high-capacity ventilation systems.

TABLE 3.1 DATA FROM INCREMENTAL AIR SAMPLERS, SHOT UMBRELLA

Location	Station	Total Counts/min Corrected for Decay to $H = 10$ Minutes	Percentage of Collected Activity in each Sampler Stage*			Millipore Filter†
			Stage 1†	Stage 2†	Stage 3†	
Galley			10^6 counts/min	per	per	per
Starboard	1	2.26	1.6	1.7	4.1	64.4
Center	2	7.31	0.6	0.6	1.0	14.7
After uptake space						
Starboard	3	5.39	10.1	3.0	2.9	17.7
Port	4	1.50	1.9	1.0	0.6	53.2
After engine room						
ventilation intakes						
Starboard	5	3.25	0.2	0.3	0.8	7.9
Port	6	5.45	0.1	0.2	0.6	6.7
After crews quarters						
ventilation intake	7	11.8	0.2	0.3	0.8	19.5
After fireroom						
Port	8	3.36	0.2	0.6	2.5	5.6
Starboard	9	4.43	0.2	0.8	1.4	13.3
After engine room						
Center, Forward	10	9.85	0.1	0.3	0.6	52.0
Starboard, After	11	9.31	0.1	0.3	0.6	6.5
Port, After	12	10.1	0.2	0.6	0.9	8.7
After crews quarters						
Starboard	13	1.86	0.0	0.2	0.8	9.4
Port	14	1.07	0.1	0.3	1.4	36.0
Director platform	15	5.05	0.2	0.3	1.0	6.4

* See Figure 2.5 for calibration curves of particle size retention in each sampler stage.

† Mean particle size retention (range): Stage 1 = 5.02 to 8.9 greater than microns, Stage 2 = 2.3 to 0.7 to 3.91 microns; Stage 3 = 1.2 (0.5 to 1.8) microns; Stage 4 = 0.7 (0.3 to 1.0) micron, Millipore filter collected particles that passed through previous four stages.

TABLE 3.2 DATA FROM TOTAL AIR SAMPLERS, SHOT UMBRELLA

Station	Total Activity Decay Corrected to $H = 10$ Minutes	Total Fissions	
		10^6 counts/min	10^{12} fission
Galley	7.83		7.90
After engine room	8.66		8.12
After fireroom	3.03		2.95
After crews quarters	1.19		1.54

TABLE 3.3 SUMMARY OF SURFACE SAMPLE DATA, SHOT UMBRELLA

All sample areas were 2 in.². All other surface samples showed no activity above background.

Sample Number	Location	Sample Count Rate 10 ³ counts/min	Time of Count After Umbrella	
			hr	hr
156	Galley	3.0	12.08	
151	Galley	1.43	12.80	
152	Galley	34.3	12.88	
107	Galley	14.3	12.92	
121	Uptake space	260.0	13.23	
126	Uptake space	1.7	13.29	
123	Uptake space	2.0	13.37	
127	Uptake space	47.5	13.39	
128	Uptake space	113.6	13.33	
136	Uptake space	29.8	12.93	
137	Uptake space	70.0	12.95	
112	Forward ammo handling room	4.9	12.98	
162	Compartment housing ventilator intake trunk to crews quarters	14.9	13.16	
164	Compartment housing ventilator intake trunk to crews quarters	12.0	13.16	
173	After engine room	0.8	13.00	
174	After engine room	1.63	13.00	
176	After crews quarters	1.0	13.38	

TABLE 3.4 NORMALIZATION FACTORS USED IN SIMULATION OF DECAY-CORRECTED NONINGRESS DOSE RATE DATA

See Section 3.2.1 for explanation.

Data of Station	Normalization Factor Applied to Averages	
	Stations 2 and 3	Stations 6 and 7
9	0.325	2.737
10	0.0887	0.364
11	0.0231	0.170
17	0.0103	0.550
18	0.035	0.189
19	0.143	0.749
20	0.0224	0.125
21	0.302	1.55

TABLE A5. ESTIMATES OF EXTERNAL GAMMA DOSE, BASED ON GTR DATA, DUE TO
INGRESS OF CONTAMINANTS, DD-392 SHOT UMBRELLA

Dose rate accumulated from 0 to 24 seconds to 80 times given below.

Compartment	GTR Station	60 Seconds	280 Seconds	10 Minutes	1 Hour	30 Days	2 Years
Galley	6	13.2	44.8	4.2	2.7	6.9	6.8
	7	51.6	80.2	70.8	77.9	74.7	74.6
	8	—	—	3.2 to 1.5	1.4 to 1.5	—	—
Forward fireroom (upper level)	10	1.9	6.9	1.9	3.2	1.1	4.5
	11	11.0	13.9	16.7	17.8	19.0	19.1
	12	—	—	2.3	2.7	—	—
Forward fireroom (lower level)	11	2.1	4.2	5.2	6.9	8.4	8.6
	12	7.9	10.0	11.0	13.5	14.9	14.2
	13	—	—	2.9	2.4	—	—
After fireroom (upper level)	13	4.4	6.6	7.4	8.4	9.8	9.9
	14	21.7	22.9	24.5	25.2	26.4	26.5
	15	—	—	2.0	2.3	—	—
After fireroom (lower level)	14	3.6	7.3	8.2	9.6	11.0	11.1
	15	11.1	12.7	13.5	14.7	16.1	16.2
	16	—	—	2.4	2.8	—	—
After engine room (upper level)	19	2.1	7.1	8.3	8.9	9.1	9.2
	20	21.8	30.5	31.3	31.4	31.6	31.7
	21	—	—	0.7	0.8	—	—
After engine room (lower level)	20	6.9	12.7	13.8	14.5	14.6	14.7
	21	10.4	16.1	17.2	17.7	17.8	17.9
	22	—	—	0.4	0.5	—	—
After crews quarters	21	1.8	4.9	1.3	1.4	1.6	1.6
	22	51.9	51.1	50.6	50.3	50.4	50.5
	23	—	—	0.2 to 0.4	0.3 to 0.5	—	—

* From data derived from normalization of average for Stations 2 and 3.

† From data derived from normalization of average for Stations 6 and 7.

‡ Dose due to deposited activity. Low values for galley from data based on normalization of average for Stations 2 and 3. High values from use of average for stations 6 and 7. Reverse is true for after crews quarters.

TABLE 3.6 ESTIMATED AIRBORNE RADIOACTIVE CONCENTRATIONS AND RESULTING EXTERNAL DOSE RATES WITHIN GALLEY OF DD-592 AFTER SHOT UMBRELLA

Estimates are based on fissions per total air sampler.

Time After Shot	Fissions per Unit Volume	Gamma Energy Emission Rate	Estimated Dose Rate at Center of Volume	Disintegration Rates (Reference 14)	Estimated Air Concentration
minutes	10^6 fissions/cm ³	MeV/sec 10^6 fissions	r/hr	dis/sec/ 10^6 fissions	$\mu\text{e}/\text{cm}^3$
0.5	16.7	204	141	154	6.32
1.0	12.4	106	55	62	2.08
2.0	6.79	54	15.2	30	0.531
3.0	3.73	33.0	5.23	20	0.202
4.0	2.19	23.5	2.92	14.4	0.1048
5.0	1.42	18.0	0.854	12.0	0.0684
6.0	0.616	14.7	0.383	10.0	0.0166
7.0	0.338	12.3	0.176	8.6	0.00756
8.0	0.187	10.3	0.081	7.6	0.00344
9.0	0.103	9.0	0.039	6.8	0.00188
10.0	0.0560	7.8	0.019	6.2	0.000938
Average					0.390

TABLE 3.7 ESTIMATED AIRBORNE RADIOACTIVE CONCENTRATIONS AND RESULTING EXTERNAL DOSE RATES WITHIN THE AFTER ENGINE ROOM OF DD-592 AFTER SHOT UMBRELLA

Estimates are based on fissions per total air sampler.

Time After Shot	Fissions per Unit Volume	Gamma Energy Emission Rate	Estimated Dose Rate at Center of Sphere	Disintegration Rates (Reference 14)	Estimated Air Concentration
minutes	10^5 fissions/cm ³	MeV/sec 10^6 fissions	r/hr	dis/sec/ 10^6 fissions	$\mu\text{e}/\text{cm}^3$
0.5	33.4	204	61.6	154	1.39
1.0	29.7	106	26.7	62	0.494
2.0	23.5	54	11.5	30	0.191
3.0	18.6	33.5	5.67	20	0.101
4.0	14.7	23.5	3.15	14.8	0.0388
5.0	11.6	19.0	1.96	12.0	0.0376
6.0	9.17	14.7	1.24	10.0	0.0245
7.0	7.27	12.3	0.923	8.6	0.0169
8.0	5.74	10.3	0.545	7.6	0.0118
9.0	4.54	9.0	0.390	6.8	0.00634
10.0	3.59	7.8	0.263	6.2	0.00602
Average					0.234

CONFIDENTIAL

TABLE 38 ESTIMATED AIRBORNE RADIOACTIVE CONCENTRATIONS AND RESULTING EXTERNAL DOSE RATES WITHIN AFTER FIREROOM OF DD-592 AFTER SHOT UMBRELLA

Estimates are based on fissions per total air sampler.

Time After Shot	Fissions per Unit Volume Assumed Constant	Gamma Energy Emission Rate	Estimated Dose Rate	Disintegration Rates (Reference 14)	Estimated Air Concentration
minutes	10^6 fissions/cm ³	Mev/sec 10^4 fissions	r/hr	dis/sec/ 10^6 fissions	$\mu\text{e}/\text{cm}^3$
0.5	3.68	204	1.24	154	3.61×10^{-3}
1.0	3.68	106	0.63	62	1.65×10^{-3}
2.0	3.68	54	0.328	30	7.04×10^{-3}
3.0	3.68	33.5	0.205	20	4.62×10^{-3}
4.0	3.68	22.5	0.144	14.8	3.47×10^{-3}
5.0	3.68	16.0	0.111	12.0	2.82×10^{-3}
6.0	3.68	14.7	0.091	10.0	2.35×10^{-3}
7.0	3.68	12.3	0.076	8.6	2.02×10^{-3}
8.0	3.68	10.3	0.064	7.6	1.78×10^{-3}
9.0	3.68	9.0	0.056	6.8	1.60×10^{-3}
10.0	3.68	7.8	0.049	6.2	1.43×10^{-3}
Average					7.78×10^{-3}

TABLE 39 ESTIMATED AIRBORNE RADIOACTIVE CONCENTRATIONS AND RESULTING EXTERNAL DOSE RATES WITHIN THE AFTER CREWS QUARTERS OF DD-592 AFTER SHOT UMBRELLA

Estimates are based on fissions per total air sampler.

Time After Shot	Fissions per Unit Volume	Gamma Energy Emission Rate	Estimated Dose Rate at Center of Sphere	Disintegration Rates (Reference 14)	Estimated Air Concentration
minutes	10^6 fissions/cm ³	Mev/sec 10^4 fissions	r/hr	dis/sec/ 10^6 fissions	$10^{-3} \mu\text{e}/\text{cm}^3$
0.5	3.90	204	4.42	154	162.0
1.0	3.76	106	2.24	62	63.0
2.0	3.49	54	1.05	30	29.3
3.0	3.24	33.5	0.61	20	17.5
4.0	3.00	23.5	0.40	14.8	12.0
5.0	2.79	18.	0.29	12.0	9.05
6.0	2.58	14.7	0.213	10.0	6.97
7.0	2.40	12.3	0.167	9.6	5.58
8.0	2.22	10.3	0.130	7.6	4.56
9.0	2.06	9.0	0.106	6.8	3.79
10.0	1.92	7.8	0.096	6.2	3.22
Average					54.0

TABLE 2.10 ESTIMATED EXTERNAL GAMMA RADIATION
DOSE DUE TO AIRBORNE RADIODACTIVITY
WITHIN TEST COMPARTMENTS OF DD-392,
AFTER SHOT UMBRELLA

Dose estimate for firebox was too low to be significant.

Compartment	Dose
	r
Galley	1.75
After engine room	1.0
Crews quarters	0.8

TABLE 2.11 ESTIMATED MAXIMUM DOSE RATES DUE TO CONTAMINATED SURFACES IN
TEST COMPARTMENTS CALCULATED FROM SURFACE SAMPLES, DD-392,
SHOT UMBRELLA

$k_2 = 2.6 \times 10^{-3} \text{ in}^2 \cdot \text{min} \cdot \text{cm}^2 \cdot \text{sec}$, conversion factor for urita. $K = 1.75 \times 10^{-4} \text{ r/hr per Mev cm}^2 \cdot \text{sec}$,
gamma flux to dose rate conversion factor. $E = 1.5 \text{ Mev photon, gamma energy}$. $\delta = 1.17 \times 10^3$, decay
factor to convert dose rate at time of sample count to dose rate at H + 10 minutes. $g = 0.05 \text{ counts/photon}$,
detection efficiency of counter. $A = \text{sample area, in}^2$.

Compartment	Area of Disk	Radius of Sphere	Distance from Disk	Sample Count Rate	Estimated Maximum Dose Rates at H + 10 Minutes			
					ft^2	ft	10^3 counts/min	10^{-3} r/hr
Galley								
Deck	135.0	8.63	3.0	34.3			153.0	
Forward after bulkhead	140.0	6.67	5.0	3.0			12.0	
Port starboard bulkhead	70.0	4.72	10.0	3.0			2.0	
Total							167.0	
After crews quarters								
Deck	567.0	13.4	3.0	1.0			6.0	
Forward bulkhead	245.0	5.61	5.0	1.0			1.4	
Port starboard bulkhead	147.0	6.89	17.0	1.0			0.4	
After bulkhead	94.0	3.6	5.25	1.0			1.6	
Total							9.4	
After engine room								
Deck	1,218.0	10.9	3.0	1.63			12.6	
Forward after bulkhead	640.0	14.3	21.0	1.63			2.4	
Port starboard bulkhead	540.0	16.4	16.0	1.63			4.8	
Total							19.8	

TABLE 3.12 ESTIMATED DOSE RATES AND DOSE IN GALLEY
FROM H=1 TO H=10 MINUTES DUE TO DEPOSITED
CONTAMINANTS, DD-392, SHOT UMBRELLA

Time After Shot minutes	Dose Rate μR/μR	Dose μR
1	31.1	
2	4.10	
3	2.00	
4	1.11	
5	0.740	
6	0.550	
7	0.390	
8	0.248	
9	0.210	
10	0.167	0.23
120	0.009	

113 TOTAL DOSE AND SUMMARY OF ESTIMATES OF EXTERNAL GAMMA DOSE DUE TO
THE INGRESS OF CONTAMINANTS, DD-392, SHOT UMBRELLA

Department	GTR Station	Total Dose		Ingress Dose		Dose Based on Air Sample Data	Dose Based on Surface Sample Data
		GTR	Film Badge Average at GTR Location	GTR	Based on GTR Data		
Galley	9	290 ± 58	288 ± 43	2 to 78*	2	1.8	0.3
Crews quarters	21	184 ± 37	158 ± 24	1.5 to 50	0.5	0.1	—
Forward fireroom upper levels	10	59 ± 12	52 ± 8	4 to 14	3	—	—
After fireroom upper levels	17	63 ± 13	65 ± 10	5 to 26	2	—	—
After engine room upper levels	19	85 ± 19	81 ± 12	9 to 31	1	1.0	—
Forward fireroom lower levels	11	26 ± 5.2	25 ± 3.5	8 to 13	4	—	—
After fireroom lower levels	18	25 ± 5.6	28 ± 4.2	11 to 15	3	—	—
After engine room lower levels	20	52 ± 6.4	26 ± 3.9	14 to 18	0.5	—	—

* Deposit dose estimate was substituted for negative dose estimate.

Station	Gamma Survey		Gamma Survey	
	Readings, Shot Wahou, H + 22 Hours	Corrected for Decay, Shot Umbrella H + 22 Hours	Readings, Shot Umbrella, H + 2 Hours	Readings, Shot Wahou, H + 2 Hours
Pantail	30	3 to 4	30 to 40	30 to 40
Starboard maindeck	100 to 200	11	100 to 120*	100 to 120*
Port maindeck	40 to 100	11	100 to 120*	100 to 120*
Director platform	150	19	200	200
Galley	150	8	40 to 100	40 to 100
Upple space	25 to 40	10	100	100
5-inch-ammo handling room	25	4 to 5	40 to 50	40 to 50
Fan space	35	—	—	—
After cross quarters				
Centerline	20	4 to 8	40 to 40	40 to 40
Port and starboard	40	—	—	—
After fireroom, lower level	40	11	120	120
After engine room				
Upper level	10	3	30	30
Upper level, port and starboard	15	—	—	—

* GITR dose rates at H + 2 Hours were: Station 2, port, 90 mr/hr; Station 3, starboard, 137 mr/hr.

TABLE 3.15. AVERAGE 24-HOUR GAMMA DOSES ABOARD DD-592,
BASED ON FILM RANGE DATA, AND RATIO OF
SHOT WAHOU DOSES TO SHOT UMBRELLA DOSES

Compartment or Area	Shot Wahou	Shot Umbrella	Wahou/Umbrella
Above waterline, 16 to 33 ft			
All weather decks*	520	351	1.48
Main weather deck	8537	549	>1.53
Bridge complex	511	229	2.23
Above waterline, 11 to 16 ft			
Forward quarters	518	204	2.54
Radio central	527	196	2.69
Galley	552	242	1.98
Crews washroom	603	307	1.97
Above waterline, 2 to 6 ft			
Crews mess	219	92.4	2.37
Forward fireroom	153	65.6	1.71
Forward engine room	121	64.4	1.88
After fireroom	177	95.4	1.80
After engine room	164	108	1.52
After cross quarters	410	210	1.97
Steering gear room	316	215	1.47
Below waterline, 3 to 6 ft			
Stateroom	214	79.1	2.70
Forward fireroom	35.6	16.7	2.16
Forward engine room	31.1	10.7	2.90
After fireroom	31.1	21.6	2.37
After engine room	62.4	37.6	1.66

* Project 2.0 film pack data (Reference 20).

* Assuming some values greater than the recommended range of film dose to be valid, the average dose would be approximately 1,130 r.

DUE TO EXTERNAL CONTAMINATED
AND UNMIXED

Compartment	Based on compartment average 24-hour film badge doses			All doses in roentgens		
	Shot Wahoo		Shot Umbrella			
	Average Film Badge Dose	Film Badge Dose Difference	Average Film Badge Dose	Film Badge Dose Difference		
Bridge complex*	514	—	229	—		
Galley	532	38	282	33		
Crews mess*	219	—	92.0	—		
Average	367	—	161	—		
After crewquarters	410	33	219	58		
Forward engine room*						
(upper level)	121	—	64.4	—		
Forward fireroom	153	32	69.6	23		
After fireroom	177	56	94.4	34		
After engine room	164	43	108	44		
Forward engine room*						
(lower level)	31.1	—	10.7	—		
Forward fireroom	38.6	7.5	18.7	8.0		
After fireroom	31.1	20.0	21.0	11.0		
After engine room	62.4	31.3	37.6	27.0		

* Noningress controls.

**TABLE 3.17 ESTIMATED EXTERNAL DOSE IN FORWARD FIREROOM DUE TO
GONTAMINATED BOILER COMBUSTION AIR: DD-474, DD-592,
AND DD-593; SHOTS WAHOO AND UMBRELLA**

Compartment	All doses in roentgens					
	Shot Wahoo			Shot Umbrella		
	DD-474	DD-592	DD-593	DD-474	DD-592	DD-593
Upper level total dose						
Forward engine room†	223	121	45.1	31	75.4	56
Forward fireroom	153	153	68.7	40	134	92
Upper level ingress dose	130	32	23.6	9	54	46
Lower level total dose						
Forward engine room†	76	31.1	9.5	—	16.4	23
Forward fireroom	101	34.6	18.9	—	44.3	33
Lower level ingress dose	23	7.3	9.4	—	27.0	12

* Based on compartment average 24-hour film badge doses.

† Based on GITR doses.

‡ Noningress controls.

71
CONFIDENTIAL

				0 to 10 Hours		11 to 14 Days		15 to 21 Days									
Shot Wahine																	
Director platform	M	168	178	1.698	0.628												
	GP	33.6	34.8	0.350	0.258												
Galley	M	6.28	7.23	0.072	0.030												
	GP	0.467	0.488	0.006	0.002												
After engine room	M	2.82	3.01	0.039	0.015												
	GP	0.400	0.427	0.004	0.002												
After fire room	M	1.96	2.10	0.021	0.008												
	GP	0.372	0.396	0.004	0.001												
Crews quarters	M	1.42	1.50	0.014	0.006												
	GP	0.439	0.456	0.005	0.002												
Shot Umbrella																	
Director platform	M	3.68	3.90	0.0573	0.0239												
	GP	1.123	1.160	0.0170	0.0066												
Galley	M	0.473	0.492	0.00415	0.00164												
	GP	0.0347	0.0362	0.00053	0.00023												
After engine room	M	0.4800	0.5100	0.00477	0.00190												
	GP	0.0825	0.0853	0.00019	0.00016												
After fire room	M	0.2030	0.2110	0.00204	0.00081												
	GP	0.027	0.029	0.00027	0.00011												
Crews quarters	M	0.0114	0.0152	0.00002	0.00007												
	GP	0.0141	0.0139	0.00127	0.0005												

TABLE 3.19 INTERNAL DOSE TO ORGANS OF ANIMALS ON DIRECTOR PLATFORM
OF DD-572

Organ	M (male), GP (female, pigs)	All doses in μ curies/pig			
		Animal	Early Dose 0 to 10 Hours	Long-Term Dose 0 to 7 Days	Long-Term Dose 7 to 14 Days
Shot Wahine					
Skeleton (dibr)	M	131.0	152.5	0.6	0
	GP	39.3	44.1	0.6	0
Respiratory tract	M	437.0	464.0	6.0	1.0
	GP	7.99	10.9	0.1	0
Gastrointestinal tract	M	1,042.0	1,200.0	3.0	0
	GP	40.0	49.8	0	0
Liver	M	107.6	121.3	0.7	0
	GP	2.40	2.59	0	0
Shot Umbrella					
Skeleton (dibr)	M	21.4	24.0	0.3	0
	GP	4.97	5.57	0.06	0
Respiratory tract	M	8.14	8.83	0.14	0
	GP	1.63	2.22	0.02	0.01
Gastrointestinal tract	M	15.3	20.5	0.1	0
	GP	3.16	4.06	0.01	0
Urinary	M	7.8	8.1	0	0
	GP	1.64	2.02	0.01	0
Liver	M	7.06	8.0	0	0
	GP	1.57	1.56	0	0

Organ	M, mice	GP, guinea pigs	All Doses in Rad		
			0 to 1 Days	1 to 14 Days	14 to 21 Days
Shot Wahoo					
Skeleton/Ribc	M	15.6	19.2	0.3	0
	GP	5.94	6.43	0.12	0
Respiratory tract	M	7.65	9.33	0.49	0
	GP	0.624	0.629	0.004	0
Gastrointestinal tract	M	1.153	1.9	0.017	0
	GP	3.61	4.03	0.03	0
Liver	M	1.13	1.59	0.045	0
	GP	0.147	0.19	0	0
Shot Umbrella					
Skeleton/Ribc	M	4.35	5.0	0.07	0
	GP	1.07	1.15	0.01	0
Respiratory tract	M	3.52	3.95	0.04	0
	GP	0.38	0.33	0.01	0
Gastrointestinal tract	M	3.38	4.14	0.018	0
	GP	0.31	0.37	0	0
Thymus	M	3.22	3.62	0	0
	GP	0.24	0.36	0.03	0.02
Liver	M	0.43	0.37	0	0
	GP	0.34	0.37	0	0

TABLE 3.21 INTERNAL DOSE TO ORGANS OF ANIMALS IN AFTER ENGINE
RADIUM-226 DD-392

Organ	M, mice	GP, guinea pigs	All Doses in Rad		
			Early Dose 0 to 1 Hours	0 to 1 Days	Long-Term Dose 1 to 14 Days
Shot Wahoo					
Skeleton/Ribc	M	10.93	20.6	0.25	0
	GP	3.59	4.42	0.08	0
Respiratory tract	M	7.03	7.34	0.025	0.005
	GP	1.78	2.42	0.03	0.003
Gastrointestinal tract	M	4.32	4.34	0.005	0
	GP	1.13	1.05	0.10	0
Liver	M	2.72	3.07	0.005	0
	GP	0.812	0.752	0	0
Shot Umbrella					
Skeleton/Ribc	M	2.46	4.24	0.05	0
	GP	1.06	2.17	0.03	0
Respiratory tract	M	4.1	4.76	0.06	0.01
	GP	0.61	0.81	0	0
Gastrointestinal tract	M	2.14	3.74	0	0
	GP	0.56	0.46	0	0
Thymus	M	0.17	4.49	0	0
	GP	0.09	1.24	0.11	0.04
Liver	M	1.22	1.37	0	0
	GP	0.50	0.63	0	0

Organ	Animal	Early Dose			Long-Term Dose	
		0 to 50 Hours	0 to 7 Days	7 to 14 Days	14 to 21 Days	
Shot Wahoo						
Skeleton (tibia)	M	0.12	10.35	0.07	0	
	GP	2.08	2.23	0.028	0	
Respiratory tract	M	0.32	3.73	0.12	0	
	GP	2.08	2.76	0.02	0.01	
Gastrointestinal tract	M	1.32	2.37	0.01	0	
	GP	1.16	1.41	0.003	0.003	
Liver	M	2.72	3.00	0.01	0	
	GP	0.066	0.071	0	0	
Shot Umbrella						
Skeleton (tibia)	M	1.44	2.16	0.12	0	
	GP	2.23	3.19	0.27	0	
Respiratory tract	M	1.60	1.63	0.03	0	
	GP	0.86	1.18	0	0	
Gastrointestinal tract	M	1.01	1.24	0	0	
	GP	0.22	0.26	0.04	0	
Thyroid	M	1.56	1.61	0	0	
	GP	0.70	0.61	0	0	
Liver	M	0.30	0.34	0	0	
	GP	0.06	0.05	0	0	

TABLE 3.23 INTERNAL DOSE TO ORGANS OF ANIMALS IN CREWS QUARTERS
OF DD-S92

Organ	Animal	Early Dose			Long-Term Dose	
		0 to 50 Hours	0 to 7 Days	7 to 14 Days	14 to 31 Days	
Shot Wahoo						
Skeleton (tibia)	M	10.32	11.52	0.08	0	
	GP	2.093	2.20	0.04	0	
Respiratory tract	M	1.97	4.33	0.04	0.01	
	GP	0.66	0.902	0.008	0.002	
Gastrointestinal tract	M	4.53	6.57	0.01	0	
	GP	1.792	2.12	0.04	0.005	
Liver	M	5.93	6.13	0.01	0	
	GP	—	—	—	—	
Shot Umbrella						
Skeleton (tibia)	M	1.14	1.68	0.04	0	
	GP	0.353	0.633	0.004	0	
Respiratory tract	M	0.516	0.562	0.008	0.001	
	GP	0.176	0.241	0.001	0.001	
Gastrointestinal tract	M	0.38	0.468	0	0	
	GP	0.176	0.212	0.001	0.001	
Thyroid	M	1.993	2.05	0	0	
	GP	0.237	0.374	0.031	0.013	
Liver	M	0.118	0.133	0.001	0	
	GP	0.317	0.342	0	0	

CONFIDENTIAL

TABLE 3-24 INTERNAL DOSE TO MAN: ESTIMATED FROM MOUSE AND GUINEA PIG DATA: SHOT AVAILO

Organ	M. dose based on mouse data. GP. dose based on guinea pig data. All doses in rads.									
	Director Platform		Galley		After Landing Room					
	30 Hours	7 Days	30 Hours	7 Days	30 Hours	7 Days				
Skeleton (tibia)	M	21.8	25.3	2.63	3.04	2.09	3.13	1.12	1.72	1.92
	GP	19.4	22.5	2.99	3.22	1.95	2.41	1.12	1.13	1.11
Respiratory tract	M	72.7	76.0	1.28	1.39	0.38	0.42	1.62	0.66	0.72
	GP	4.0	5.5	0.314	0.414	0.38	0.41	1.79	0.33	0.45
Gastrointestinal tract	M	173.6	412.5	0.24	0.32	0.59	0.74	0.32	0.75	0.93
	GP	26.0	24.4	1.005	2.215	3.76	6.59	1.70	6.96	1.06
Liver	M	19.8	20.2	0.18	0.21	0.15	0.51	1.47	3.31	1.02
	GP	1.2	1.3	0.221	0.240	0.236	0.276	0.43	0.36	0.34

TABLE 3-25 INTERNAL DOSE TO MAN: ESTIMATED FROM MOUSE AND GUINEA PIG DATA: SHOT UMBRELLA

Organ	M. dose based on mouse data. GP. dose based on guinea pig data. All doses in rads.									
	Director Platform		Galley		After Landing Room					
	30 Hours	7 Days	30 Hours	7 Days	30 Hours	7 Days				
Skeleton (tibia)	M	4.07	4.66	1.39	1.60	0.95	1.15	0.36	0.52	0.51
	GP	2.48	2.79	0.51	0.55	0.59	1.09	1.42	1.39	0.317
Respiratory tract	M	1.36	1.47	0.59	0.66	0.73	0.79	0.54	0.31	0.076
	GP	0.82	1.11	0.19	0.27	0.31	0.42	0.42	0.59	0.121
Gastrointestinal tract	M	2.55	3.12	0.56	0.69	0.51	0.64	1.17	5.21	6.63
	GP	2.08	2.53	0.16	0.19	0.23	0.41	0.13	0.69	0.106
Thyroid	M	1.30	1.35	0.59	0.60	0.13	0.75	1.26	0.27	0.34
	GP	3.04	4.61	0.12	0.18	0.19	0.62	0.45	0.44	0.10
Liver	M	1.14	1.33	0.14	0.14	0.20	0.23	0.05	0.06	0.019
	GP	0.67	0.59	0.17	0.14	0.30	0.33	0.07	0.10	0.159

CONFIDENTIAL

TABLE 3.26 COMPARISON OF AIR SAMPLE AND ANIMAL DATA,
SHOT UMBRELLA

Location	Early Whole-Body		Air Sample	
	Internal Dose Mice	Internal Dose Guinea Pigs	Activity to 8 + 10 Minutes	Estimated Average Airborne Concentration $\mu\text{c cm}^{-3}$
Galley	0.175	0.040	7.31	0.006
After engine room	0.008	0.081	10.1	0.231
After fire room	0.203	0.027	4.32	0.008
Crews quarters	0.002	0.012	1.93	0.1
Director platform	3.68	1.132	5.95	—

TABLE 3.27 ESTIMATED EXTERNAL AND INTERNAL DOSES DUE TO THE
INGRESS OF CONTAMINANTS, DD-502

Location	Shot Wahoo*		Shot Umbrella	
	Internal Dose†	Internal Dose‡	Minimum§	External Dose§
Galley	3 to 2.7	0.6 to 1.6	2	2 to 78
Crews quarters	1.1 to 1.9	0.3 to 0.6	0.5	1.5 to 50
After engine room	3.2 to 3.4	1.1 to 1.2	1	9 to 31
	(0.7 to 7.8)			
After fire room	1.1 to 1.8	0.4 to 1.6	3	11 to 15

* External ingress dose for Shot Wahoo estimated to be equal to or greater than for Shot Umbrella.

† Maximum 0- to 7-day dose to critical organ (skeleton).

‡ Maximum external dose is taken as the overestimate of ingress dose due to deposited radioactivity, based on GITR data.

§ 0- to 7-day dose to GI tract.

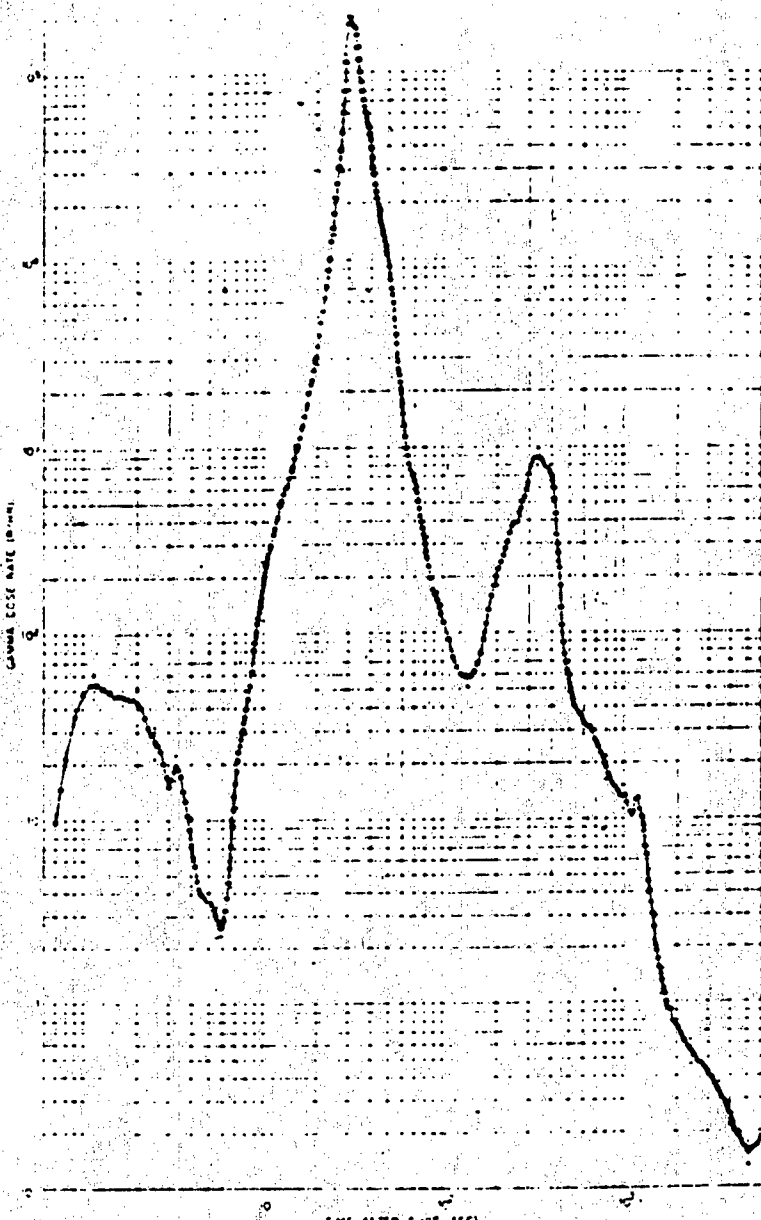


Figure 3.1 Average gamma dose rates on weather decks of DD-392 after Shot Umbrella. Vertical bars indicate estimates of probable error.

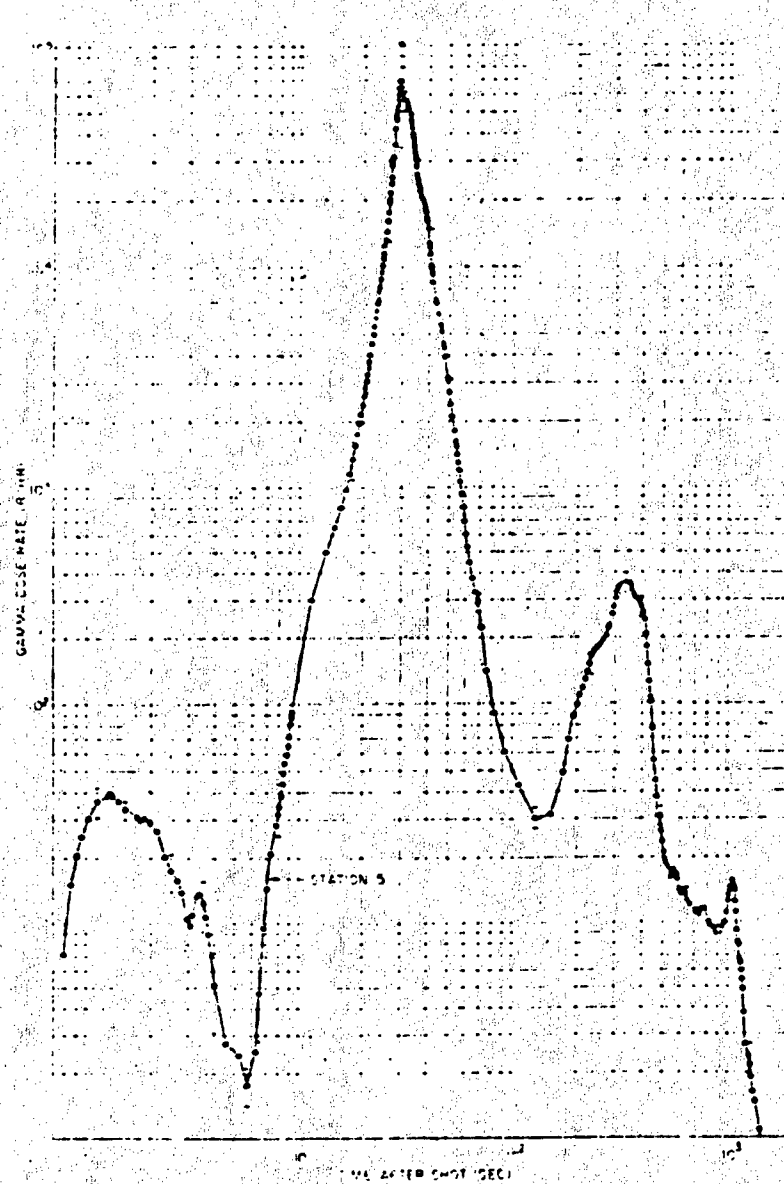


Figure 3.2. Gamma dose rates in vicinity of DD-392 after Shot Underhill. Compartment sealed, no ventilation. Vertical bars indicate estimates of probable error.

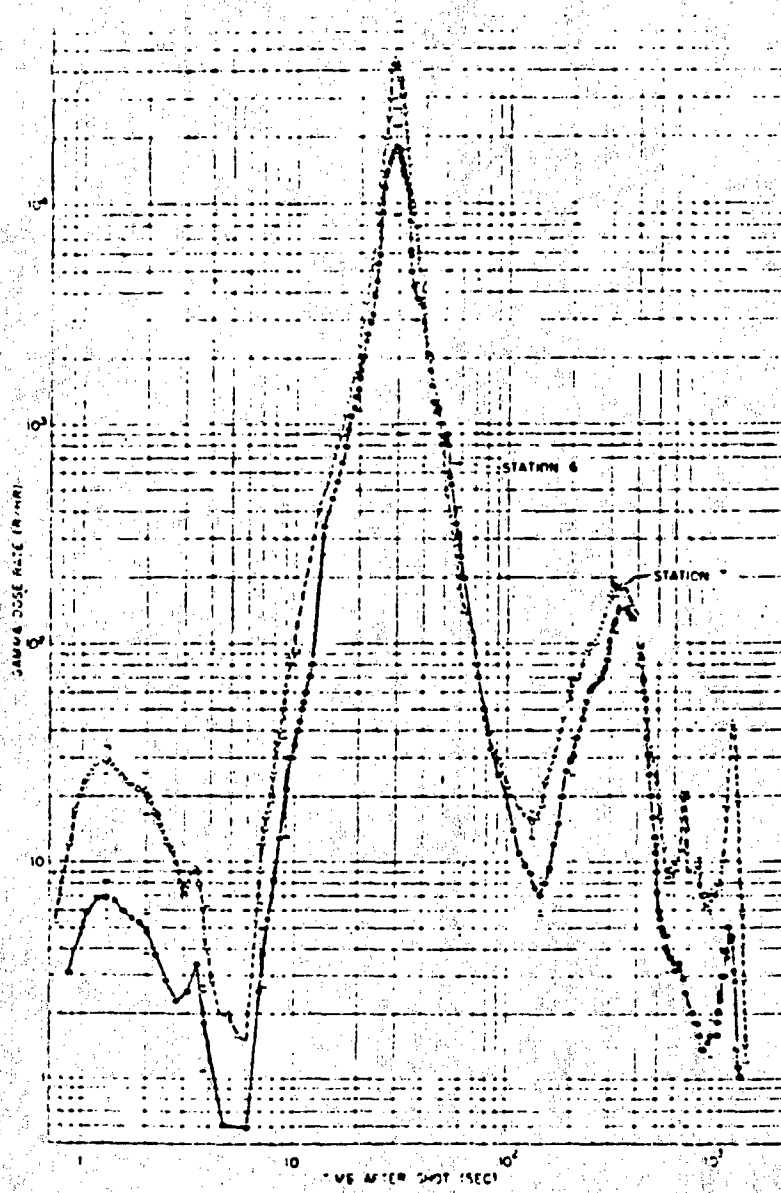


Figure 3-3. Gamma dose rates in crew's mess of D10-592 after Shot Umbrella. Compartment sealed, no ventilation. Vertical bars indicate estimates of probable error.

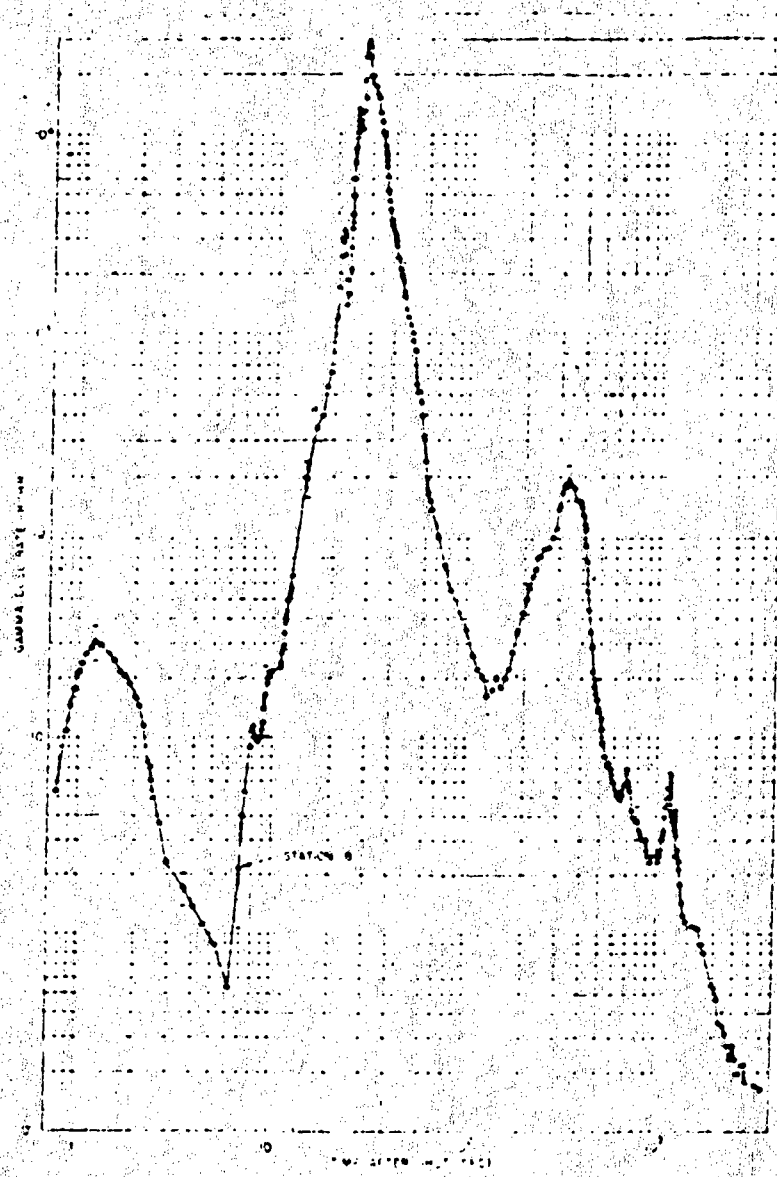


Figure 3.4 Gamma dose rates in magazine of DD-592 after shot Umbrella. Compartment sealed, no ventilation. Vertical bars indicate estimates of probable error.

80

CONFIDENTIAL

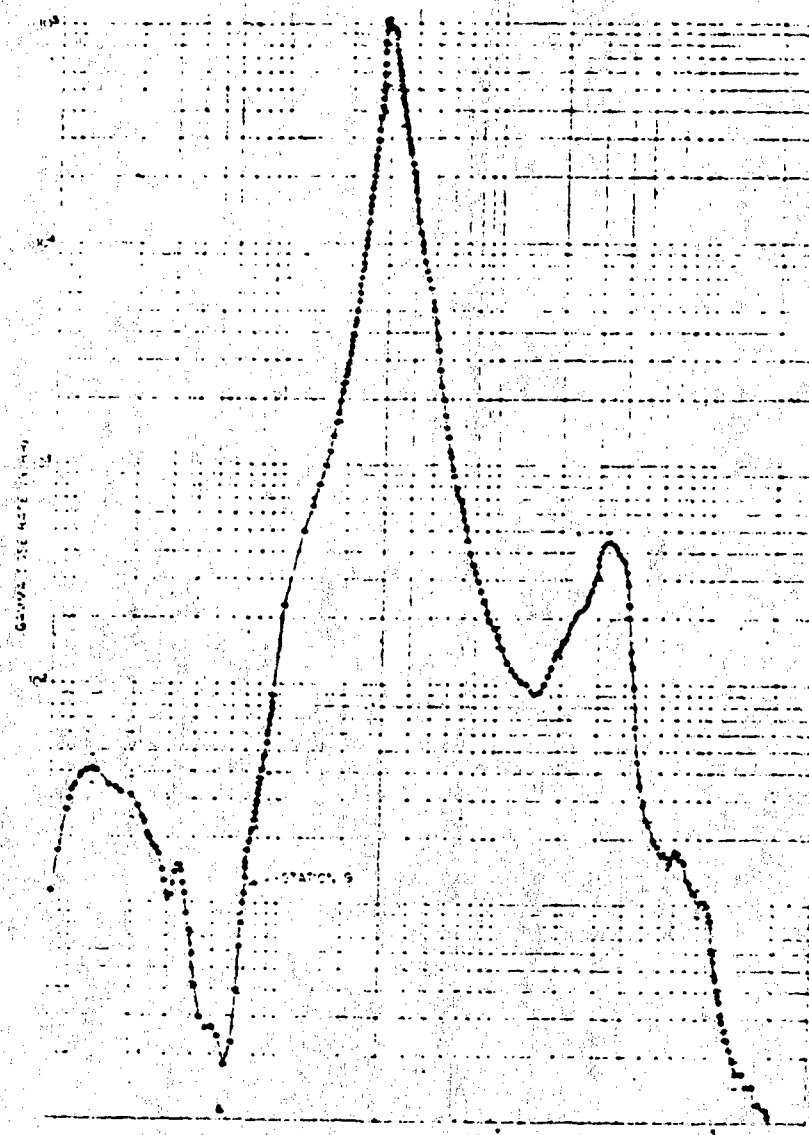


Figure 3.5 Gamma dose rates in eddy of FD-592 after Shot Umbrella. Controlled ventilation, 100 seconds for one air change. Vertical bars indicate estimates of probable error.

81

CONFIDENTIAL

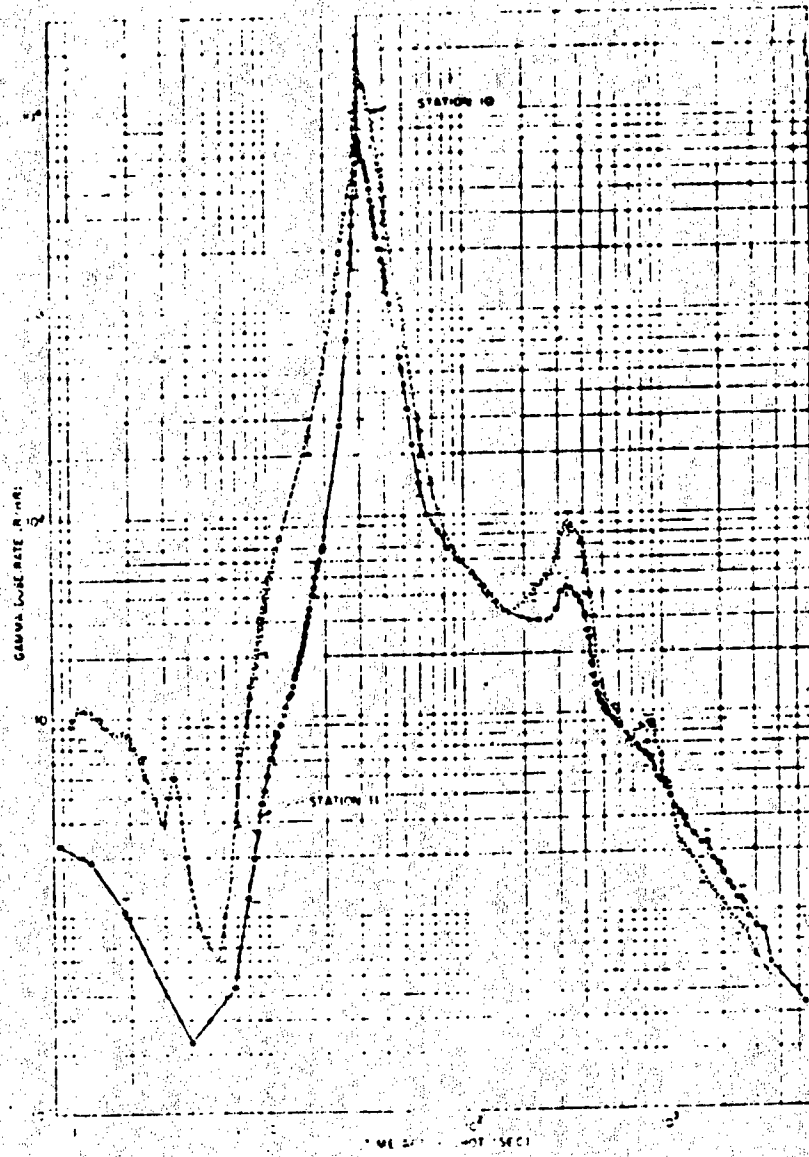


Figure 3.6. Gamma dose rates outward from room of DD-592 after Shot Umbrella. Compartment sealed, no ventilation, one boiler operating with half of full power airflow. Vertical bars indicate estimates of probable error.

CONFIDENTIAL

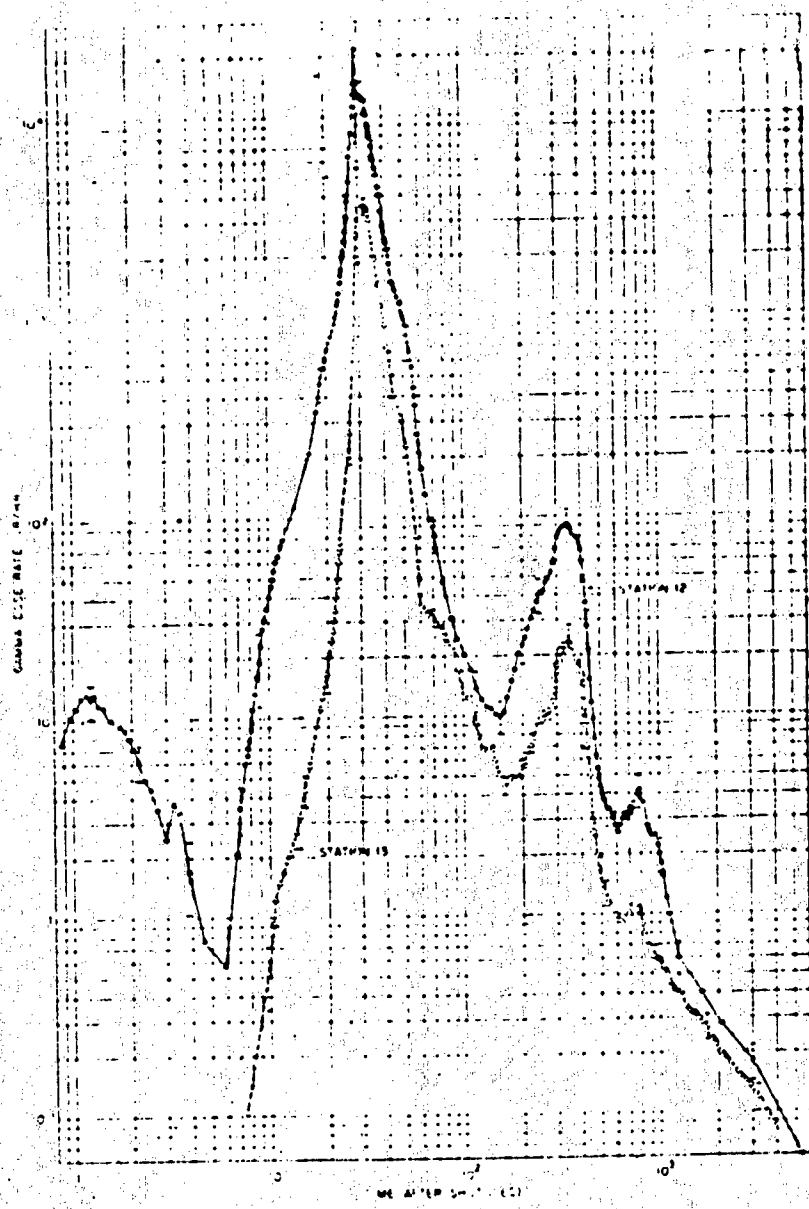


Figure 3.7 Gamma dose rates in forward engine room of DD-592 after Shot Unbr. 11a. Compartment sealed, no ventilation. Vertical bars indicate estimates of probable error.

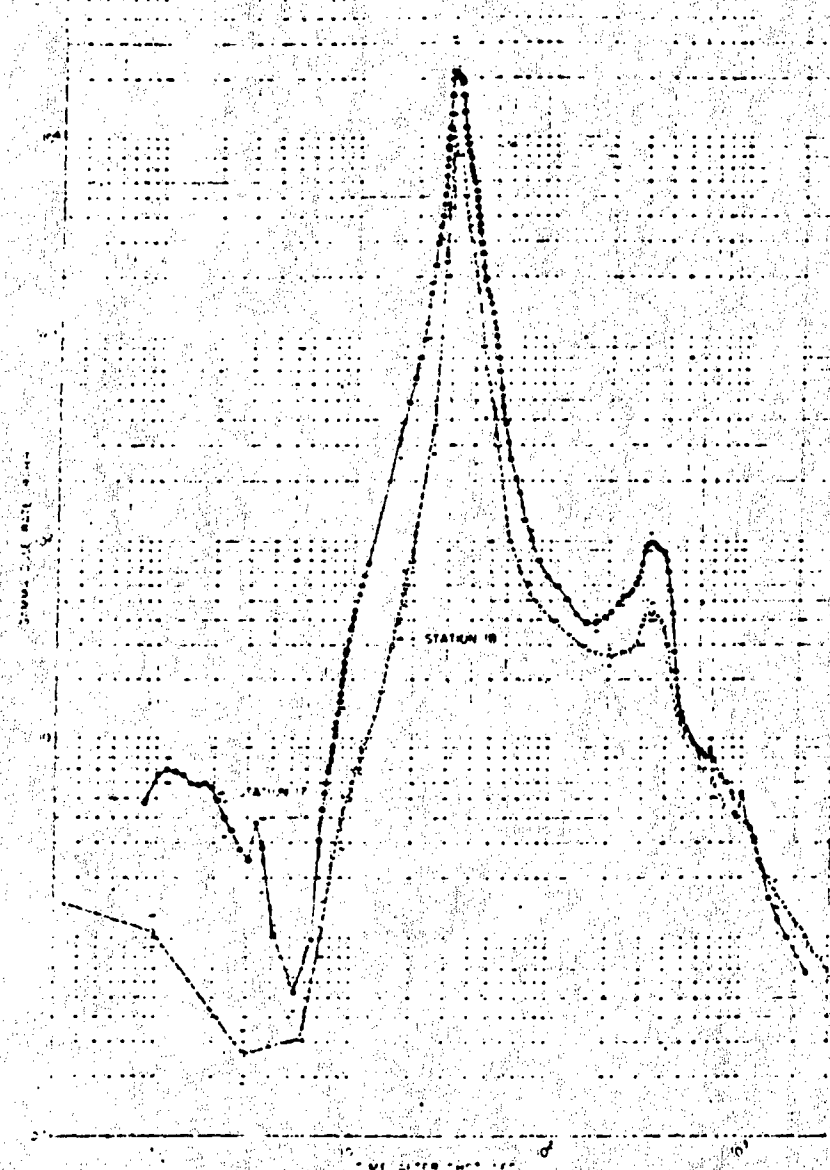


Figure 3-6. Gamma dose rates in after fireroom of DD-592 after Shot Umbrella. Compartment sealed, no ventilation, full-power airflow through one undivided boiler. Vertical bars indicate estimates of probable error.

CONFIDENTIAL

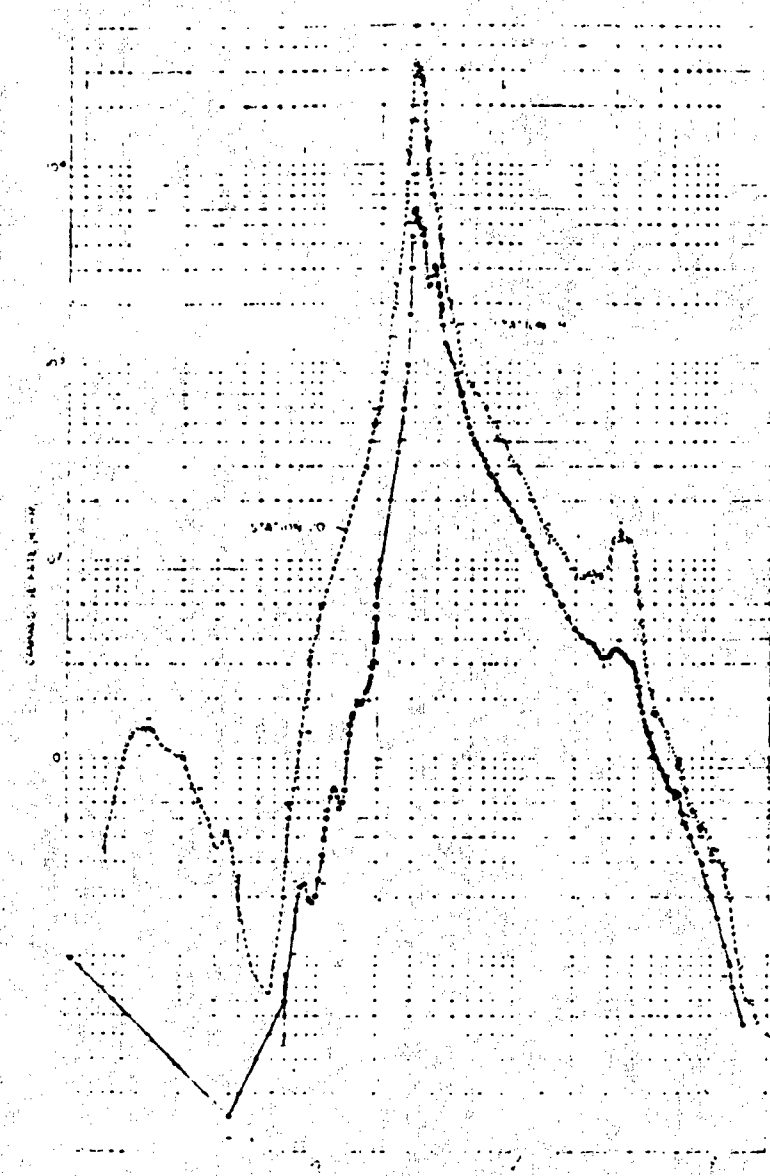


Figure 3.9. Gamma dose rates in after engine room of DD-592 after Shot Umbrella. Controlled ventilation, 253 seconds for one air change. Vertical bars indicate estimates of probable error.

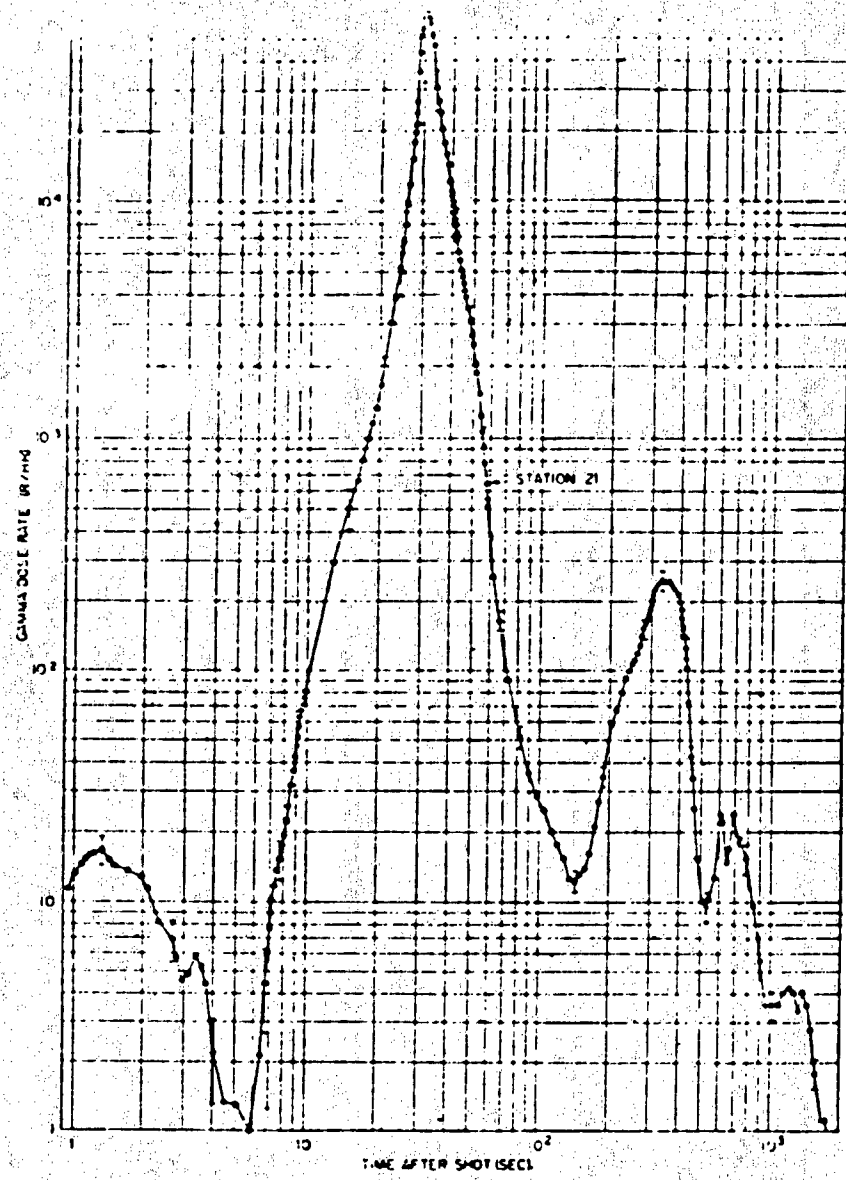


Figure 3.10 Gamma dose rates in after crews quarters of DD-592 after
Slit Umbrella. Controlled ventilation, 800 seconds for one air change.
Vertical bars indicate estimates of probable error.

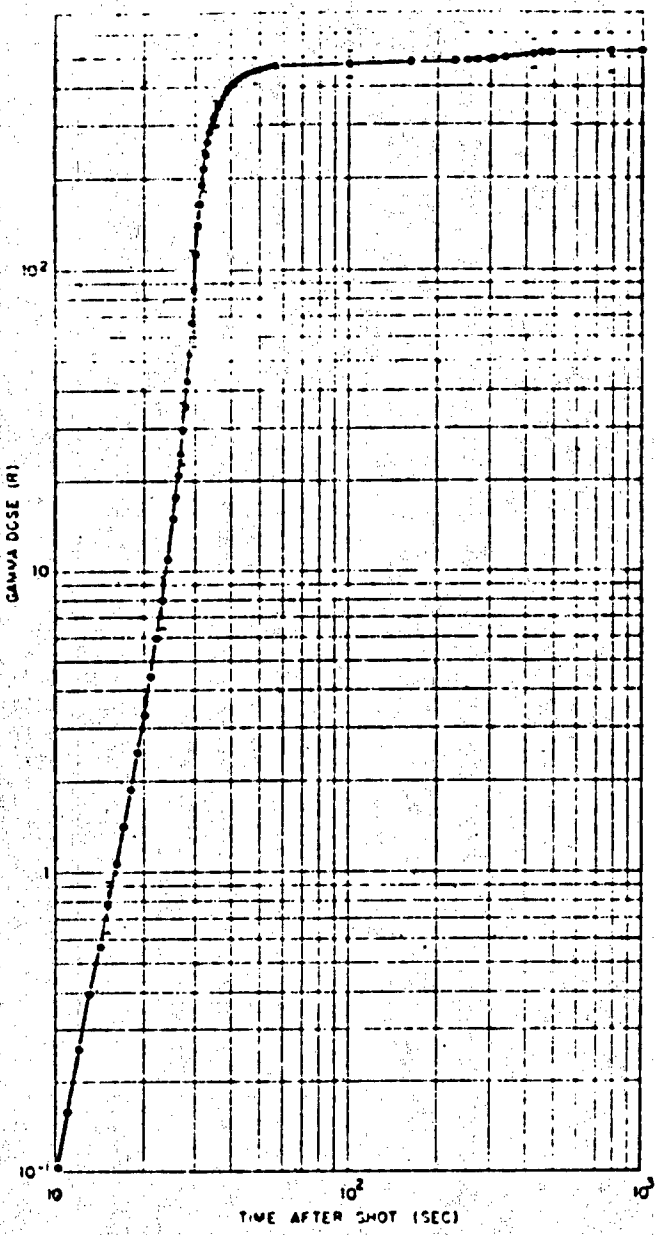


Figure 3.11 Average gamma dose on weather decks of DD-592 after Shot Umbrella. Vertical bars indicate estimates of probable error.

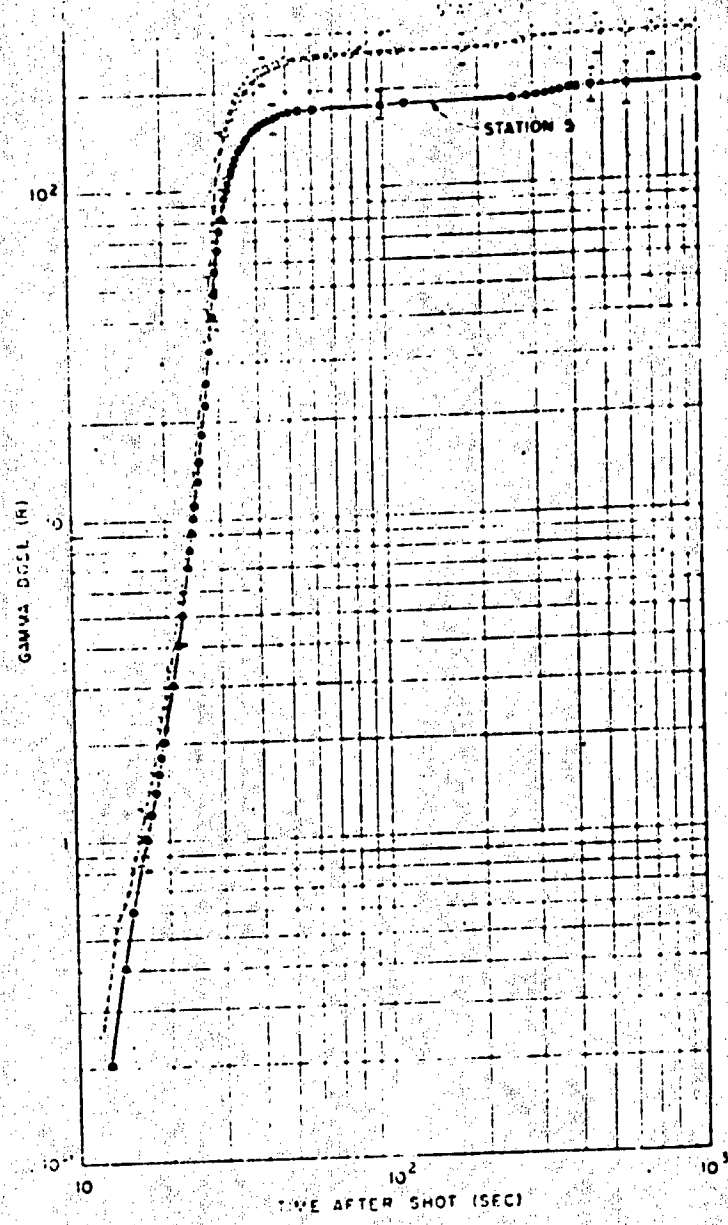


Figure 3.12 Gamma dose γ in wheelhouse and gallery of DD-362 after Shot Umbrella. Wheelhouse sealed, no ventilation. Controlled ventilation in gallery, 100 scuds for one air change. Vertical bars indicate estimates of probable error.

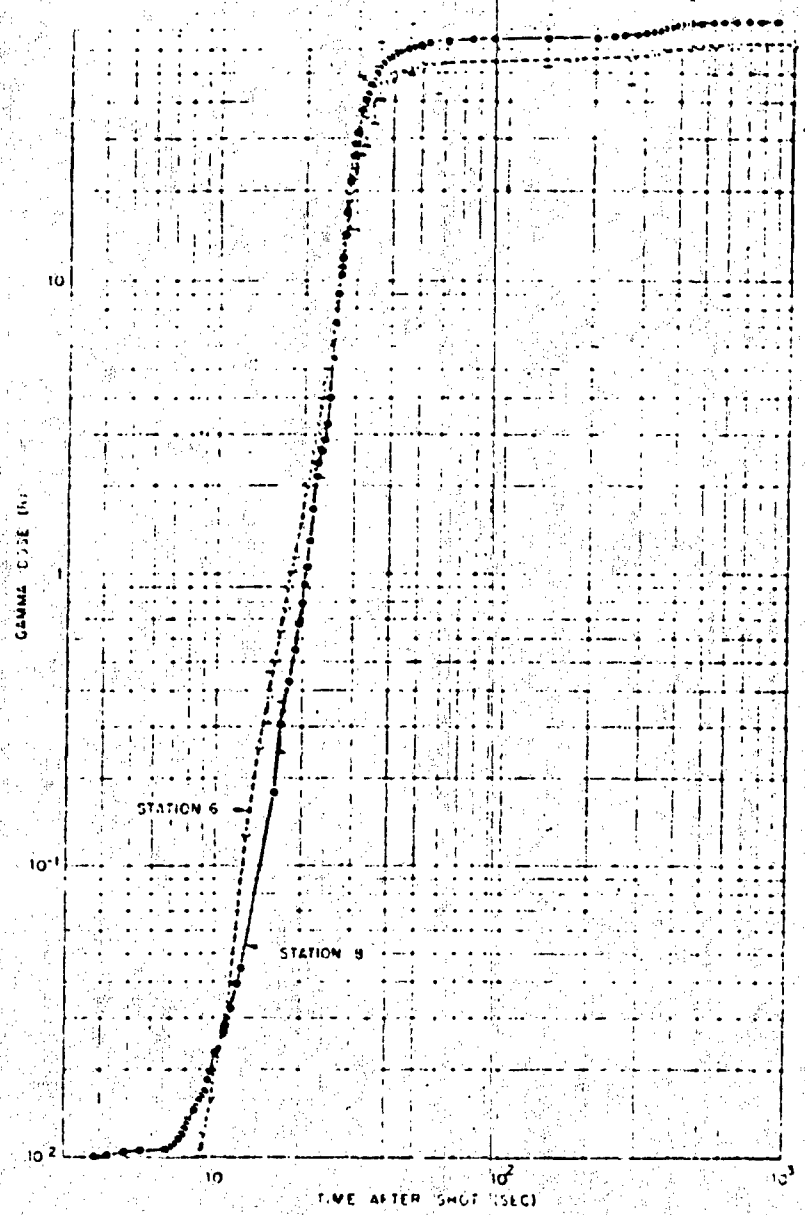


Figure 3.13. Gamma doses in crews mess (portside) CITR Station 6) and magazine of DD-502 after Shot Umbrella. Both compartments sealed, no ventilation. Vertical bars indicate estimates of probable error.

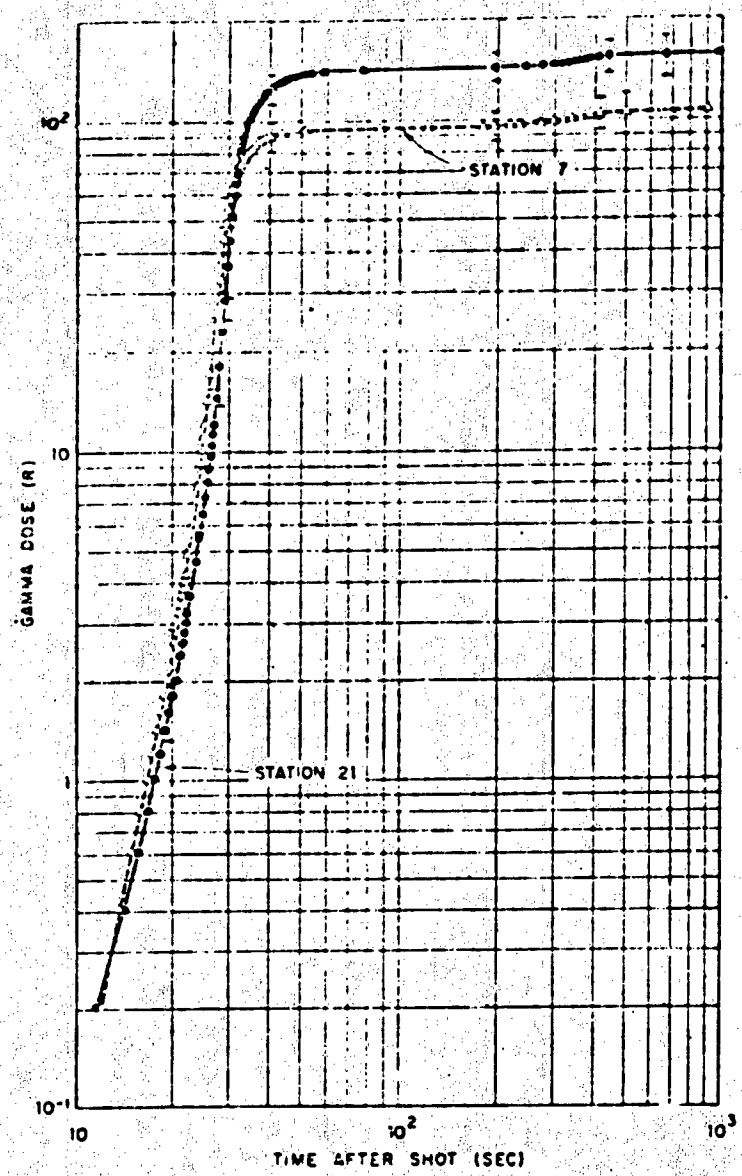


Figure 3.11. Gamma doses in crew mess (starboard side, GITR Station 7) and after crew's quarters of DD-542 after Shot Umbrella. Crews mess sealed, no ventilation. Controlled ventilation in after crew's quarters, 800 seconds for one air change. Vertical bars indicate estimates of probable error.

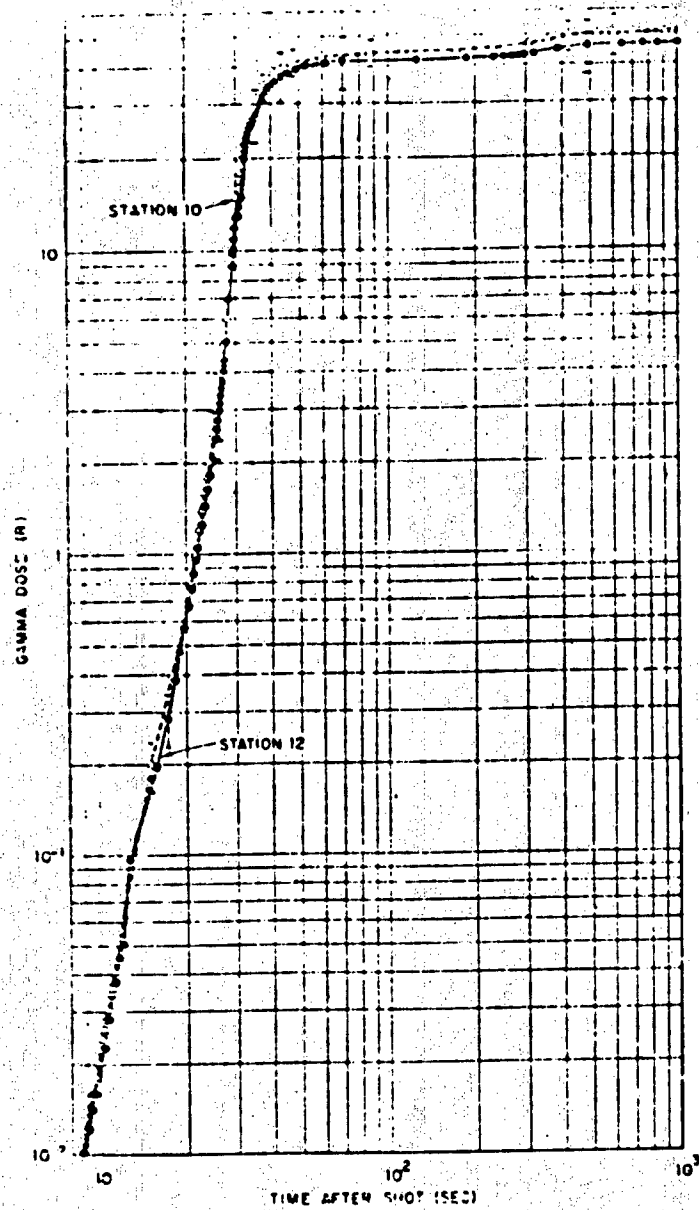


Figure 3.15 Gamma doses in upper levels of forward fireroom and forward engine room of DD-592 after Shot Umbrella. Both compartments sealed, no ventilation. One boiler operating in forward fireroom with half of full-power airflow. Vertical bars indicate estimates of probable error.

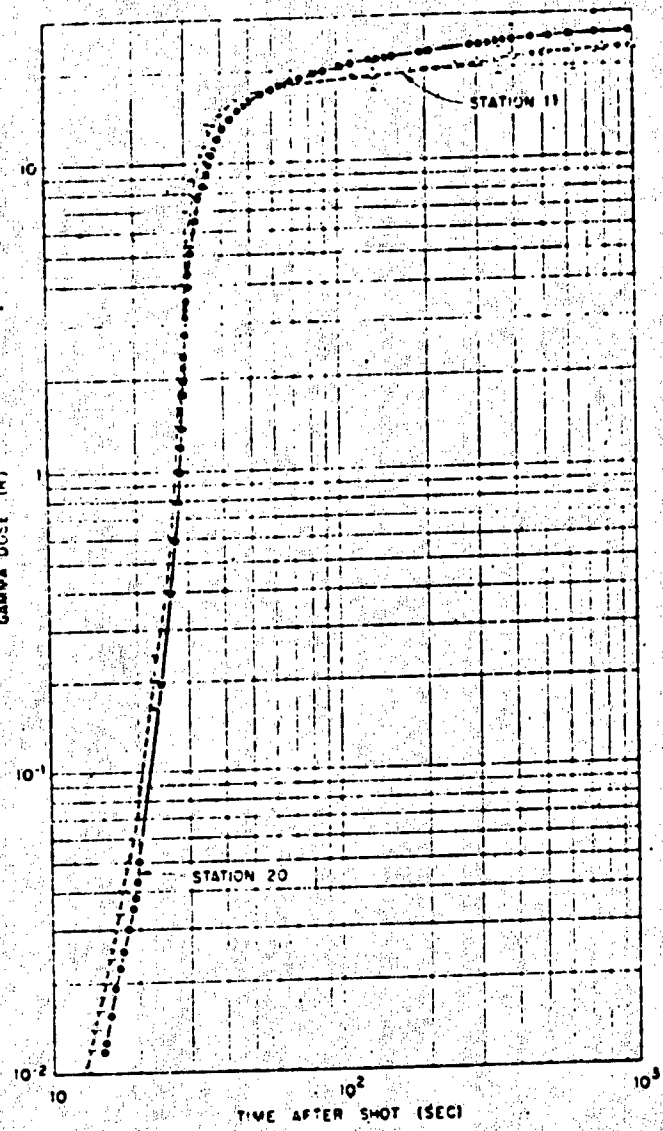


Figure 3.10 Gamma doses in lower levels of forward fireroom and after engine room of DD-512 after shot Umbrella. Forward fireroom sealed, no ventilation, but one boiler operating with half of full-power airflow. Controlled ventilation in after engine room, 233 seconds for one air change. Vertical bars indicate estimates of probable error.

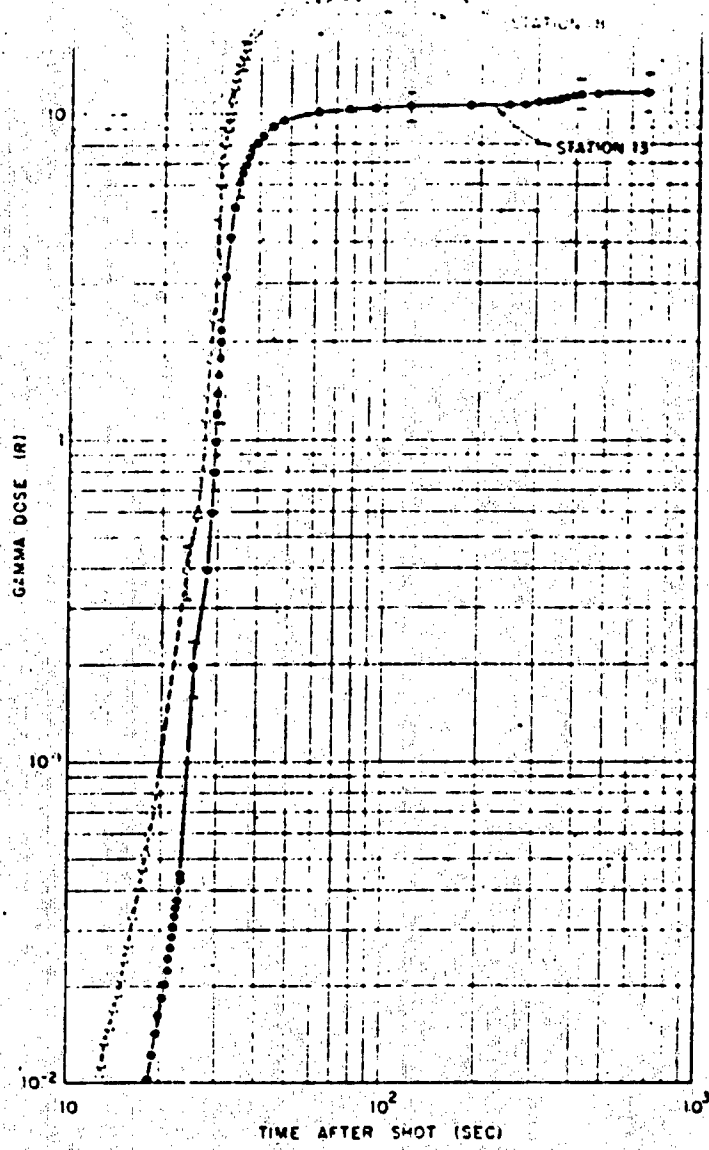


Figure 3.17 Gamma doses in lower levels of forward engine room and after fireroom of DD-512 after Shot Umbrella. Both compartments sealed, no ventilation, but full-power airflow through one boiler in after fireroom. Vertical bars indicate estimates of probable error.

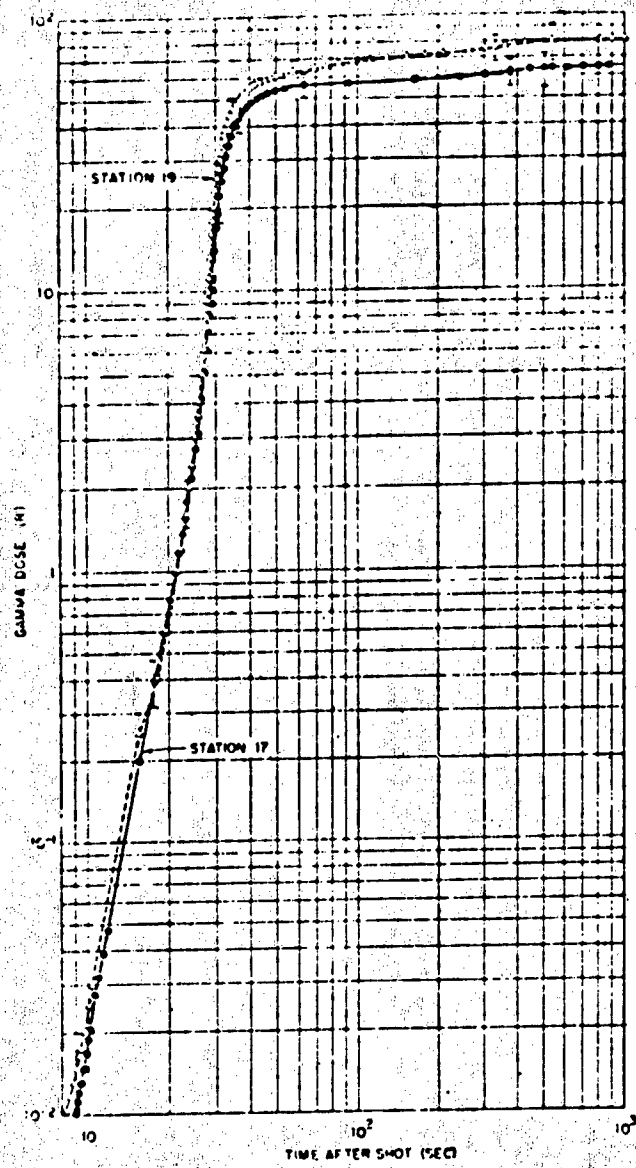


Figure 3.18 Gamma doses in upper levels of after engine room and after fireroom of DD-592 after Shot Umbrella. Controlled ventilation in after engine room, 255 seconds for one air change. After fireroom sealed, no ventilation, but full-power airflow through one undred boiler. Vertical bars indicate estimates of probable error.

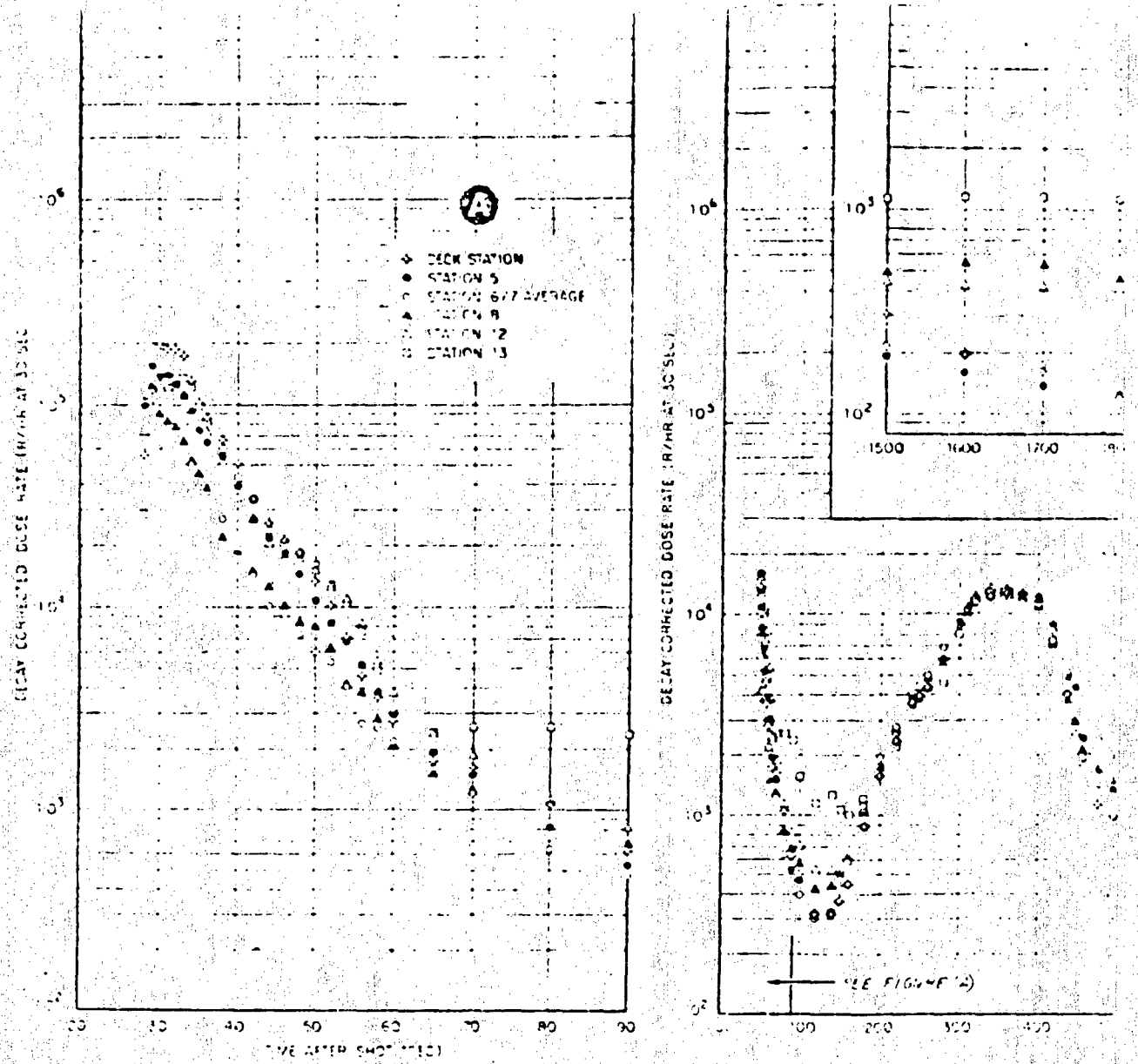
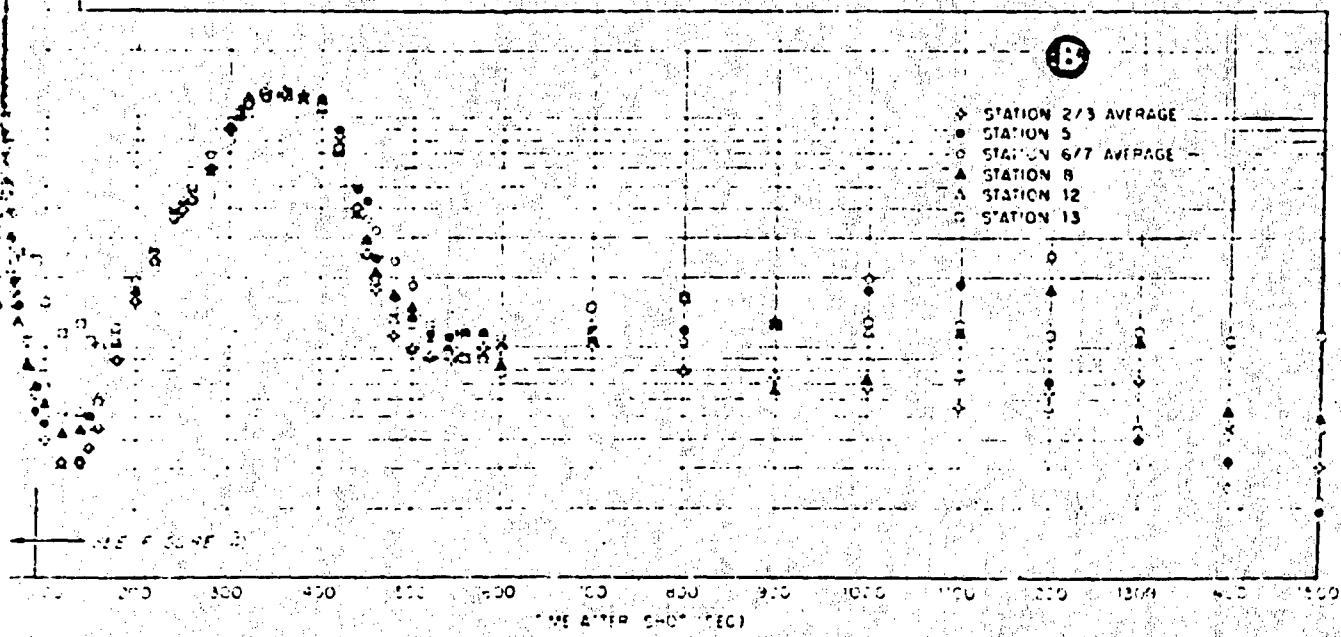
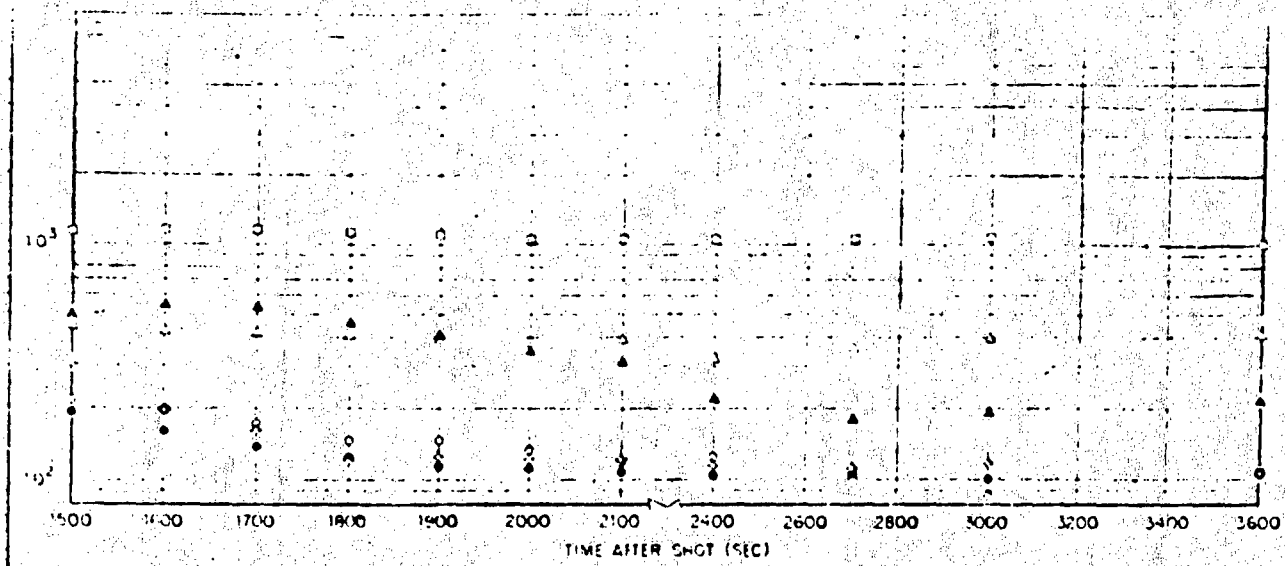


Figure 3.21 Decay-corrected dose rates for all nonanguss stations normalized to the average of Stations 2 and 3 at 300 seconds.

97-98

CONFIDENTIAL



Corrected dose rates for all nonmeasured stations at all GTR stations
except Stations 2 and 3 at 3 sec. (DD-592, Shot Umbrella)

01-92

CONFIDENTIAL

2

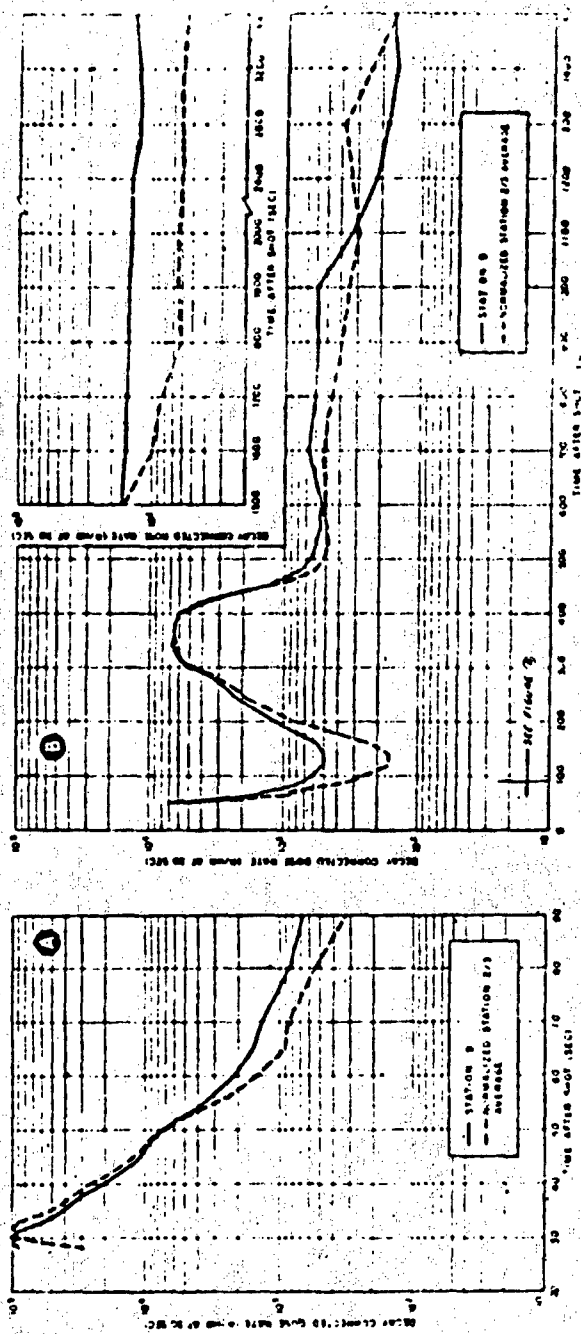


Figure 3.22. Decay-corrected dose rates for the galley GITR Station 9, and for the normalized average of Stations 2 and 3; DD-392, Ship Umbrella. Difference at 360-second normalization point is equal to difference at 520 seconds.

CONFIDENTIAL

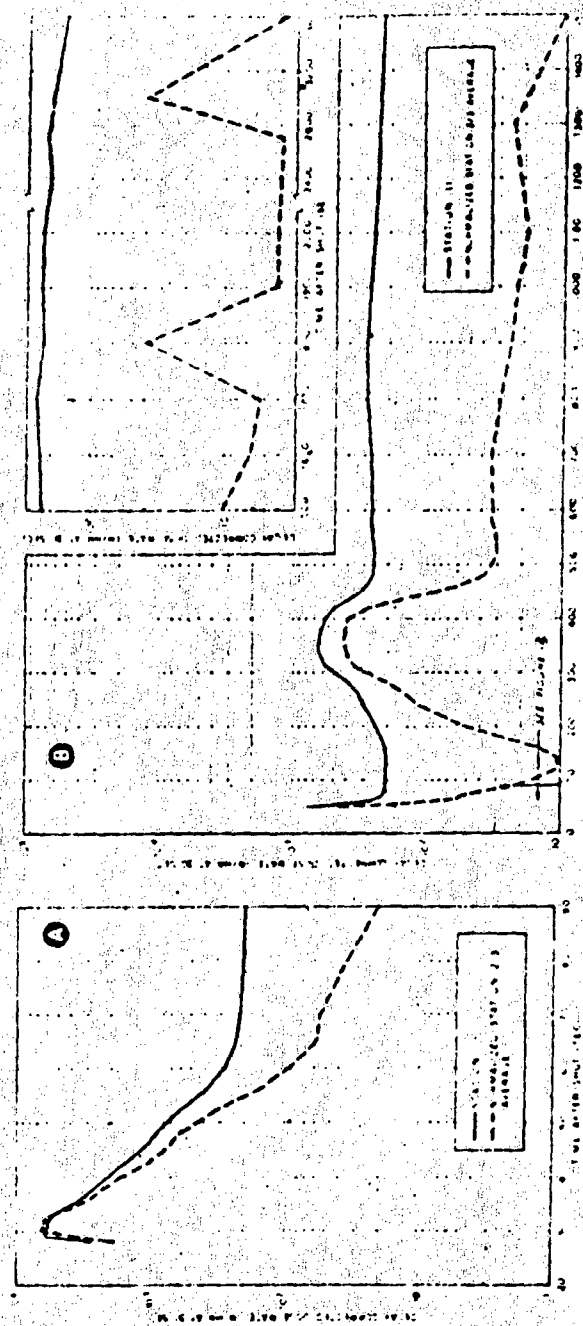


Figure 3.23. Dose-corrected dose rates for the lower level of the forward fireroom
 GIFT Station 11, and for the normalized average of Stations 2 and 3; 101-532; Shot
 Umbrella. Difference at 360-second normalization point is equal to difference at
 520 seconds.

CONFIDENTIAL

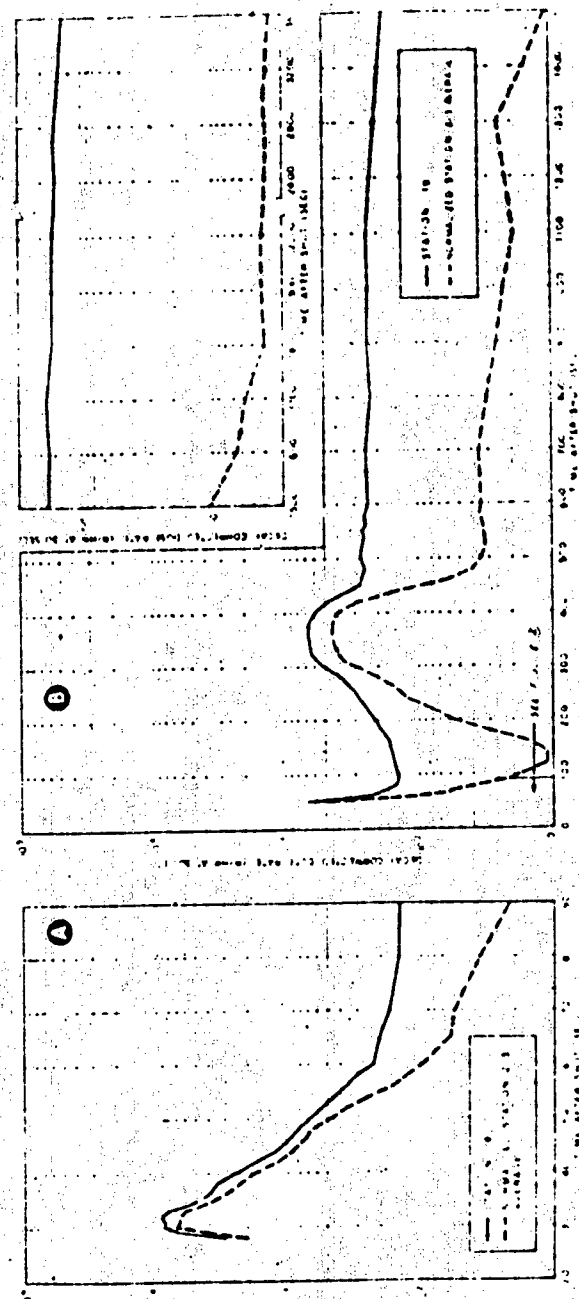


Figure 3.24 Decay-corrected dose rates for the lower level of the after-bomb GTR Station 10, and for the normalized average of Stations 2 and 3. Dose Rate, Shot Umbrella. Difference at 360-second normalization point is equal to difference at 520 seconds.

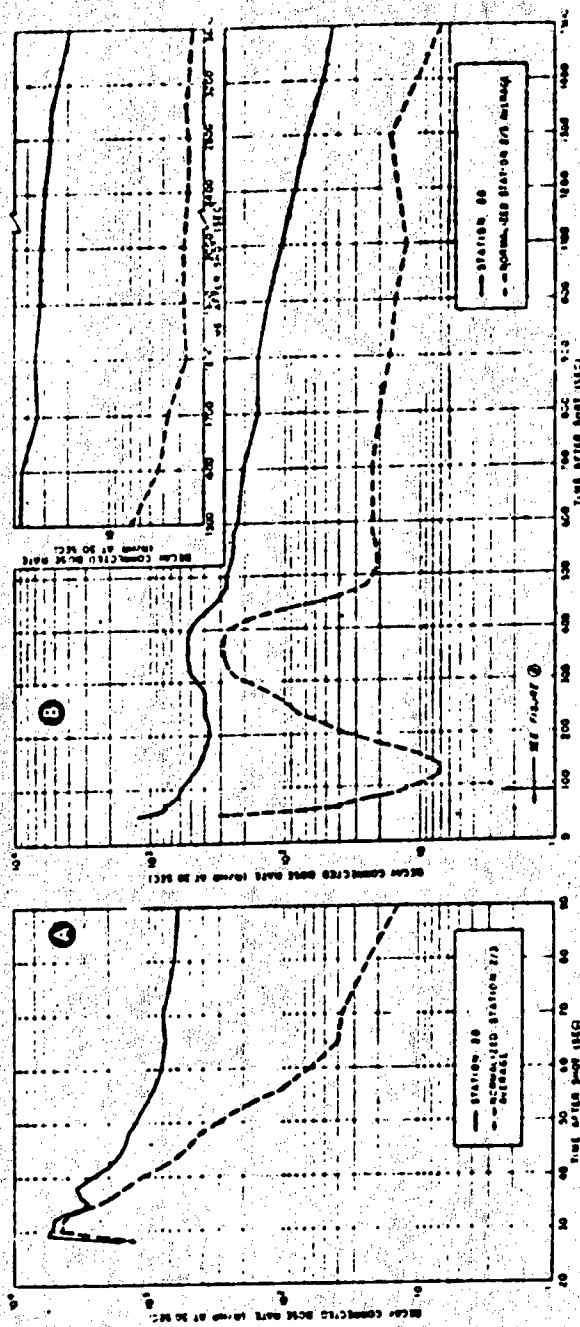


Figure 3.25 Decay-corrected dose rates for the lower engine room GITR Station 20, and for the normalized average of Stations 3 and 20; DD-392, Ship Umbrella. Difference at 360-second normalization point is equal to difference at 320 seconds.

CONFIDENTIAL

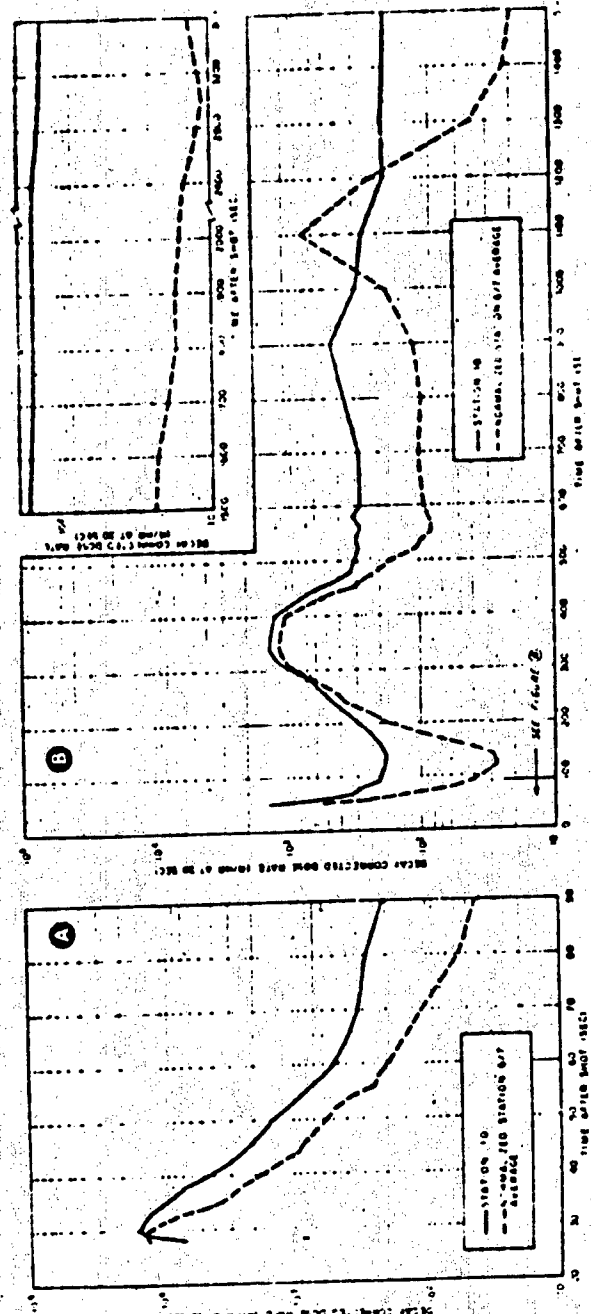


Figure 3.26 Decay-corrected dose rates for the upper level of the forward 11' x 11' room. GTR Station 10, and for the normalized average of Stations 6 and 7; DD-592, Shot Umbrella. Difference at 360-second normalization point is equal to difference at 500 seconds.

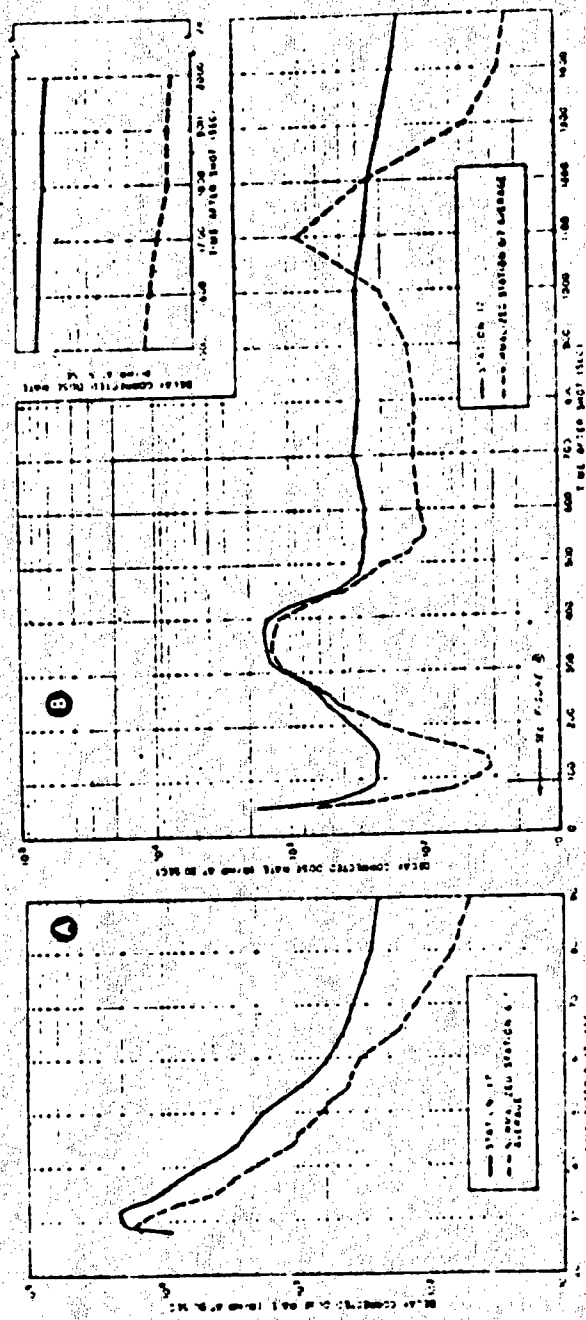


Figure 3.27. Decay-corrected dose rates for the upper level of the after-burner. Information GITT Station 17, and for the normalized-average of Stations 6 and 7. Dose 360, Shot Guitrella. Difference at 360-second normalization point is equal to difference at 540 seconds.

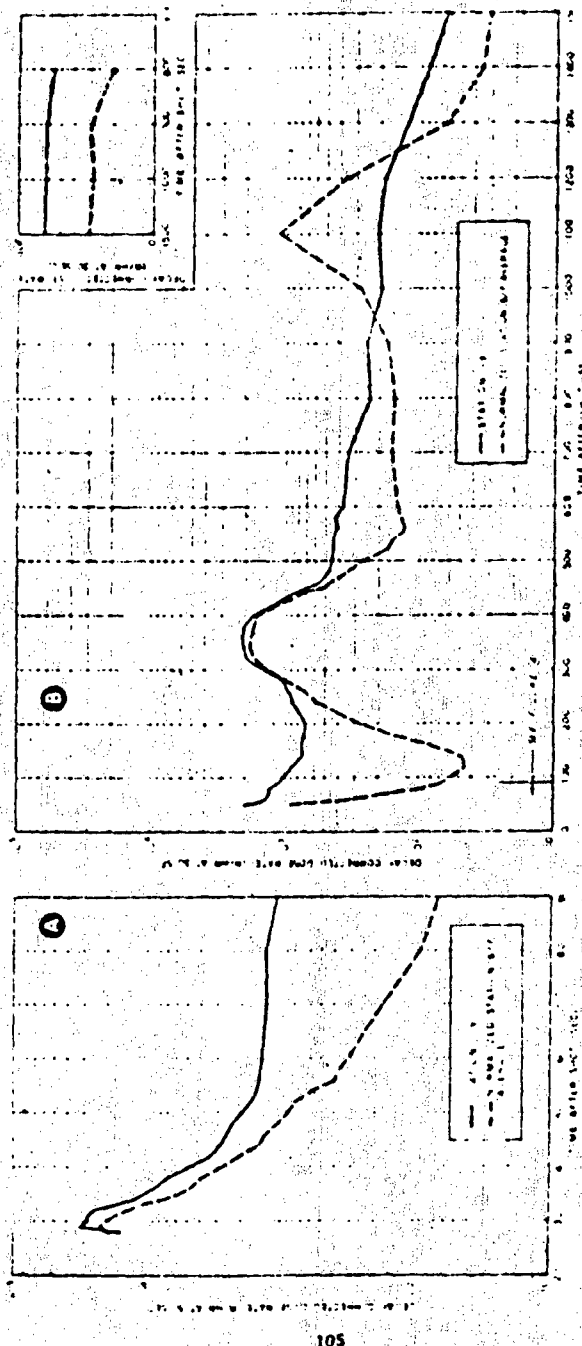


Figure 3.28 Decay-corrected dose rates for the upper level of the alter chamber room GTTR Station 15, and for the normalized average of Stations 6 and 7. Dose rate at umbrella difference at 260-second normalization point is equal to difference at 500 seconds.

CONFIDENTIAL

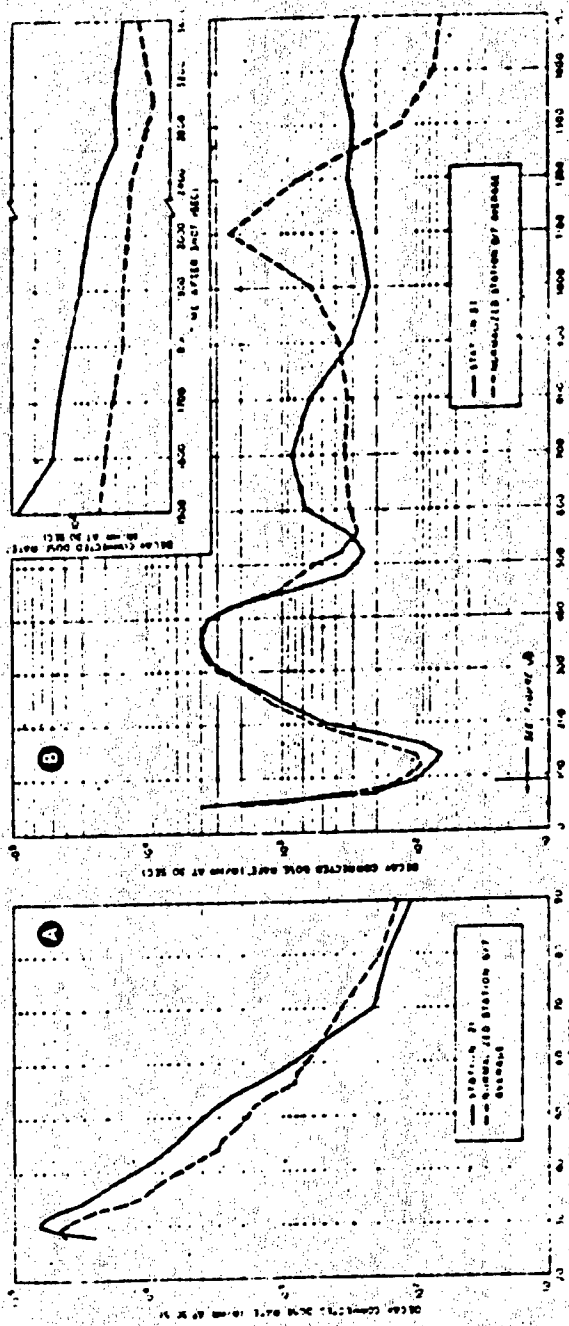


Figure 3.29 Decay-corrected dose rates for the after crew quarters
 GTR Station 21, and for the normalized averages of Stations 6 and 7;
 DD-592, Shot Umbrella. Difference at 360-second normalization point
 is equal to difference at 360 seconds.

CONFIDENTIAL

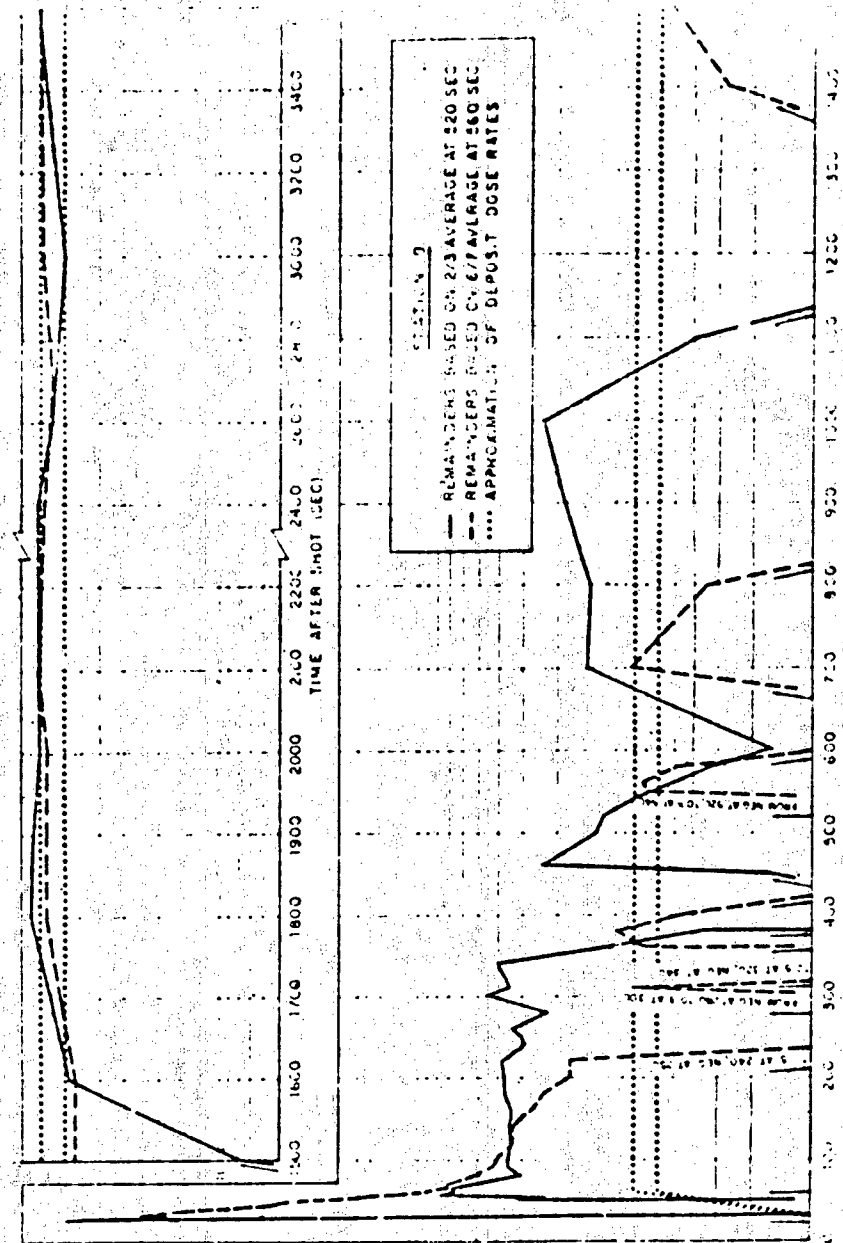


Figure 3.30 Estimated dose rates in the gallery due to the dispersal of contaminants into the DD-592 for Shot Unicella, using CTR data.

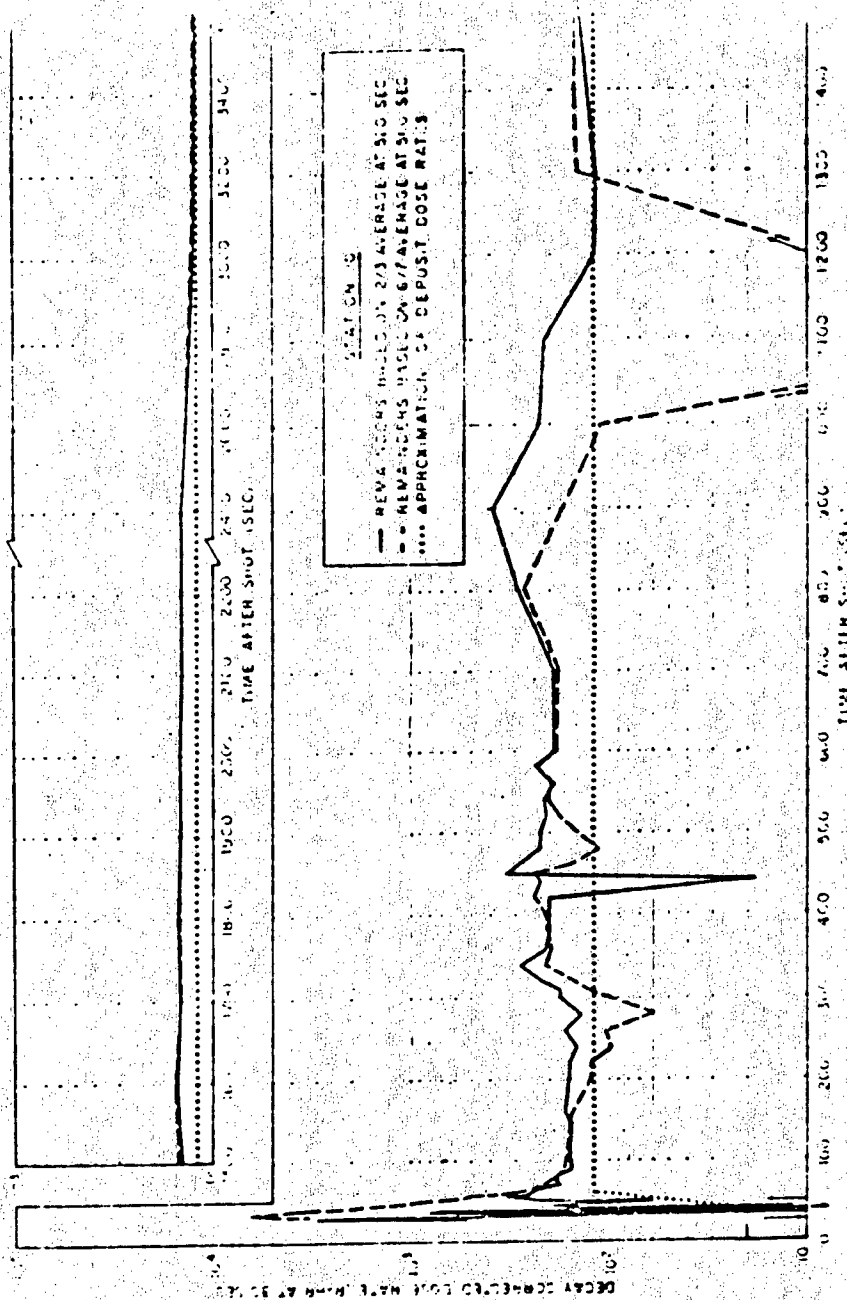


Figure 3.3-1. Estimated dose rates in the upper level of the forward fireroom, due to the ingress of contaminants into the D-532 for SMC-100, using GITR data.

CONFIDENTIAL

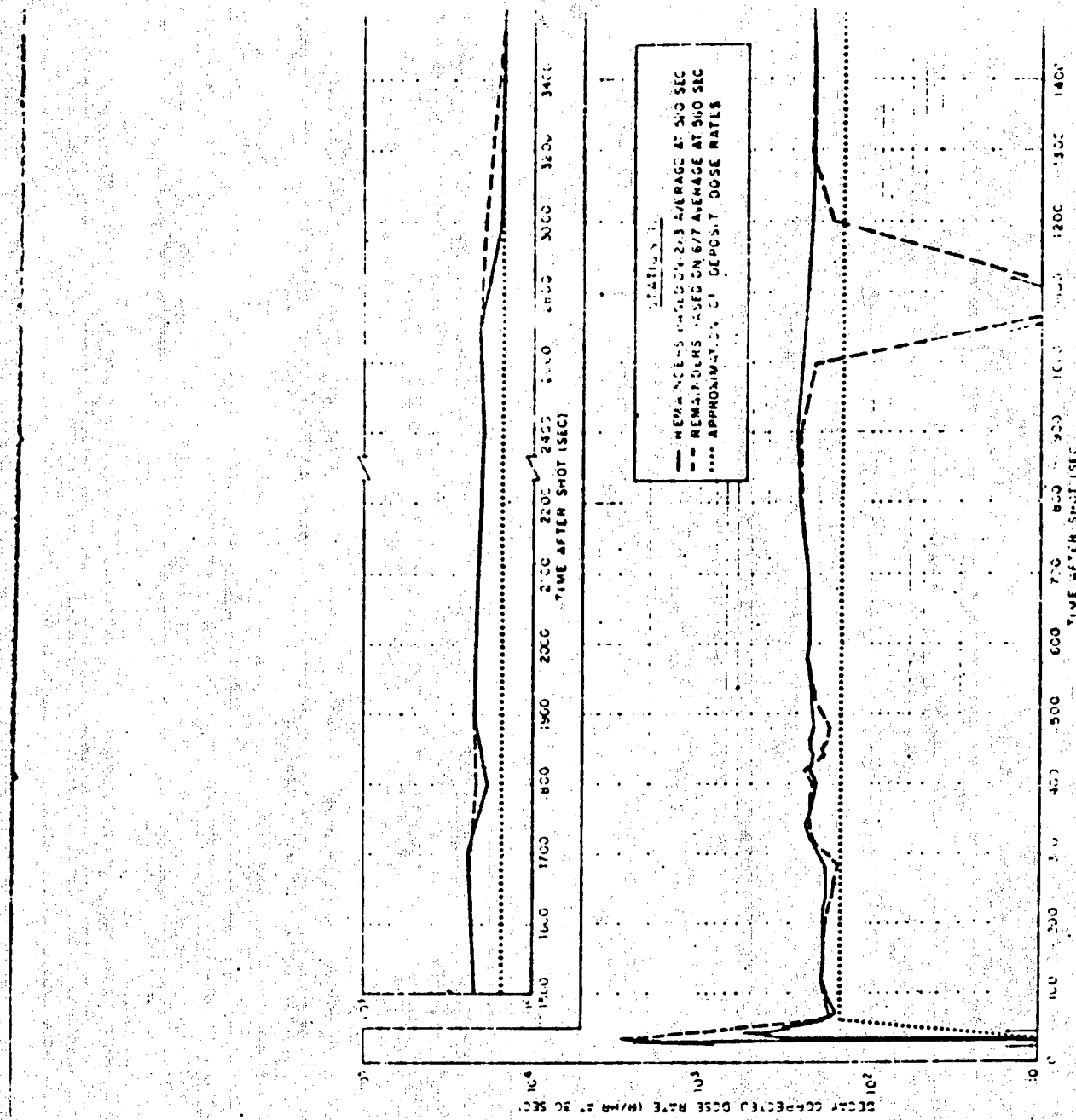
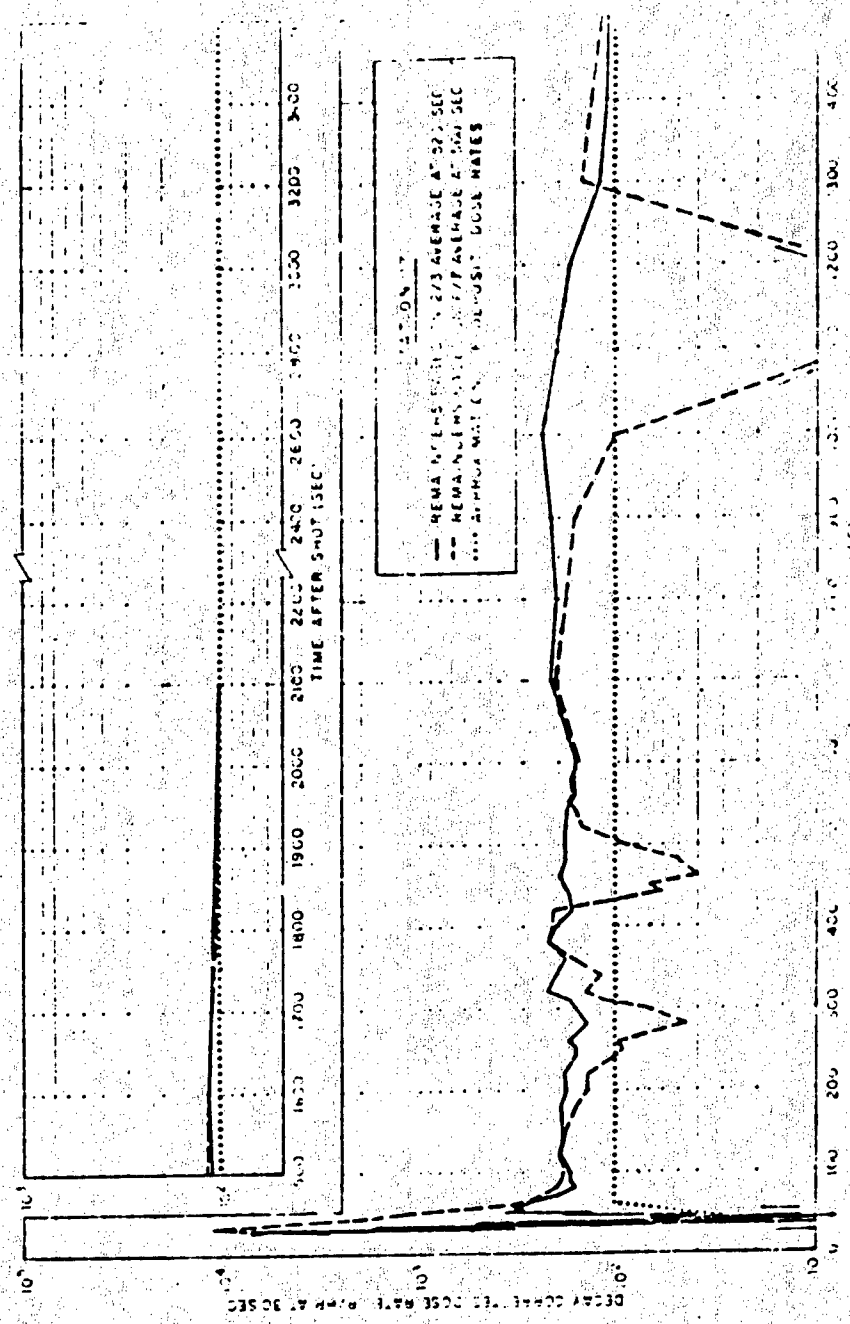
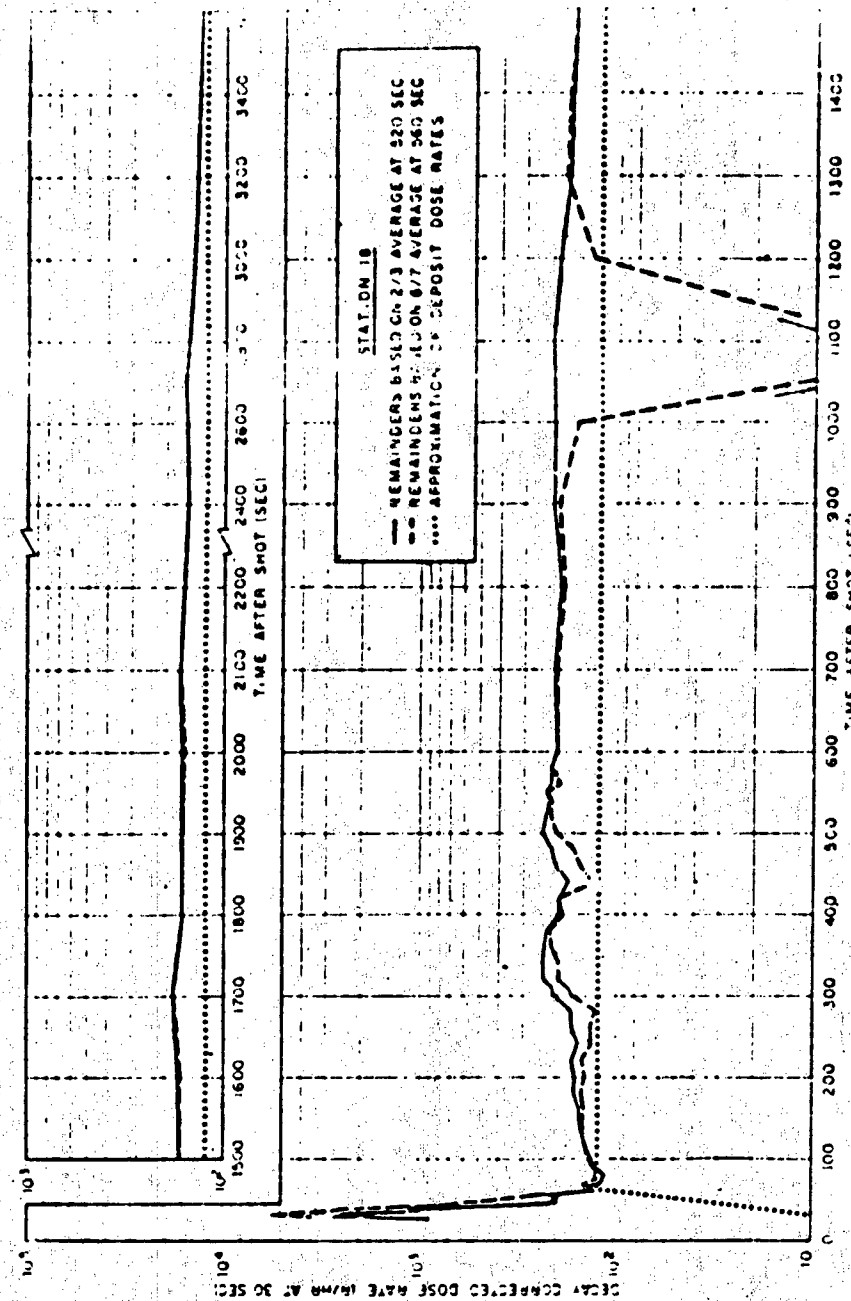


Figure 3-32. Estimated dose rates in the lower level of the lower room due to the ingress of contaminants into the DD-552 test shot. Data, using GITR data.



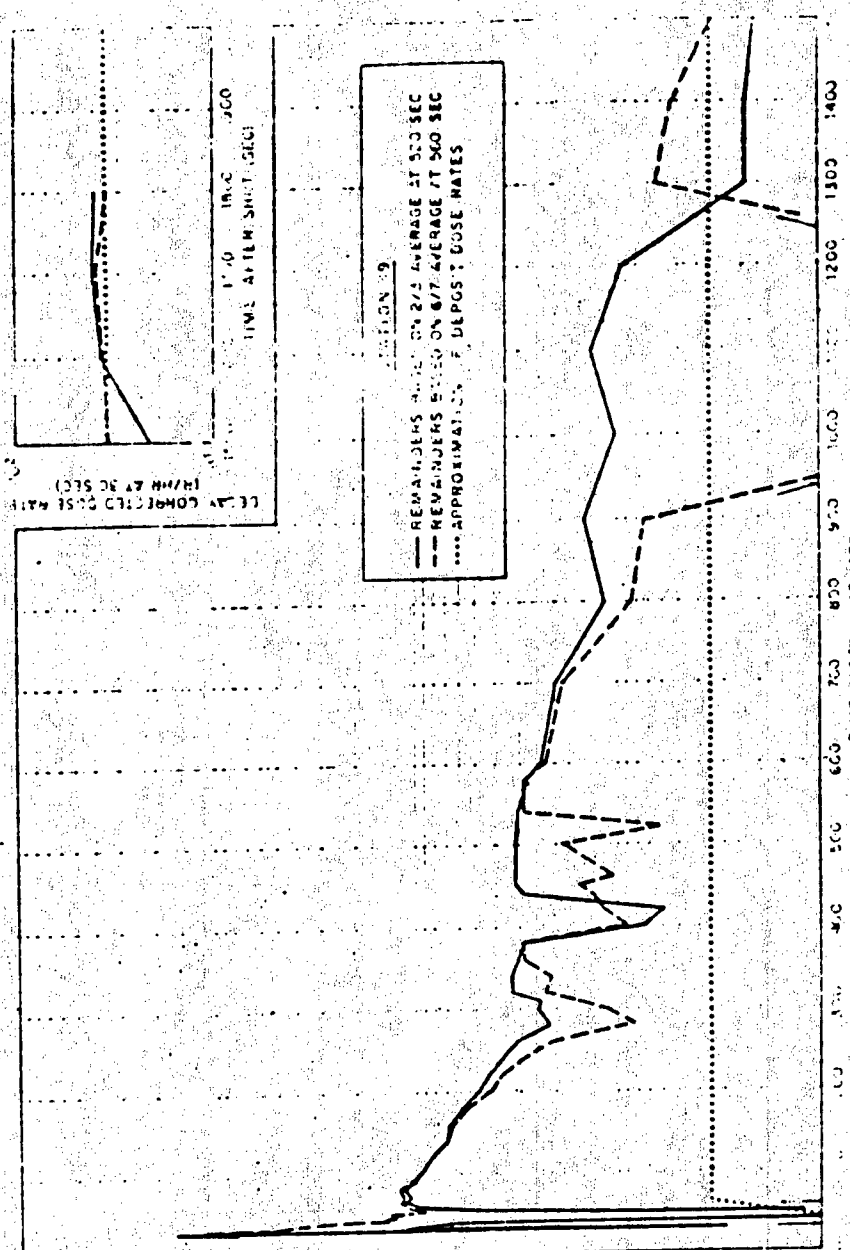
CONFIDENTIAL

Figure 3.33 Estimated dose rate (RADS/SEC) versus time after shutdown due to the ingress of contaminants into the DD-552 fire shaft Unit 114, using GTR data.



CONFIDENTIAL

Figure 3.34 Estimated dose rates in the lower level of the inner 7th tier room, due to the ingress of contaminants into the DD-392 for Shot Unit 1, using CITR data.



the 22nd of January, 1863, in the name of the Commonwealth of Massachusetts.

卷之三

THE AMERICAN MUSEUM

卷之三

~~CONFIDENTIAL~~

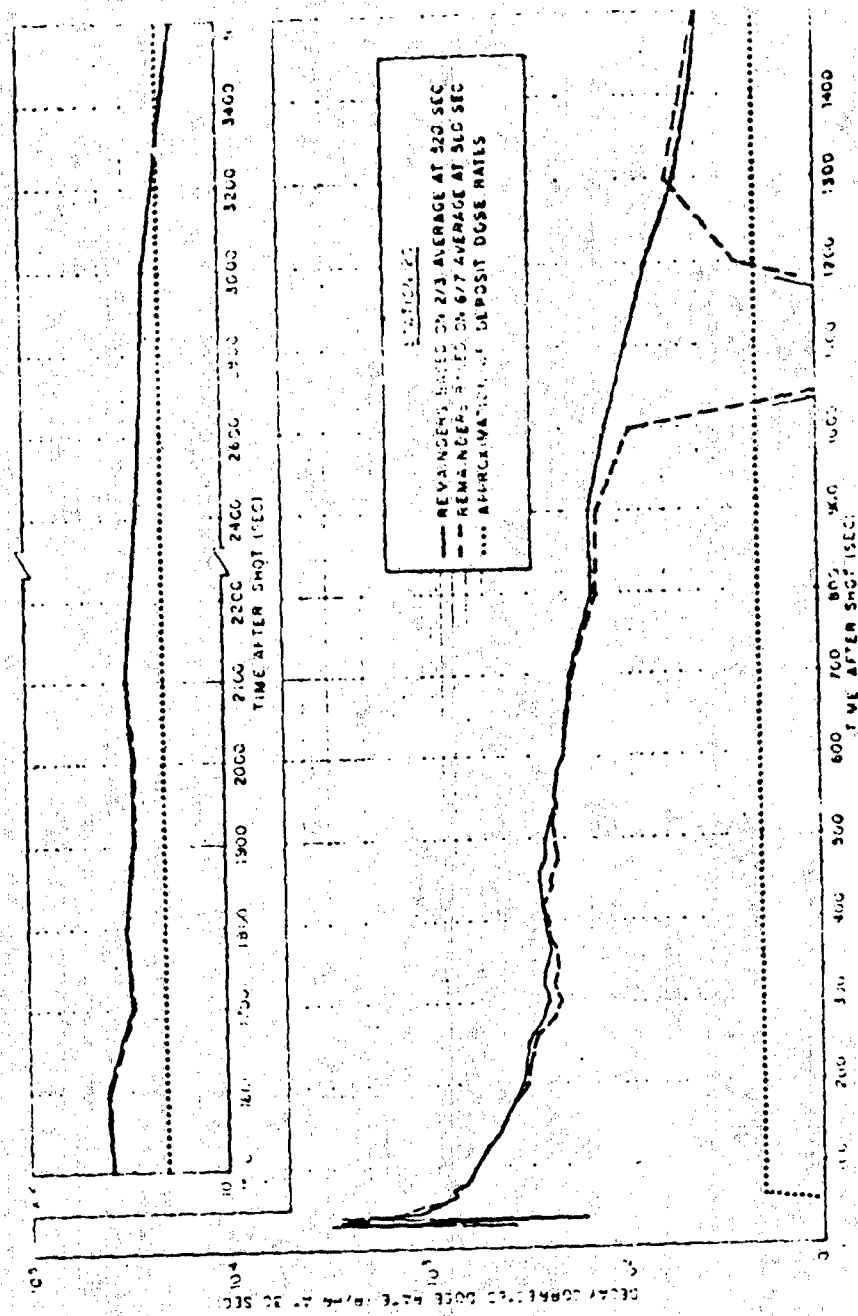


Figure 3-36 Estimated dose rates in the lower level of the alpha science room, due to the impact of contaminants from Shot U-1, using GTR data.

CONFIDENTIAL

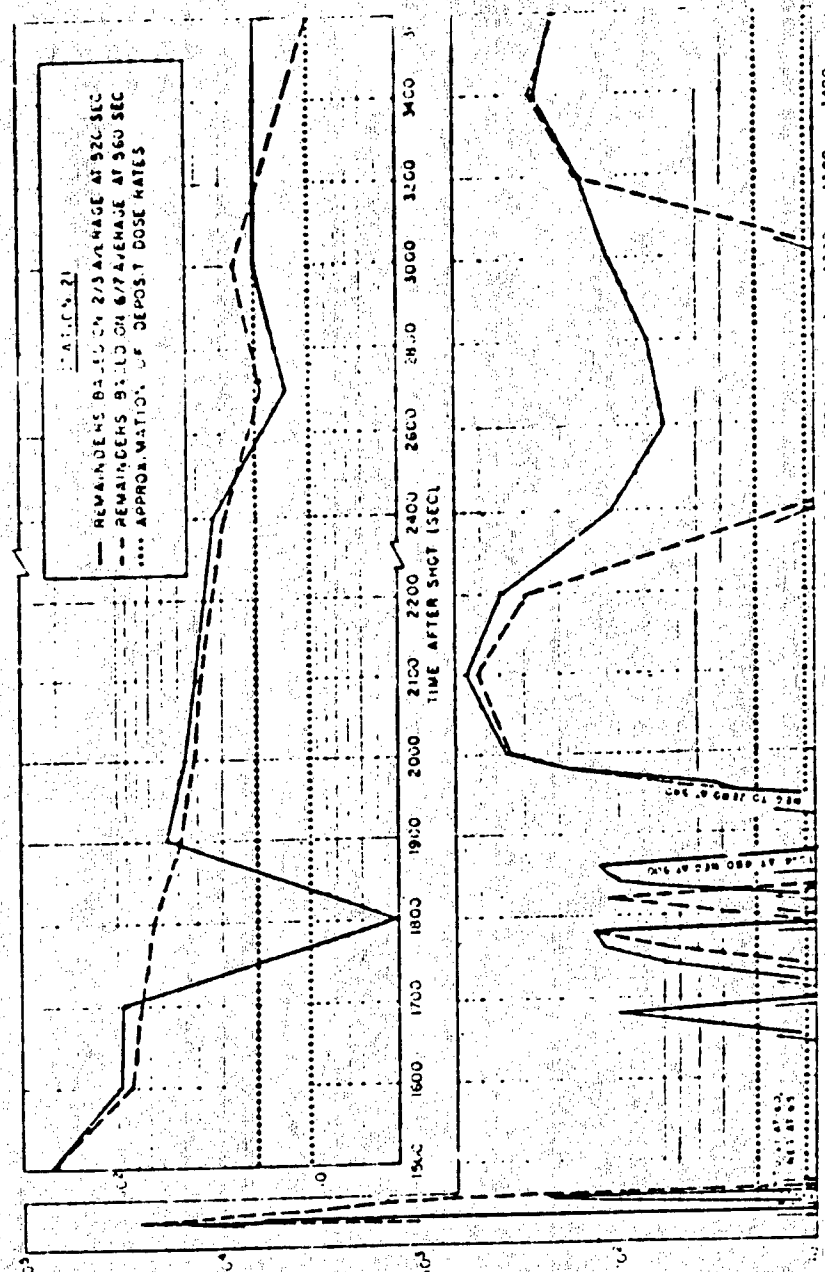
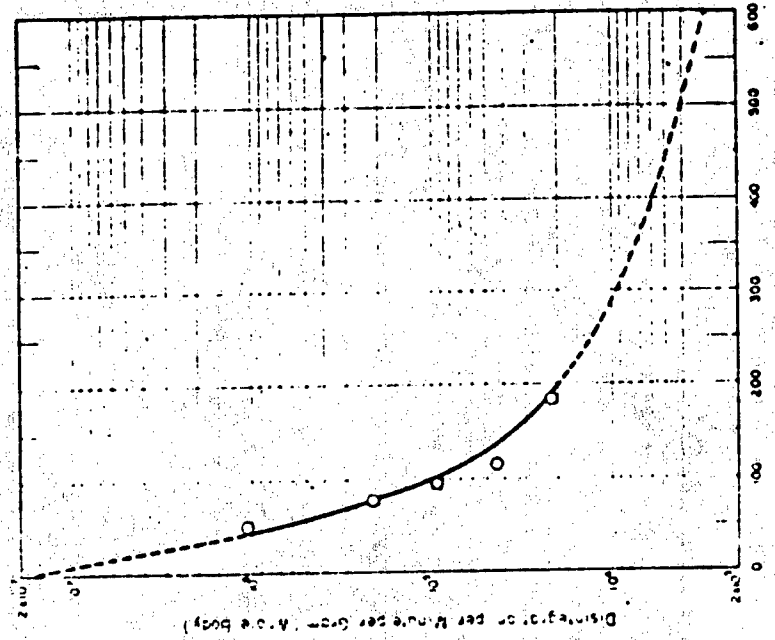
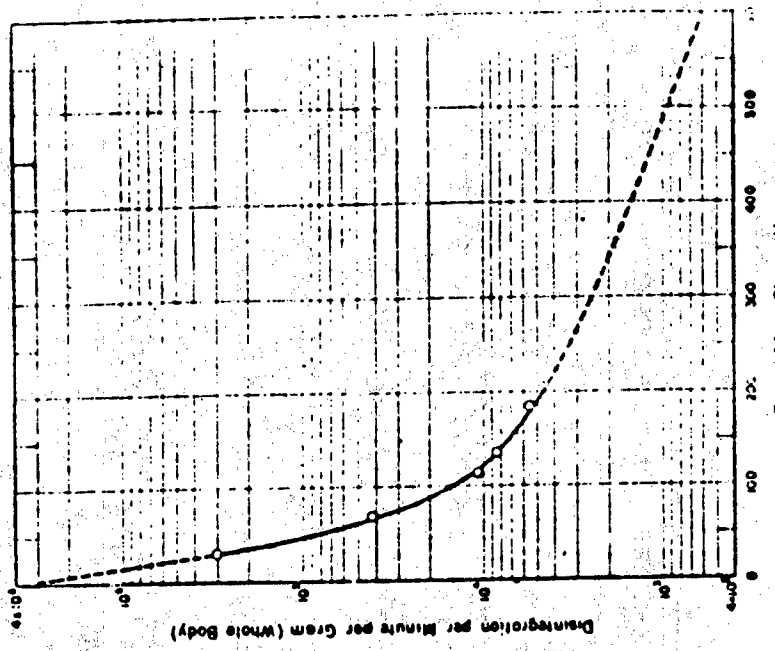
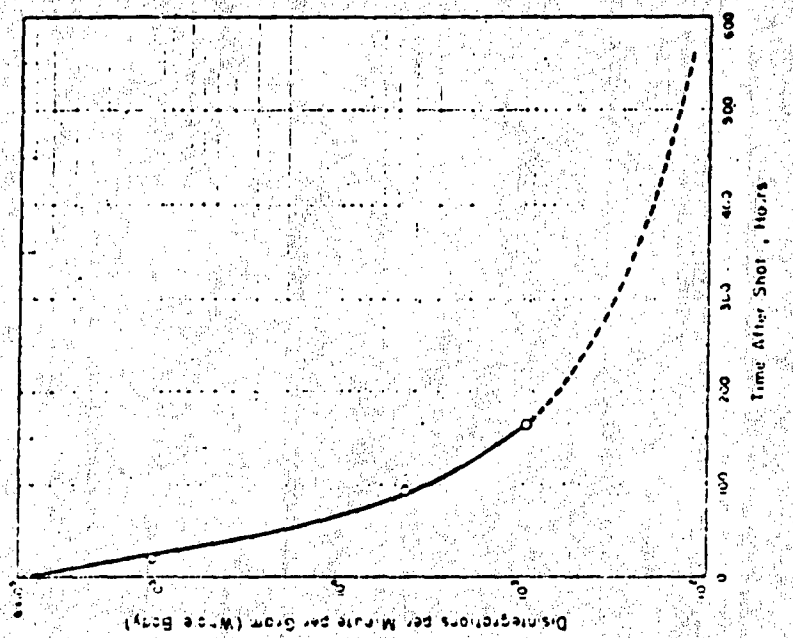
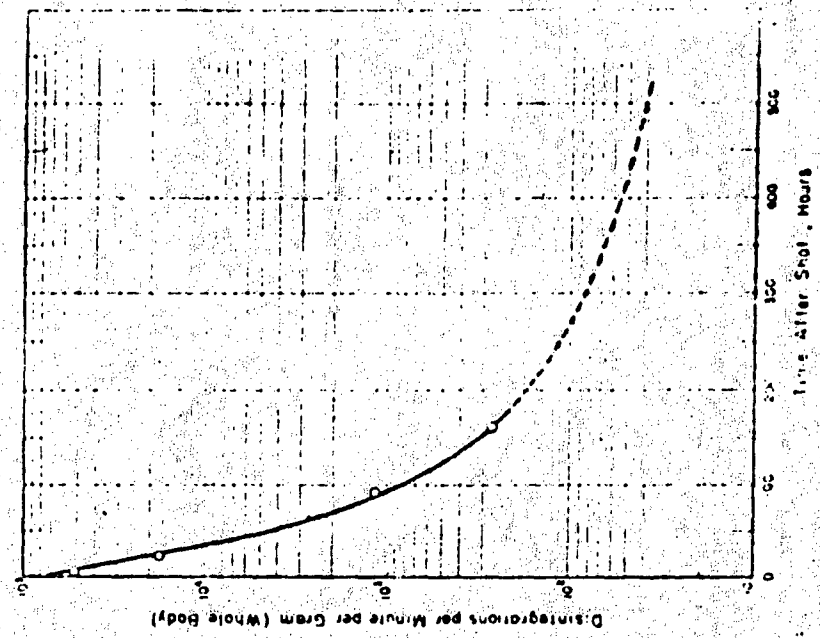


Figure 3.37 Estimated dose rates in the crew's quarters, due to the ingress of contaminants into the DD-592 slot, Umbrella, using GITR data.



CONFIDENTIAL



116

CONFIDENTIAL

Figure 44. Results of experiments on the absorption of 1000 Rads. by the whole body. Points show data points on plateau. Shaded areas points on water test data points. Curve allows laboratory to determine curve normalized to 1000 Rads. by whole body.

Figure 45. Results of experiments on the absorption of 116 Rads. by the whole body. Points show data points on plateau. Shaded areas points on water test data points. Curve allows laboratory to determine curve normalized to 1000 Rads. by whole body.

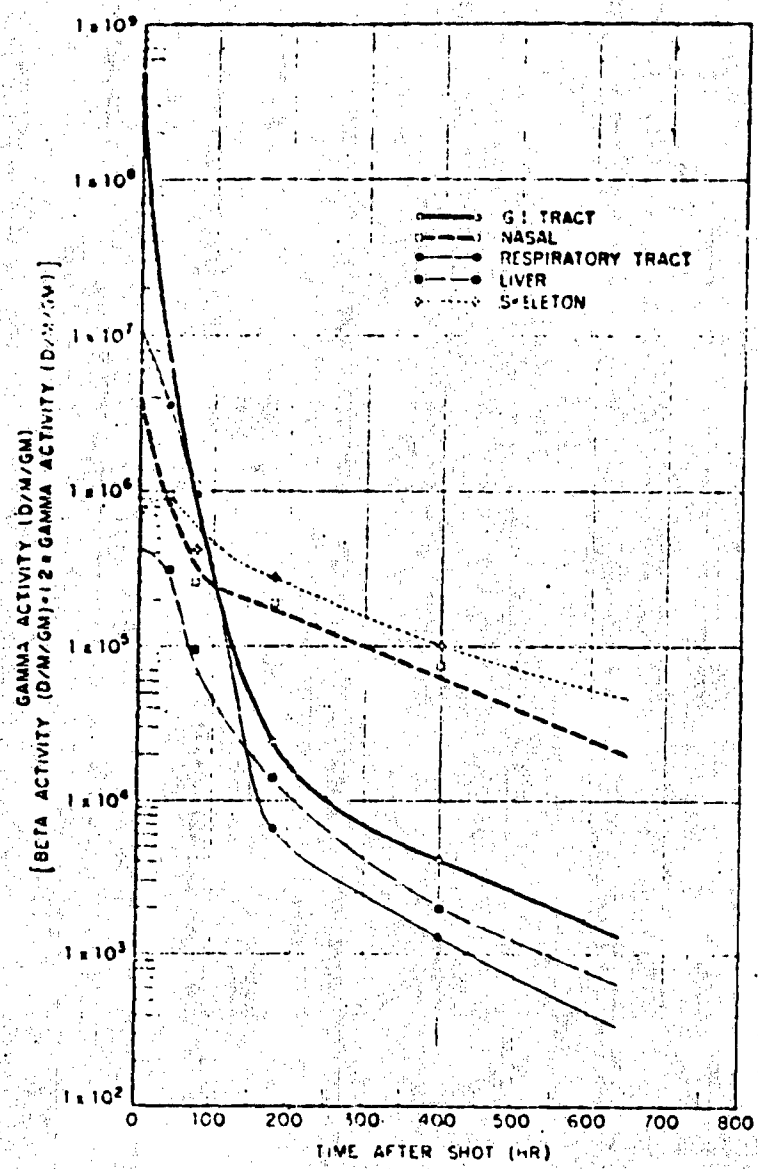


Figure 2-42. Radioactivity in various tissues following a single bolus injection of ⁹⁰Sr. The curves are plotted on a semi-logarithmic scale. The time axis is in hours. The curves are normalized to the same initial value.

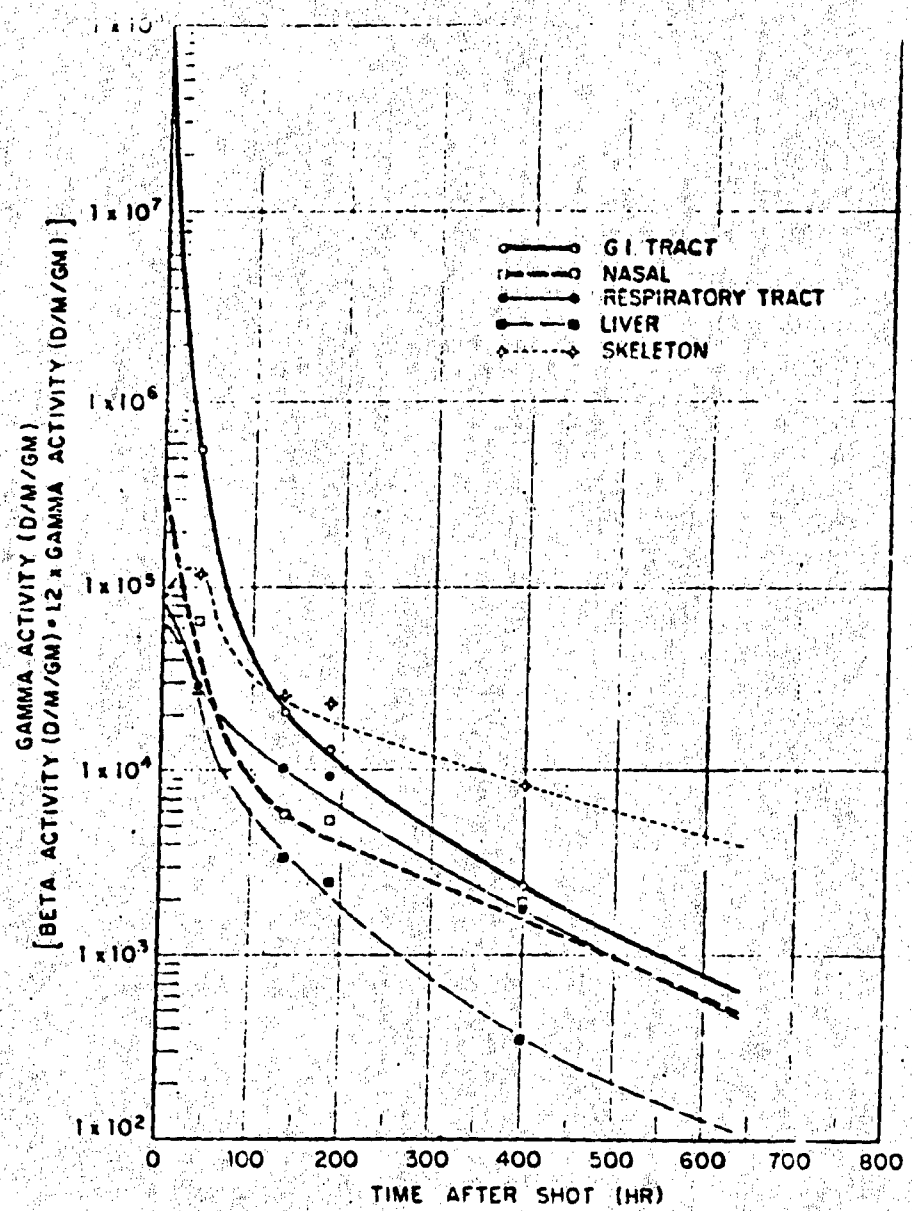


Figure 3-12. Radioisotope and biological decay curves for tritium-labeled trinitrotoluene. (Data from R. H. St. John and W. H. H. Smith, 1961. Points shown are to be data points. Curves shown are fits to data + experimental curves normalized to fit to data points.)

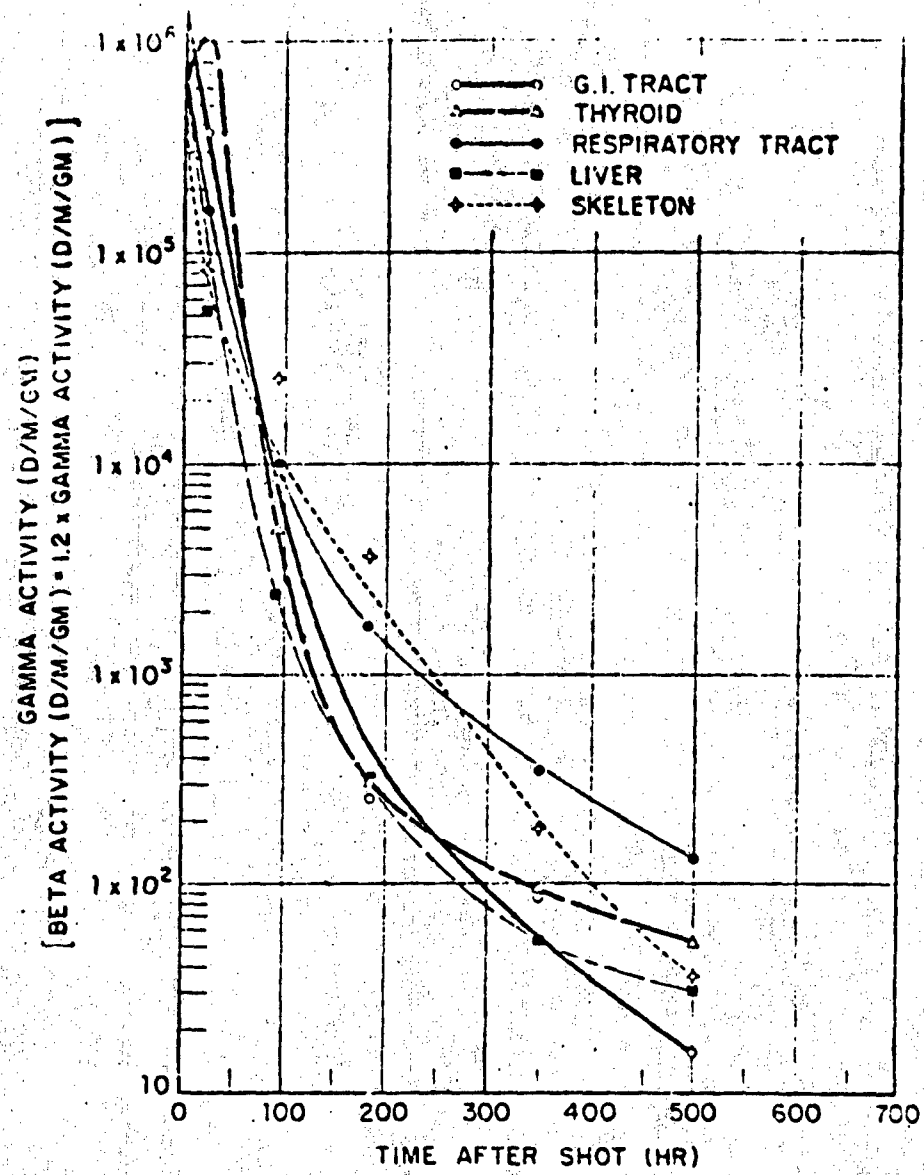


Figure 3.44. Radiological and biological decay curves for individual organs of mice, direct radiation, 500 rads/0.1 hr. Points shown are 1/2 hr. data points. Curves shown are laboratory experimental curves normalized to fit these data points.

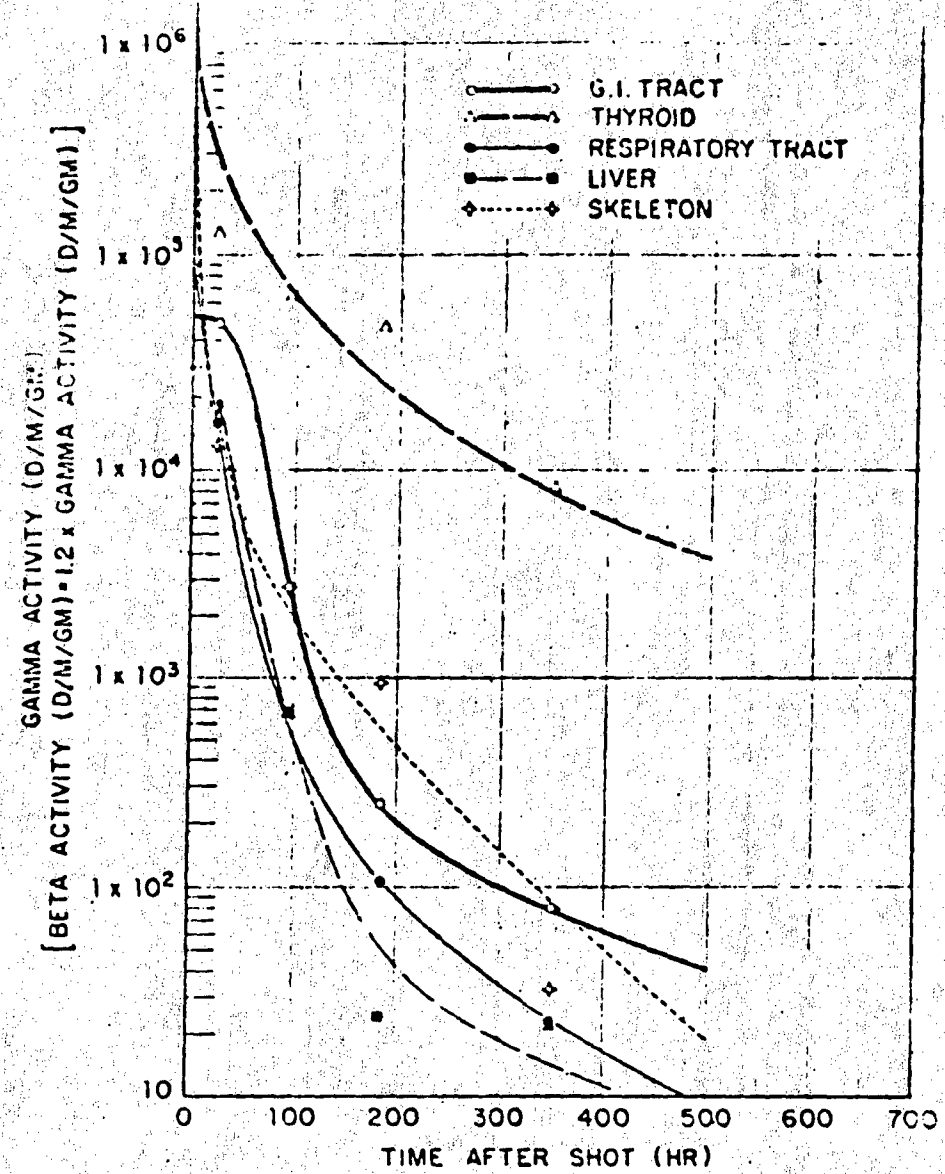


Figure 3-35. Radiological and biological decay curves for individual organs of guinea pigs, director pattern, Site Umbrella 1A. Points shown are field data points. Curves shown are laboratory experimental curves normalized to fit field data points.

Chapter 4

CONCLUSIONS AND RECOMMENDATIONS

4.1 CONCLUSIONS

For the target destroyers moored in the downwind sector of the base surge, fallout, or cloud after Shots Wahoo and Umbrella, with ventilation systems open (but fans secured) and boilers operating, it was concluded that:

1. The dose due to the ingress of contaminants was secondary to the doses due to transient radiation sources exterior to the ship.
2. The dose due to radioactivity deposited in the body was always insignificant compared to the total exposure dose.
3. No dose due to the ingress of contaminants was of a magnitude that would result in casualties or any reduction in combat effectiveness to personnel.
4. If shielding were provided to reduce the dose due to exterior transient radiation sources for operations in the base surge, cloud, or fallout, then the doses due to the ingress of contaminants would require consideration under any concept of dosage control for repeated exposures.
5. For Shot Umbrella, the doses due to the ingress of contaminants decreased with distance downwind from surface zero.
6. For Shot Wahoo, the doses due to the ingress of contaminants decreased with distance downwind from surface zero to the DD-592 position, but there was no further decrease downwind to the DD-593 position.
7. For the one case, DD-592 Shot Umbrella, where air samples were obtained in ventilated spaces, the sample activities were principally associated with particle sizes that were readily airborne and capable of being respired.

4.2 RECOMMENDATIONS

No recommendations for the use of the data are made in view of the uncertainty in the estimates of the major radiological effects due to ingress of radioactive sources into ships' compartments and the fact that, at a maximum, they were secondary to the much larger concomitant external dose from transient sources external to the ships. If analysis of other radiation data from Operation Hardtack and shipboard operation requirements indicate a need for a more quantitative evaluation of the possible hazards from contamination entering ship compartments and the important parameters responsible for this ingress, then it is clear that such determinations can only be made as the result of a coordinated laboratory research and field testing program.

Appendix A

EQUATIONS FOR ESTIMATION OF GAMMA DOSE RATES FROM RADIOACTIVITY MEASUREMENTS OF AIR AND SURFACE SAMPLE COLLECTIONS AS A FUNCTION OF TIME IN A SHIPBOARD COMPARTMENT

The gamma dose rates due to airborne and deposited radioactivity within several shipboard compartments were estimated for the approximate center of each compartment, because this point was near a detector measuring dose rate and permitted a simplified analytic approach, namely, that the point is the center of a spherical volume of uniformly contaminated air.

A.1 GAMMA DOSE RATE DUE TO AIRBORNE ACTIVITY

Assume Point P at the center of a contaminated spherical volume, and also assume:

- R = dose rate at Point P, at time t, rads/hr
- r = radial distance from P to the shell of the sphere, feet
- r_0 = maximum radius of the sphere, feet
- S = sample count rate, counts/min
- V = volume of air from which sample was obtained, ft^3
- K = detection efficiency of counter, counts/photon
- f = fraction of sample retained by filter, dimensionless
- E = gamma energy, Mev/photon
- μ = linear absorption coefficient, ft^{-1}
- B = multiple scattering buildup factor, dimensionless
- K = gamma flux to dose rate conversion factor, $\text{rads}/\text{hr per Mev cm}^2\text{-sec}$
- k_1 = conversion factor for units, $1.8 \times 10^{-3} \text{ ft}^2\text{-min cm}^2\text{-sec}$
- δ = decay factor to convert dose rate at time of sample count, t_0 , to dose rate at time t, dimensionless

The dose rate at P contributed by a shell of the contaminated sphere at radius r, will be:

$$\frac{dR}{dt} = \frac{k_1 K S E \delta 4\pi r^2 dr B e^{-\mu r}}{16 V - 4\pi r^2} \quad (A.1)$$

When $0 \leq \mu r \leq 1$, B can be represented in the form

$$B = 1 + b \mu r, \text{ or } b = \frac{B-1}{\mu r} \quad (A.2)$$

where Equation A.2 defines b. Therefore,

$$\frac{dR}{dt} = \frac{k_1 K S E \delta}{16 V} (1 + b \mu r)^{-\mu r} dr \quad (A.3)$$

Integrating between the limits $r = 0$ and $r = r_0$,

$$R = \frac{k_1 K S E \delta}{16 V} \int_0^{r_0} e^{-\mu r} dr + \frac{k_1 K S E \delta}{16 V} b \int_0^{r_0} r e^{-\mu r} dr \quad (A.4)$$

Evaluating the integral and collecting terms,

CONFIDENTIAL

$$\frac{R_{14V}}{k_1 K S E \delta r_0} = \left(\frac{1}{w r_0} \right) \left[1 - e^{-w r_0} \left(\frac{1 + b w r_0}{1 + b} \right) \right] \quad (A.5)$$

Equation A.5 can be expanded into a series form,

$$\frac{R_{14V}}{k_1 K S E \delta r_0} = 1 - (1 - b) \frac{\mu r_0}{3!} + (1 - 2b) \frac{\mu r_0^2}{3!} - \dots \quad (A.6)$$

In application of Equation A.6, the distance r_0 will be 30 feet or less. For values of E between 0.5 and 6 Mev, $w r_0$ will be less than 0.1, and values of b will be less than 2. Therefore, in this range of energies and radii,

$$R = \frac{k_1 K S E \delta r_0}{14V} \text{, within } \pm 5 \text{ percent} \quad (A.7)$$

Values of K from Figure 27 of Reference 25:

E Mev	K $\times 10^{-6}$
0.5	2.1
1.0	1.9
2.0	1.6
3.0	1.4
4.0	1.3

Example, let

$$\begin{aligned} r_0 &= 30 \text{ feet} \\ S &= 300 \text{ counts/min (at 30 hours after shot)} \\ V &= 2 \text{ ft}^3 \\ g &= 0.3 \text{ count/photon} \\ f &= 0.9 \\ E &= 1 \text{ Mev/photon} \\ k_1 &= 1.8 \times 10^{-6} \text{ ft}^2 \cdot \text{min/cm}^2 \cdot \text{sec} \\ K &= 1.9 \times 10^{-6} \text{ r/hr per Mev/cm}^2 \cdot \text{sec} \\ t &= 6 \text{ minutes} = 0.1 \text{ hour} \\ t_0 &= 30 \text{ hours} \end{aligned}$$

The following decay function is assumed:

$$d = R_0 (R_0/t)^{1.3}$$

Where: R_0 = dose rate at time t

R_0 = dose rate at time of sample count t_0

From Equation A.5 and A.6,

$$\begin{aligned} R &= \frac{k_1 K S E \delta r_0}{14V} = \frac{k_1 K S E r_0}{14V} (R_0/t)^{1.3} \\ &= \frac{1.8 \times 10^{-6} \times 1.9 \times 10^{-6} \times 3 \times 10^3 \times 1 \times 3 \times 10}{0.9 \times 0.3 \times 2} (30/0.1)^{1.3} \\ &= 0.5 \text{ mr/hr} \end{aligned}$$

A.2 GAMMA DOSE RATES DUE TO AIRBORNE ACTIVITY AND ESTIMATION OF AIRBORNE ACTIVITY CONCENTRATIONS FROM TOTAL AIR SAMPLE DATA

For a method of estimating the dose rate from total air sampling data, the following are defined:

t_1 = time after shot of instantaneous influx of contaminated air into compartment, minutes

w = volume of air sampled at constant rate between times t_1 and t_2 , cm^3

t_2 = time after shot when air sampling stopped, minutes

t_0 = an assumed time after shot of instantaneous influx of contaminated air uniformly distributed throughout compartments, minutes

Then: $\frac{f_1}{V_1(t_2-t_1)} = \text{the collection rate of fissions on an air sample.}$

A collection efficiency of 100 percent is assumed.

Because no time-dependent air sampling data was obtained, assume:

$$f_1 = f_0 e^{-k_2(t-t_0)} \quad t_0 \leq t \leq t_1$$

$$f_2 = f_0 e^{-k_2(t_2-t_1)} \quad t_1 \leq t$$

An exponential dilution equation from Reference 20

where: f_1 = number of fissions in compartment at time t , fissions

f_0 = number of fissions after instantaneous influx of contaminated air at time t_0 , fissions

t_1 = time after shot when ventilation blowers stopped, minutes

k_2 = ratio of ventilation airflow rate to compartment volume.

Then

$$\frac{w}{V_1(t_2-t_1)} \int_{t_1}^{t_2} f_1 dt = F \quad (A.8)$$

Where: F = total number of fissions collected on sample as determined by a radiochemical analysis for Mo^{99} content.

Then

$$\begin{aligned} F &= \frac{w f_0}{V_1(t_2-t_1)} \left[e^{k_2 t_0} \int_{t_0}^{t_1} e^{-k_2 t} dt + e^{-k_2(t_1-t_0)} \int_{t_1}^{t_2} dt \right] \\ F &= \frac{w f_0}{V_1(t_2-t_1)} \left[\frac{e^{k_2 t_0}}{k_2} e^{-k_2 t_0} - e^{-k_2 t_1} + \frac{k_2}{k_2} (t_2-t_1) e^{-k_2(t_2-t_1)} \right] \\ F &= \frac{w f_0}{k_2 V_1(t_2-t_1)} \left[1 + e^{-k_2(t_1-t_0)} \left\{ k_2(t_2-t_1) - 1 \right\} \right] \end{aligned}$$

Therefore:

$$\frac{f_1}{V_1} = \frac{k_2(t_2-t_1)}{w} \frac{F}{\left\{ 1 + e^{-k_2(t_1-t_0)} \left\{ k_2(t_2-t_1) - 1 \right\} \right\}} \quad t \geq t_1 \quad (A.9)$$

$$\frac{f_1}{V_1} = \frac{F}{w} \frac{k_2(t_2-t_1)}{\left(k_2(t_2-t_1) - 1 \right)} \quad t \geq t_1 \quad (A.10)$$

Now, for a sphere of radius r (cm), assuming no absorption or buildup,

$$R = 10^{-6} \frac{f_1}{V_1} \text{ MrK} \quad (A.11)$$

Where: R = dose rate at the center of the sphere at time t , $\text{r} \cdot \text{hr}$

$\frac{f_1}{V_1}$ = concentration in fis/cm^3 as determined by Equations A.8 and A.9

UNCLASSIFIED

For a quarter circle, $\delta = 0.25$; for a semi-circle, $\delta = 0.5$; for a full circle, $\delta = 1.0$; for a quarter circle, $k_1 = 3.74 \times 10^2$ for the center, and 8.96×10^2 for every quarter.

K = gamma dose rate conversion factor, $\text{r/hr per Mev/cm}^2 \cdot \text{sec}$

Values for M were obtained from Reference 25. Values for K were obtained from Reference 24—
 1.85×10^{-6} at $H = 10$ seconds and 1.92×10^{-6} at $H = 10$ minutes.

A.3 GAMMA DOSE RATE DUE TO DEINTEGRATED ACTIVITY

In this case the surface (deck, bulkhead, and the like) is assumed to be a uniformly contaminated disk. In addition to those quantities defined in Section A.1 above, the following are defined:

R = dose rate at Point P, h feet above the center of a contaminated disk at time t , r/hr

r = radial distance from center of disk, feet

r_0 = maximum radius of disk, feet

h = perpendicular distance of Point P from disk, feet

A = annular area, in^2

k_2 = conversion factor for units, $2.6 \times 10^{-2} \text{ in}^2 \cdot \text{min} \cdot \text{cm}^3 \cdot \text{sec}$

The dose rate R at Point P, h feet above the center of a uniformly contaminated disk, contributed by an annular incremental area, is

$$dR = \frac{k_2 K S E \delta \times 2\pi r dr B_0}{g A} \cdot e^{-\mu (r^2 + h^2)^{1/2}} \quad (A.12)$$

but for $(r_0^2 + h^2)^{1/2} \approx 30$ feet, where $0.5 \leq E \leq 4$ Mev

$$B_0 \approx e^{-\mu (r_0^2 + h^2)^{1/2}} = 1 \text{ (0.5 percent)}$$

Therefore,

$$dR = \frac{k_2 K S E \delta}{2gA} \times \frac{r dr}{(r^2 + h^2)} \quad (A.13)$$

Now, let $t^2 = r^2 + h^2$; $tdt = r dr$

$$\text{Hence, } dr = \frac{dt}{t} \quad (A.14)$$

Integrating Equation A.4, then,

$$R = \frac{k_2 K S E \delta}{2gA} \int_{h^2}^{(r_0^2 + h^2)^{1/2}} \frac{dt}{t} \quad (A.15)$$

$$= \frac{k_2 K S E \delta}{2gA} \ln(1 + (r_0^2/h^2)^{1/2})$$

$$= \frac{k_2 K S E \delta}{4gA} \ln(1 + (r_0^2/h^2))$$

UNCLASSIFIED

Appendix B

DECAY FACTORS TO CONNECT $\tau_{1/2}$ TO EQUIVALENT $\tau_{1/2}$ AT $t = 30$ SECONDS

Used with GITR data only.

Decay factors from $t = 30$ to $t = 360$ seconds from preliminary experimental data of low chamber decay measurements by J. Mackin and others, NRDL, September 1958 (report in preparation). Decay factors from $t = 360$ to $t = 7,200$ seconds from Reference 18 normalized to early decay measurements at $t = 360$ seconds.

Time After Shot sec	Decay Factor	Time After Shot sec	Decay Factor	Time After Shot sec	Decay Factor
28	0.930	140	5.277	560	30.00
29	0.968	150	5.714	600	36.77
30	1.000	160	6.154	700	48.71
31	1.033	180	7.059	800	48.15
32	1.057	200	8.136	900	55.17
33	1.096	220	9.091	1,000	63.16
34	1.127	240	10.21	1,100	70.59
35	1.165	250	10.67	1,200	77.42
36	1.200	260	11.27	1,300	85.71
38	1.258	280	12.18	1,400	92.31
40	1.304	300	13.33	1,500	100.00
42	1.364	310	13.79	1,600	109.1
44	1.429	320	14.29	1,700	117.1
46	1.500	310	15.19	1,800	124.4
48	1.569	360	16.23	1,900	133.3
50	1.633	380	17.27	2,000	141.2
52	1.690	400	18.18	2,100	150
54	1.763	420	19.20	2,400	178
56	1.832	440	20.17	2,700	203
58	1.905	450	20.51	3,000	233
60	1.967	460	21.24	3,600	289
63	2.143	480	22.22	4,200	346
70	2.330	500	24.00	4,800	407
80	2.727	520	25.83	5,400	471
90	3.117	540	26.97	6,000	522
100	3.525	550	27.59	7,200	632
120	4.364	560	27.91		

UNCLASSIFIED

REFERENCES

1. F. R. Holden and others; "Radioactive Contamination of Ventilation Supply System, USS Crittenton, from Baker Explosion"; Operation Crossroads, Report No. AD-200(X), 14 February 1950; U. S. Naval Radiological Defense Laboratory, San Francisco, California; Confidential.
2. J. D. Terest, R. W. Shmider, and H. R. Rinnert; "Personnel Radiation Hazards Incident to Ship Boiler Operation Following an Underwater Atomic Attack"; Technical Report No. 16, 14 September 1954; U. S. Naval Radiological Defense Laboratory, San Francisco, California; Secret.
3. "Maximum Permissible Body Burdens and Maximum Permissible Concentrations of Radioactivities in Air and in Water for Occupational Exposure"; Handbook 69, 1959; National Bureau of Standards; U. S. Department of Commerce, Washington, D. C.; Unclassified.
4. "Armed Forces Medical Policy Council Handbook of Atomic Weapons for Medical Officers"; NavMed P-1330, also DA Pm8-11, and AFM 160-11, Armed Forces Special Weapons Project, June 1951; Unclassified.
5. R. W. Shmider and C. E. Morris; "Significance of Breaks in Integrity of Weather Envelope of Ships Operating During an Underwater Atomic Attack"; Technical Report No. 51, 4 April 19; U. S. Naval Radiological Defense Laboratory, San Francisco, California; Confidential.
6. G. G. McMullumphy and M. M. Digger; "Proof Testing of Atomic Weapons Ship Countermeasures"; Project 6.4, Operation Castle, WT-927, 25 October 1957; U. S. Naval Radiological Defense Laboratory, San Francisco 24, California; Confidential.
7. S. H. Cohn and others; "Some Effects of Ionizing Radiation on Human Beings"; July 1956; United States Atomic Energy Commission; Chapter V; Unclassified.
8. F. Smith, D. W. Biddy, and M. Goldman; "Biological Injury from Particle Inhalation"; Project 2.7, Operation Jangle, WT-396, 18 June 1952; National Institutes of Health, Bethesda, Maryland; Secret Restricted Data.
9. "Experimental Data Obtained in the Field"; Annex 2.4, Parts I, II, and III, Operation Greenhouse, WT-43, January 1953; Los Alamos Scientific Laboratory, Los Alamos, New Mexico; Secret Restricted Data.
10. W. H. Langham and others; "The Radiation Hazards to Personnel Within an Atomic Cloud"; Project 4.1, Operation Upshot-Knothole, WT-743, December 1953; Air Force Cambridge Research Center, Cambridge, Massachusetts; Secret Restricted Data.
11. C. A. Sonnhaus; "Ratio of Lung Beta Dose to Whole Body Dose During Given Time Intervals After Atomic Bomb Detonation"; NRDRL-394, 31 December 1952; U. S. Naval Radiological Defense Laboratory, San Francisco, California; Unclassified.
12. S. H. Cohn and others; "Studies on the Metabolism of Inhaled Aerosols of Strontium and Lanthanum"; Technical Report No. 175, 27 May 1957; U. S. Naval Radiological Defense Laboratory, San Francisco, California; Unclassified.
13. P. E. Palm, J. M. McNerney, and T. Hatch; "Respiratory Dust Retention in Small Animals: A Comparison with Men"; Arch. Ind. Health 13, April 1956, Pages 355 to 365; American Medical Association, Chicago, Illinois; Unclassified.

UNCLASSIFIED

15. S. H. Cohn and others: "The Preparation and Biological Application of Airborne Simulants of Fallout From Nuclear Detonation"; Journal of Air Pollution Control Association, Vol. 7, Pages 20 to 25, May 1957; Unclassified.

16. S. H. Cohn and others: "Uptake, Distribution and Retention of Fission Products in Tissues of Mice Exposed to a Simulant of Fallout From a Nuclear Detonation. Simulant of Fallout from a Detonation Under Sea Water"; Technical Report No. 77, 5 December 1955; U. S. Naval Radiological Defense Laboratory, San Francisco, California; Unclassified.

17. S. H. Cohn and others: "Radiotoxicity Resulting from Exposure to Fallout Simulant"; Technical Report No. 118, 12 January 1957; U. S. Naval Radiological Defense Laboratory, San Francisco, California; Unclassified.

18. M. M. Bicker, H. R. P. Scott, and H. A. Zagerites: "Shipboard Radiation From Underwater Nuclear Bursts"; Project 2.1, Operation Hardtack, WT-1619, 24 March 1961; U. S. Naval Radiological Defense Laboratory, San Francisco, California; Confidential.

19. N. H. Farlow: "Quantitative Determination of Chloride Ion in 10^{-6} to 10^{-12} Gram Particles"; Analytical Chemist, 7, Page 883, June 1957; American Chemical Society, Washington, D. C.; Unclassified.

20. E. C. Evans III and T. H. Shirasawa: "Characteristics of the Radioactive Cloud from Underwater Bursts"; Project 2.3, Operation Hardtack, WT-1621; U. S. Naval Radiological Defense Laboratory, San Francisco, California; Confidential Formerly Restricted Data.

21. C. F. Miller and P. Levy: "Ionization Rate and Photon Pulse Decay of Fission Products from the Slow-Neutron Fission of U^{235} "; NRD-TR-247, 4 August 1958; U. S. Naval Radiological Defense Laboratory, San Francisco, California; Unclassified.

22. C. L. Prosser and others: "Comparative Animal Physiology"; 1950; W. B. Saunders Co., Philadelphia, Pennsylvania; Unclassified.

23. F. C. Albrecht: Handbook, "Standard Values in Blood"; 1952; W. B. Saunders Co., Philadelphia, Pennsylvania; Unclassified.

24. W. Spector: "Handbook of Biological Data"; 1956; W. B. Saunders Co., Philadelphia, Pennsylvania; Unclassified.

25. Reactor Shielding Design Manual; TID-7004, March 1956; Naval Reactors Branch Division of Reactor Development, United States Atomic Energy Commission; Unclassified.

26. "Permissible Dose for External Sources of Ionizing Radiation"; Handbook 59, 1954; National Bureau of Standards, U. S. Department of Commerce, Washington, D. C.; Unclassified.

27. J. Young: "Natural Variation Studies Aboard USS Worcester (CL-144)"; 22 December 1955; Naval Research Laboratory, Washington 25, D. C.; Confidential.

28. P. D. L. Rutherford: "Early-Time Gamma Ray Properties of U^{235} Gross Fission Products"; Technical Memorandum No. 5, 9 July 1956; U. S. Naval Radiological Defense Laboratory, San Francisco, California; Unclassified.

UNCLASSIFIED

DISTRIBUTION

Aliment & Distribution (aliment).

NETT ACTIVITIES

A high-contrast, black and white image showing a dense, abstract pattern of dots and lines, possibly a scan of a textured surface or a specific type of noise pattern. The pattern is composed of numerous small, dark dots scattered across a lighter background, with some horizontal and vertical lines suggesting a grid or a series of connected points. The overall effect is grainy and lacks a clear, recognizable subject.

UNCLASSIFIED

UNCLASSIFIED

130

UNCLASSIFIED